

PROTECTION AGAINST WATER HAMMER
IN PUMP-DISCHARGE LINES

DESIGN FOR PROTECTION AGAINST
WATER HAMMER IN PUMP-DISCHARGE LINES

By

ATEF M. KASSEM, B.SC.

A Thesis

Submitted to the School of Graduate Studies

in Partial Fulfilment of the Requirements

for the Degree

Master of Engineering

McMaster University

March 1976

MASTER OF ENGINEERING (1976)
(Civil Engineering)

McMASTER UNIVERSITY
Hamilton, Ontario

TITLE: Design for Protection Against Water Hammer in Pump-Discharge
Lines

AUTHOR: Atef M. Kassem, B.Sc., Cairo University

SUPERVISOR: Dr. William James

NUMBER OF PAGES: xiii, 164

ABSTRACT

A computer program has been developed to compute water hammer transients in pump-discharge lines (forcemains), resulting from power failure at the pumps. The program incorporates various boundary conditions as subroutines. Hence the pump(s) can be placed anywhere in the pipeline, with or without discharge valves (or check valves), and the program can accept a large number of surge-control devices, similarly placed anywhere in the pipeline. Such devices include valves, check valves, surge tanks, one-way surge tanks, and pressure vessels.

An explicit finite-difference scheme employing the method of characteristics is used throughout. It proved to be accurate and stable. The program is written in a dimensionless and general form.

Several checks were made to prove the validity of the computer model. Comparisons with field observations, graphical analysis, and/or water hammer design charts were made, depending on the data available in the literature for each boundary condition. An exhaustive search through the literature was made. Computer plots are developed which proved valuable in presenting the results.

The computer model was applied to the water hammer problem in the Ancaster forcemain, and a "best" protective device is suggested.

ACKNOWLEDGEMENTS

I wish to express my sincere appreciation to Dr. W. Jamés for his invaluable guidance and encouragement in carrying out this study.

I would also like to acknowledge with thanks the helpful suggestions by Dr. J. Ransford, of FENCO in Toronto.

I am also grateful to Mr. J. W. Disher and Mr. C. Cordahi, of C. C. Parker and Assocs., for providing the opportunity to test the Ancaster forcemain and pumps.

Thanks are also due to Miss Erie Long for typing this thesis.

This investigation was made possible through grants to Dr. James provided by the Science and Engineering Research Board of the McMaster University, to whom I extend my sincere thanks.

TABLE OF CONTENTS

CHAPTER		PAGE
1	INTRODUCTION	
	1.1 History of Water Hammer	1
	1.1.1 Early Studies Up to the 19th Century	1
	1.1.2 Development in the 19th Century	2
	1.1.3 Development in the 20th Century	4
	1.2 Recent Studies	6
	1.3 Scope of the Study	10
2	THEORY OF WATER HAMMER	
	2.1 Basic Equations	16
	2.2 Normalization	18
	2.3 Method of Characteristics Solution	21
	2.4 Solution Plane	23
	2.5 Stability	24
	2.6 Solution For Interior Points	25
	2.7 Some Simple Boundary Conditions	26
	2.7.1 Reservoir at the Upstream End	29
	2.7.2 Reservoir at the Downstream End	30
	2.7.3 Valve at the Upstream End	31
	2.7.4 Valve at the Downstream End	32

TABLE OF CONTENTS - continued

CHAPTER		PAGE
3	WATER HAMMER IN PUMP DISCHARGE LINES	
	3.1 Effect of Power Failure	35
	3.2 Pump Characteristics	36
	3.3 Pump Inertia	40
	3.4 Pump Analysis	42
	3.4.1 Pump Connected to a Reservoir	42
	3.4.1.1 Single Pump Without Discharge Valve	42
	3.4.1.2 Pump With a Discharge Valve	46
	3.4.1.3 Identical Pumps in Parallel	50
	3.4.2 Pump In-Line	51
	3.4.2.1 Pump In-Line Without Discharge Valve	52
	3.4.2.2 Pump In-Line With Discharge Valve	54
	3.5 Pipeline Protection Against Water Hammer	56
	3.5.1 Valve In-Line	57
	3.5.2 Surge Tanks	59
	3.5.3 One-Way Surge Tanks or Discharge Tanks	63
	3.5.4 Air Chamber or Pressure Vessel	66
4	DEVELOPMENT OF THE COMPUTER MODEL	
	4.1 Representation of the Pipeline Profile	72
	4.2 General Method	74
	4.3 The Pump	77

TABLE OF CONTENTS - continued

CHAPTER		PAGE
5	VALIDATION OF THE COMPUTER MODEL	
	5.1 Water Hammer Due to Valve Operation	80
	5.1.1 Valve Operation at the Downstream End of a Pipe	80
	5.1.1.1 Sudden Valve Closure	81
	5.1.1.2 Gradual Valve Closure	81
	5.1.2 Valve Operation at the Upstream end of a Pipe	87
	5.1.3 Surge Tank Near the Downstream Valve	87
	5.2 Water Hammer Due to Pump Shut-Down	94
	5.2.1 Pumps Without Any Discharge or Check Valves, Connected Directly to the Suction Reservoir	94
	5.2.2 Pumps With Butterfly Valves Connected Directly to the Suction Reservoir	98
	5.2.3 Pumps Connected to Both Suction and Delivery Pipes	103
	5.2.4 Effect of Valve Operation at the Pump	108
	5.2.5 Effect of the Inertia of Rotating Elements	110
	5.2.6 Effect of Friction on Water Hammer Pressures	110
6	THE ANCASTER PUMP STATION AND FORCEMAIN	
	6.1 Introduction	118
	6.2 Protection of the Pipeline	124
	6.2.1 Increasing Inertia	124
	6.2.2 Surge Tanks	124
	6.2.3 One-Way Surge Tanks	130
	6.2.4 Air Vessel	133

TABLE OF CONTENTS - continued

CHAPTER		PAGE
6	6.2.5 Air Vents	137
	6.3 Conclusion	137
7	CONCLUSIONS	138
	BIBLIOGRAPHY	140
	NOTATION	146
APPENDICES		
A	PUMP CHARACTERISTICS	150
B	LISTING OF COMPUTER PROGRAM	158

LIST OF FIGURES

FIGURE		PAGE
2.1	Free-Body Diagram for Derivation of the Water Hammer Equations	15
2.2	Rectangular Grid for Solution of Characteristics Equations	23
2.3	Diagrammatic Sketch of a Pipeline Connecting Two Reservoirs with Valves Near the Reservoirs	26
3.1	Transient Conditions Following Power Failure at Pump Motor	37
3.2	Diagrammatic Sketch of a Pump-Discharge Line with the Pump(s) Connected to the Suction Reservoir	43
3.3	Diagrammatic Sketch of a Pump-Discharge Line with the Pump(s) Connected to Suction and Delivery Pipes	51
3.4	In-Line Valve	57
3.5	Schematic for Simple Surge Tank	61
3.6	Schematic for One-Way Surge Tank	64
3.7	Schematic for Pressure Vessel	67
4.1	Flow Chart	73
4.2	A Hypothetical Pipeline to Illustrate The General Method	75
5.1	Pressure Distribution Along Pipe Due to Sudden Valve Closure	82
5.2	Maximum and Minimum Pressures Along the Pipe Due to Gradual Valve Closure at the Downstream End	83
5.3	Pressure Transients Due to Gradual Valve Closure - Comparison with an Analytical Solution	84
5.4	Valve Closure Time Relationship	85

LIST OF FIGURES - continued

FIGURE		PAGE
5.5	Effect of Friction on the Pressure Transients Due to Gradual Valve Closure at the Downstream End of a Pipe	86
5.6	Maximum and Minimum Pressures Along the Pipe Due to Gradual Valve Closure at the Upstream End	88
5.7	Pressure Transients Due to Gradual Valve Closure at the Upstream End of a Pipe	89
5.8	Effect of Surge Tank on Reducing the Transient Pressures Along the Pipeline	91
5.9	Surge Levels in a Simple Surge Tank	92
5.10	Surge Levels in a Simple Surge Tank; With Pipe Friction Neglected	93
5.11	Transient Pressure Gradients Due to Power Failure at Pump Motors	95
5.12	Transient Conditions Due to Power Failure - Comparison Between Graphical Analysis and Computer Results	97
5.13	The Tracy Pumping Plant - Butterfly Valve Closure Relation	100
5.14	The Tracy Pumping Plant - Transient Conditions Due to Power Failure - Comparison Between Field Tests and Computer Results	101
5.15	The Tracy Pumping Plant - Transient Conditions Due to Power Failure - Comparison Between Graphical Analysis and Computer Results	102
5.16	The Granby Pumping Plant - Transient Conditions Due to Power Failure	105
5.17	The Granby Pumping Plant - Transient Pressure Gradients Due to Power Failure	106
5.18	Effect of Valve Operation at the Pump on the Pressure Transients	109
5.19	Effect of Pump and Motor Inertia on the Pressure Transients - No Valves at the Pump	111

LIST OF FIGURES - continued

FIGURE		PAGE
5.20	Effect of Pump and Motor Inertia on the Pressure Transients - Check Valve at the Pump	112
5.21	Effect of Pump and Motor Inertia on the Transient Pressure Gradients - No Valves at the Pump	113
5.22	Effect of Pump and Motor Inertia on the Transient Pressure Gradients - Check Valve at the Pump	114
5.23	Transient Conditions Due to Power Failure - Case of High Friction Losses	116
5.24	Transient Pressure Gradients Due to Power Failure - Case of High Friction Losses	117
6.1	The Ancaster Forcemain - Operating Heads	119
6.2	The Ancaster Forcemain - Transient Heads and Velocities Along the Pipeline for One-Pump Operation	121
6.3	The Ancaster Forcemain - Transient Heads and Velocities Along the Pipeline for One-Pump Operation (New Impellor)	122
6.4	The Ancaster Forcemain - Transient Heads and Velocities Along the Pipeline for Two-Pump Operation	123
6.5	The Ancaster Forcemain - Transient Conditions Due to Power Failure for $WR^2 = 400.0 \text{ lb.ft}^2$; for One-Pump Operation	125
6.6	The Ancaster Forcemain - Transient Conditions Due to Power Failure for $WR^2 = 400.0 \text{ lb.ft}^2$; for Two-Pump Operation	126
6.7	The Ancaster Forcemain - Transient Pressure Gradients for $WR^2 = 400.0 \text{ lb.ft}^2$	127
6.8	The Ancaster Forcemain - Effect of Surge Tank on the Transient Pressure Gradients: Ultimate Design Conditions	128
6.9	The Ancaster Forcemain - Surge Levels in Surge Tank	129
6.10	The Ancaster Forcemain - Effect of One-Way Surge Tank on the Transient Pressure Gradients: One-Pump Operation	131
6.11	The Ancaster Forcemain - Transient Conditions Due to Power Failure; With a One-Way Surge Tank	132

LIST OF FIGURES - continued

FIGURE		PAGE
6.12	The Ancaster Forcemain - Effect of Pressure Vessel on the Transient Pressure Gradients	134
6.13	The Ancaster Forcemain - Pressure Variations at the Air Vessel	135
6.14	The Ancaster Forcemain - Pressure Variations at the Midlength of Discharge Line; With the Air Vessel Installed	136
A.1	Dimensionless-Homologous Torque Data for Centrifugal Pumps - $N_s = 1800$ (gpm units)	150
A.2	Dimensionless-Homologous Head Data for Centrifugal Pumps - $N_s = 1800$ (gpm units)	150
A.3	Dimensionless-Homologous Torque Data for Mixed Flow Pumps - $N_s = 7600$ (gpm units)	151
A.4	Dimensionless-Homologous Head Data for Mixed Flow Pumps - $N_s = 7600$ (gpm units)	152
A.5	Dimensionless-Homologous Torque Data for Axial Flow Pumps - $N_s = 13500$ (gpm units)	153
A.6	Dimensionless-Homologous Head Data for Axial Flow Pumps - $N_s = 13500$ (gpm units)	154

LIST OF TABLES

TABLE		PAGE
5.1	Comparison with Parmakian's Graphical Analysis and Kinno's Charts	98
5.2	The Granby Pumping Plant - Transient Conditions Due to Power Failure - Comparison Between Computer Results and (a) Field Tests; (b) Water Hammer Charts	107
A.1	Dimensionless-Homologous Torque and Head Data for Centrifugal Pumps - $N_s = 1800$ (gpm units)	155
A.2	Dimensionless-Homologous Torque and Head Data for Mixed Flow Pumps - $N_s = 7600$ (gpm units)	156
A.3	Dimensionless-Homologous Torque and Head Data for Axial Flow Pumps - $N_s = 13500$ (gpm units)	157

1. INTRODUCTION

Water hammer occurs in a closed conduit flowing full whenever the flow is retarded or accelerated. Rapid pressure changes occur and travel back and forth along the pipe at the speed of sound. This phenomenon governs the design of most pump-pipelines or forcemains.

1.1 History of Water Hammer

This historical review has been distilled from a comprehensive report by F. M. Wood⁽¹⁾, who traced the development of water hammer from the seventeenth century to the middle of the twentieth century. The references cited in this present review (all of Section 1.1) are listed separately within the bibliography at the end of this thesis. Further reference should also be made to Wood's report.

1.1.1 Early Studies Up to the 19th Century. Euler in 1775 was the first to deal with the subject of water hammer⁽²⁾, in an investigation of blood flow in arteries. At this time, mathematicians were interested in other similar fields, such as the propagation of waves on shallow water and the propagation of sound waves in air. These studies, although no detailed solution was obtained until the development of calculus and the solution of partial differential equations, became the basis for the development of water hammer theory. Among the mathematicians that should be mentioned

are René Descartes (1596-1650), B. Cavalieri (1598-1647), Isaac Barrow (1630-1677), Isaac Newton (1642-1727) who had invented the calculus through his theory of fluxions and his study of the propagation of sound waves in air⁽³⁾ and water waves in canals, Wilhelm Leibniz (1646-1716), Jean L. Bernoulli (1667-1748), Brooks Taylor (1685-1731) who had derived his series in 1712, one of the fundamental theorems; and Leonhard Euler (1707-1783) who developed a detailed theory of sound wave propagation in air⁽⁴⁾. He developed and solved the partial differential equation for wave propagation and discussed the significance of the functions F and f which represent waves travelling up and down the pipe with the velocity of propagation a . Joseph L. Lagrange (1736-1813) obtained solutions for the movement of compressible and incompressible fluids⁽⁵⁾. Gaspard Monge in 1789 developed a graphical integration of partial differential equations⁽⁶⁾ and used the method of characteristics. Pierre S. Laplace (1749-1827) developed the Laplace equation, the criterion of equilibrium of homogeneous fluids⁽⁷⁾.

1.1.2 Development in the 19th Century. In the first half of the 19th century, there had been much experimental work on air and water surges in pipes. Herman von Helmholtz (1821-1894) was the first in 1848 to discuss the effect of elasticity of pipe walls on the velocity of wave propagation in a water pipe. Werthein⁽⁸⁾ gave the same explanation in 1848. In 1860, B. Riemann⁽⁹⁾ developed the equation of motion in its general three dimensional form and used its simplified one dimensional form in the problem of sound wave propagation. In 1850, Wilhelm Weber⁽¹⁰⁾ conducted experiments to measure the velocity of propagation. He studied

the case of an incompressible fluid in an elastic pipe⁽¹¹⁾. He was the first to develop the two first order equations, the continuity and the dynamic equation, which are the basis for our theoretical studies in water hammer. Other experimenters that should be mentioned are Wertheim⁽⁸⁾ in 1848, Kundt⁽¹²⁾ and Dvorak⁽¹³⁾ in 1875. In 1875, Dr. Marey published the results of his experiments on the propagation of water waves⁽¹⁴⁾ and reached the conclusion that the reflected wave has the same velocity as the propagated wave. In 1876, H. Resal⁽¹⁵⁾ published his development of the second order wave equations assuming an incompressible fluid and elastic pipe. He obtained the same results as Weber. In 1878, D. J. Korteweg⁽¹⁶⁾ was the first to consider the elasticity of both the pipe wall and the fluid; however, he was interested only in the velocity of propagation and not with the transient pressure velocity relationship. In 1878, Jules Michaud⁽¹⁷⁾ made extensive studies into the design and use of air chambers and safety valves in pipelines to reduce the effect of sudden and gradual closure of gates and valves. In 1883, V. I. Gromeka⁽¹⁸⁾ seems to be the first to have considered the effect of friction.

During the years 1885 to 1899 experiments had been made by several engineers in the United States. Some engineers used air chambers, and some tried to develop a theoretical relationship between the velocity reduction and pressure increase. The most notable of these engineers were E. B. Weston⁽¹⁹⁾ in 1885, I. P. Church^(20,21) in 1890 and 1898, and R. C. Carpenter⁽²²⁾ in 1893, but there was little success. In 1897, J. P. Frizell⁽²³⁾ presented an analytical solution for the velocity and pressure surges due to water hammer. He also considered the case of branched pipelines and wave reflection and discussed cases of slow

closure. At the same time in 1897, N. Joukowski⁽²⁴⁾ in Moscow ran extensive experiments on the relationship between the velocity and pressure changes. He also derived his own theory of water hammer and compared the theoretical results with his experiments. He considered the elasticity of both the pipe and the fluid. In 1902, L. Allievi⁽²⁵⁾ published his general water hammer theory. His theory is similar to that of Korteweg, but more accurate for the acceleration terms. Allievi's work covers the whole field of operation including gradual gate closure and he derived general charts and tables.

1.1.3 Development in the 20th Century. Water hammer studies have become more specialized and the methods more accurate. During the first twenty years of the 20th century much work was done by engineers in Europe and North America applying the theories developed by Allievi and Joukowski. The main object was the application to practical design of water works and hydro-electric plants. In 1915, M. M. Warren⁽²⁶⁾ published a paper on penstock and surge tank problems. In 1920, G. Constantinescu⁽²⁷⁾ presented his invention of a mechanism to transmit mechanical energy by the use of water hammer waves. In the same year, N. R. Gibson presented a paper⁽²⁸⁾ on pressure surges due to gradual closure and he derived a reasonably applicable relation between the discharge and the pressure loss through a partially closed gate. He also used a coefficient that can be used for any non-uniform closure. In 1926, Strowger and Kerr presented an important paper⁽²⁹⁾ on the speed regulation of hydraulic turbines. They used the method given by Gibson⁽²⁸⁾ for computing velocities and pressure changes due to both uniform and non-uniform gate movement. In

1928, R. L'wy published his text on water hammer⁽³⁰⁾ in which he presented the solution of surges in a pipeline using the step-by-step method. Since that time, engineers started to study the pipeline as an integral part connected with various elements, such as pumps, turbines, relief valves, air chambers, and surge tanks. They also obtained the solution for compound pipes and considered friction and low moduli of elasticity. In 1929, O. Schnyder⁽³¹⁾ used the graphical method in the case of pipelines connected to centrifugal pumps. In 1931, Louis Bergeron⁽³²⁾ applied the graphical method and managed to obtain an analytical relationship between velocities and pressures at any two points on the pipeline. In 1932, Schnyder⁽³³⁾ introduced the effect of friction to the graphical solution. At the 1933 Symposium of the ASME and ASCE at Chicago⁽³⁴⁾, engineers from North and South America presented many papers on high-head penstocks, compound pipes, surge tanks and centrifugal pump installations equipped with relief valves and air chambers. In 1935, R. W. Angus⁽³⁵⁾ presented a paper on the graphical method and used lumped friction. In 1937, the second water hammer symposium of the ASME, ASCE, and AWWA was held in New York in which many papers were presented by engineers from America and Europe, including Allievi⁽³⁶⁾, Angus⁽³⁷⁾, K. J. De Juhasz⁽³⁸⁾, F. Knapp⁽³⁹⁾, R. T. Knapp⁽⁴⁰⁾, Schnyder⁽⁴¹⁾, Strowger⁽⁴²⁾ and F. M. Wood⁽⁴³⁾. In 1938, Angus⁽⁴⁴⁾ studied water column separation. In 1953, H. R. Lupton⁽⁴⁵⁾ studied surges in pump discharge lines and separation of water columns. In the 1955 symposium of the ASME, ASCE and AWWA at Chicago, many papers were presented. R. T. Richards⁽⁴⁶⁾ presented a paper dealing with pump discharge lines with particular regard to water column separation, and C. P. Kittredge⁽⁴⁷⁾ compared the solution for rigid

and elastic column theories.

1.2 Recent Studies

In the middle of the twentieth century the electronic computer was brought into use and this has proved extremely valuable in the treatment of water hammer problems. The use of coarse approximations became no longer necessary, e.g. for the non-linear terms in water hammer equations. However, the graphical method has also been used extensively by many engineers. Since this time, the main thrust was the use of different boundary conditions and various hydraulic devices such as pumps, turbines, surge tanks, discharge tanks, valves, air chambers, etc.

In 1953, John Parmakian⁽⁴⁸⁾ studied pressure surges in pump discharge lines, due to power failure, graphically. He used complete pump characteristics for that purpose and obtained a time history of pump speed, pump discharge, and head at pump and midlength of discharge line covering three zones of operation; namely, normal pump, energy dissipation, and turbine operation zones. He also presented charts^(48,49) showing maximum and minimum surge heads at the pump and midlength of discharge pipe. These charts also yield the maximum reverse speed of the pump, time of flow reversal at the pump, time of zero pump speed, and time of maximum reverse pump speed. The charts were derived for pipelines having no discharge valves and where friction can be neglected. In 1958, Parmakian⁽⁵⁰⁾ used a similar analysis for pump discharge lines with one-way surge tank and concluded that one-way surge tanks offer an

effective method for eliminating the harmful effects of water column separation at high points in pump discharge lines subsequent to pump stoppage.

In 1961, B. Donsky⁽⁵¹⁾ managed to use the test data collected by Professor Hollander of the California Institute of Technology, for three pumps of different specific speeds, to develop complete pump characteristics curves covering all normal and abnormal operating conditions. These data were valuable in the transients calculations for water hammer in pump discharge lines resulting from pump stoppage.

In 1953, W. E. Evans and C. C. Crawford⁽⁵²⁾ derived a set of data in chart form from which the size of an air chamber can be determined quickly for preliminary design purposes. In the preparation of the charts it was assumed that a check valve is placed on the discharge side of the pump. This check valve closes immediately on power failure so that the pump characteristics can be eliminated from the calculations. It was also assumed that the air chamber is situated near the pump. In addition it was assumed that the pressure-volume relationship for the air in the chamber is expressed by

$$h*V^{1.2} = \text{constant}$$

where h^* is the absolute head in the chamber and V is the air volume. The static head difference between the water surface in the air chamber and the center line of the pipe below the chamber was neglected. They noted that the downsurge in the pipeline can be reduced effectively if the outward flow is kept as free as possible while the inflow to the

chamber is restricted. They recommend that a special orifice be used for that purpose and presented test results for that orifice. The friction head loss was assumed to be concentrated at the orifice. The charts represent the maximum upsurges and downsurges as a percentage of the absolute pumping head, as a function of the air volume, wave celerity, length of discharge line and the steady state discharge.

In 1962, Streeter and Chintu Lai⁽⁵³⁾ published the first study in water hammer using high speed digital computers. The effect of friction was considered and the non-linear terms included. The method of characteristics was used for the solution. They applied their method to many different gate operations and pipe connections. The method proved to be accurate and dependable through experimental verification.

In 1963 Streeter⁽⁵⁴⁾ developed equations for the closure of a valve at the downstream end of a pipeline leading from a reservoir, so that the pressures remain above their steady state values at all times, without backflow and without separation of the fluid column. His study is theoretical and an actual valve which permits these improvements has yet to be developed.

In 1964, Streeter⁽⁵⁵⁾ developed a computer program for the treatment of pump failure using complete pump data linked with pipe characteristics. He also studied the operation of discharge valves to control the surge.

In 1965, Kinno and Kennedy⁽⁵⁶⁾ presented comprehensive charts which included the effect of line friction and pump efficiency. The charts can be used to predict the minimum and maximum transient heads at the pump and midlength of discharge line. They also can be used for

predicting the time of flow reversal. Their charts are applicable for pumps of specific speeds of less than approximately 2700 (rpm-gpm-ft); they are not applicable to systems in which there is valve closure during the transients or to systems that contain water hammer control devices other than a large surge tank. Kinno and Kennedy claimed that the upsurge could be reduced considerably if reverse flow through the pumps was permitted, but with reverse rotation prevented.

In 1972, D. Stephenson⁽⁵⁷⁾ presented a simplified method for design of one-way surge tanks (or discharge tanks) and presented charts and equations for rapid determination of tank size and the resulting maximum pressure. A computer program was used to prepare the charts. Friction was not accounted for in these charts, and the pump was assumed to stop instantaneously. The charts cover the cases of one discharge tank in the line with or without an in-line reflex valve, and that with two discharge tanks in the line.

In 1972, C. S. Martin⁽⁵⁸⁾ applied the elastic wave equation to surge tank calculations, using the method of characteristics. A comparison of his analytical results to field test measurements of surge tank oscillations proved to be excellent.

In 1972, Streeter⁽⁵⁹⁾ reviewed the methods of transient calculations for liquids in metal pipes, using both the explicit and implicit formulations. He presented a comparison between both methods. He concluded that the explicit method, utilizing the method of characteristics, is more accurate and unconditionally stable as long as $(\Delta t = \Delta x/a)$, where Δx and Δt are the length and time increments used for calculations and a is the celerity of the pressure wave. On the other

hand, he found that the implicit scheme became unstable, and yielded unsatisfactory results for very sudden, sharp transients. In addition, he discussed some boundary conditions using the characteristic method.

In 1974, T. J. Sheer⁽⁶⁰⁾ discussed the use of one-way surge tanks (discharge tanks), to protect a pipeline against severe water hammer effects. He concluded that a discharge tank in combination with in-line non-return valves could eliminate severe water hammer under any operating circumstances. His study was performed on a 23 Km long pipeline of an unfavourable profile where water column separation was expected.

1.3 Scope of the Study

In this present study, water hammer is investigated, with special consideration given to pump discharge lines. The theory of water hammer is discussed and the basic non-linear partial differential equations for water hammer are presented and transformed into a dimensionless form independent of the system of units that are to be used. Since the equations cannot be solved directly, they are solved explicitly by a finite difference method based on characteristics. The solution is carried out for successive time increments in an X-T plane using a rectangular grid, such that the nodes coincide with the characteristics grid. The solution for interior points is obtained explicitly. In order to continue the solution for successive time increments, we have to formulate equations for the conditions at the boundaries. A number of different boundary conditions are investigated and derived in dimensionless

form. We start with the simple boundary conditions presented by valves and reservoirs. Reservoirs are usually placed at either the upstream or downstream ends, but valves may be placed anywhere in the pipe.

Water hammer resulting from pump stoppage, due to either power failure or pump shut-down, is one of the most severe problems that may beset a pipeline. Water hammer due to pump stoppage is the prime objective of this study and is investigated in some detail. The effect of power failure on pump speed is investigated and an inertia equation, which governs the change of pump speed, is utilized. Complete pump characteristics are presented covering three zones of operation: normal pump, energy dissipation, and turbine operation zones. The data have been presented through dimensionless plots for head and torque as a function of pump discharge and pump speed. These data have also been presented in tabular form, which is more convenient for storage and interpolation by the computer. The data were obtained by Hollander at the California Institute of Technology, and were published by Donsky⁽⁵¹⁾ for three specific speeds, 1800, 7600, and 13500 (gpm units) which represent centrifugal pumps, mixed flow pumps, and axial flow pumps, respectively. The pump (or number of pumps in parallel) can be connected directly to the suction reservoir, or through a suction pipe. A discharge valve (or check valve) can be placed at the pump or it can be omitted. The equations for the pump failure, as a boundary condition, are derived in a dimensionless form.

Surge tanks, discharge tanks, and air vessels, which are all commonly used to protect pipelines against high pressures that may follow power failure at the pump motor, are treated similarly, and the equations

describing these devices are derived in a dimensionless form.

A general computer program is developed to solve the problems described above. The program is written in ANSI FORTRAN in as general a form as possible, and is capable of handling many pump discharge lines with the pump (or number of pumps in parallel) placed anywhere in the pipeline. The program can handle pumps with or without discharge valves. The valves can be closed at the instant of flow reversal (check valves) or gradually after power failure, in a prescribed manner. The program can handle any pipeline geometry with a very large number of certain surge control devices placed anywhere in the pipeline. This is of extreme value in choosing the most effective and economical surge control device (or combination of devices) for a certain pump discharge line, and their most effective locations. Designers usually avoid using surge control devices, if possible, as the devices are expensive and in many cases require costly maintenance. The computer program can check the water hammer effects on the basic pipeline (without surge control devices). If the results show that harmful water hammer effects will occur in the pipeline, then we have to find some protective device (or a combination of devices). This is where the program is useful: as it can handle several different methods of surge control simultaneously. A description of the computer model is presented, and a listing of the program is appended. The results can be printed out after each time step showing the head and discharge at all sections along the pipeline. Also, computer plots can be obtained describing the time-history of pump speed, pump discharge, and the head variations after pump stoppage. The plots give an accurate summary of heads and discharges throughout the pipeline.

To check the results obtained from the computer program, comparison with field observations is made whenever published data are pertinent. Comparison with the graphical method of solution is presented in some situations. Water hammer charts by Parmakian⁽⁴⁹⁾, Kinno and Kennedy⁽⁵⁶⁾, and those by Evans and Crawford⁽⁵²⁾ are also used to check the computer results whenever relevant.

We start by studying the water hammer effects caused by valve operation in a pipe connected to reservoirs at different elevations, or a pipe connected to a reservoir at one end while the other is open to the air (no pumps are operated in the pipe). The pressure variation along the pipeline due to valve operation, whether suddenly or gradually, is obtained and the results are shown to be generally valid.

Water hammer effects in a pipeline due to valve closure at the downstream end where a surge tank is situated close to the valve is next examined and the resulting surges compared with those obtained from charts⁽⁴⁹⁾. The oscillations of the water surface in the tank are obtained and plotted and the effect of friction on the damping of surge tank oscillations is studied too. Next, several cases of water hammer in pump discharge lines are resolved. The effects of valve operation at the pump, pump and motor inertia, and of pipe friction is covered.

In an application of the computer program, the water hammer effects in the Ancaster forcemain, a rising pipeline pumping raw sewage, is investigated. The pipeline has twice broken down. The pipeline profile, governed by the ground profile, is unfavourable and water column separation will occur unless special protective devices are installed. Various protection devices are discussed including increasing pump and

motor inertia, a surge tank, discharge tanks, and an air chamber. The advantages and disadvantages of each surge control device are discussed and certain measures suggested.

In summary, the scope of this work is the development of a general, efficient and design-oriented computer program, capable of incorporating a large number of varied pipeline and surge-control devices. The program is to be used to select an optional and surge-safe pumping system, and utilizes the latest data and formulations in the literature. A new solution method is thus required: a normalized formulation with boundary conditions handled by subroutine calls, and such subroutines using compatible normalized algorithms.

It is not the purpose of this study to repeat or extend specific research work in the development of wholly new processes or wholly new algorithms describing some aspect of water hammer, e.g., to refine a coefficient of discharge for the changing aperture of a particular valve.

2. THEORY OF WATER HAMMER

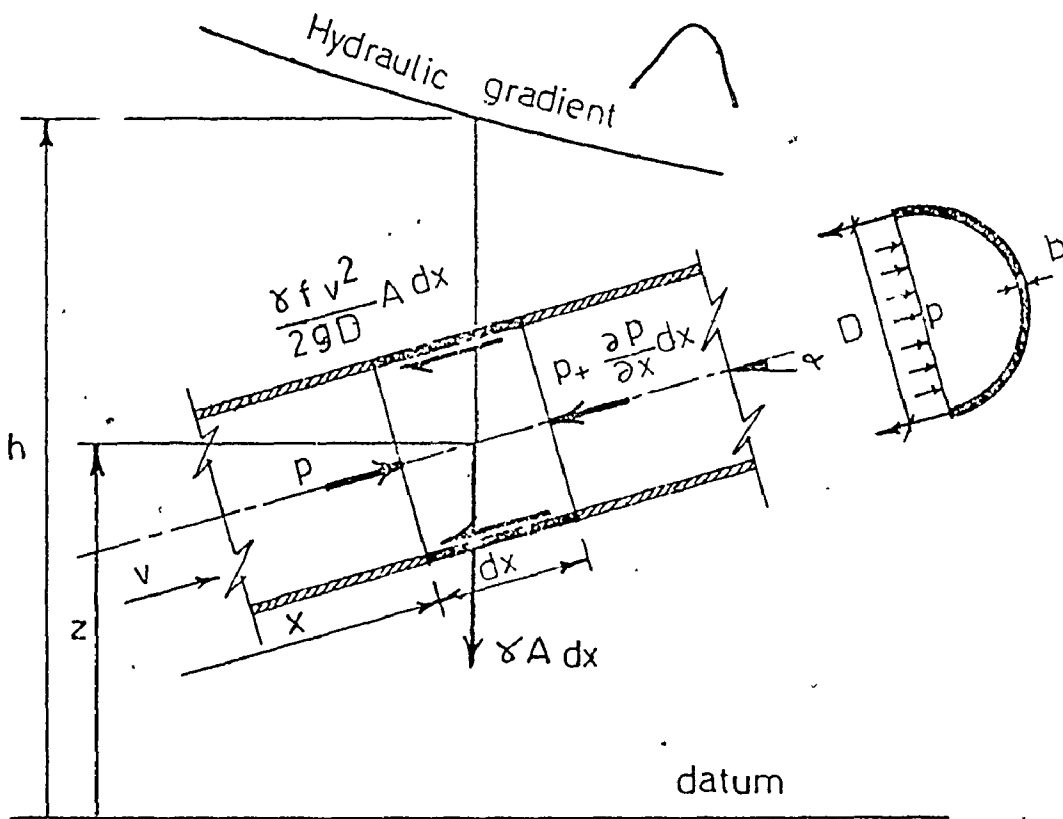


FIG. 2.1: FREE-BODY DIAGRAM FOR DERIVATION OF THE WATER HAMMER EQUATIONS

2.1 Basic Equations

In order to derive the basic partial differential equations for water hammer, consider a section of the pipe bounded by two parallel planes perpendicular to the centerline of the pipe, the distance between the two planes is dx . The forces acting on the element are shown in Fig. 2.1. There are two independent variables in the problem, namely, the distance (x) measured along the pipeline and the time (t). The dependent variables are the pressure head (h) measured from an arbitrary reference datum, and the discharge per unit cross sectional area (q) at the same section.

Using the principle of the conservation of energy (dynamic equilibrium) and the principle of the conservation of mass (the continuity equation), we can easily obtain the basic partial differential equations for water hammer. The discussion is available in many references^(50,61,62).

The basic water hammer equations are:

1. Equation of Motion:

$$\frac{\partial h}{\partial x} + \frac{1}{gA} \frac{\partial q}{\partial t} + \frac{f}{2gDA} q^2 = 0 \quad (2.1)$$

2. Equation of Continuity:

$$\frac{a^2}{gA} \frac{\partial q}{\partial x} + \frac{\partial h}{\partial t} = 0 \quad (2.2)$$

where: A = cross sectional area of pipe;

D = diameter of pipe;

f = Darcy-Weisbach friction factor;

g = acceleration due to gravity;

q = the discharge; and

a = celerity of pressure wave.

The celerity of pressure wave, a , is given by:

$$a = \frac{1}{\sqrt{\frac{\gamma}{g} \left(\frac{1}{K} + \frac{Dc_1}{Eb} \right)}} \quad (2.3)$$

where: b = pipe wall thickness;

c_1 = pipe rigidity, or a factor of pipe restriction;

E = modulus of elasticity of pipe wall material;

K = bulk modulus of elasticity of the liquid; and

γ = specific weight of fluid.

The pipe rigidity, c_1 , can take the following values⁽⁴⁹⁾:

a) For a pipe anchored at the upper end and without expansion joints:

$$c_1 = \frac{5}{4} - \mu \quad (2.4a)$$

where: μ = poisson's ratio for the pipe wall material.

b) For a pipe anchored against longitudinal movement throughout its length:

$$c_1 = 1 - \mu^2 \quad (2.4b)$$

c) For a pipe with expansion joints:

$$c_1 = 1 - \frac{\mu}{2} \quad (2.4c)$$

In the derivation of the water hammer equations (2.1) and (2.2), it is assumed that the unit discharge (or velocity) and pressure are uniform over a transverse cross section of the pipe and that the pipeline remains full of water at all times. It is assumed also that the pressure in the pipe always exceeds the vapour pressure of the flowing fluid. If, at any time, the pressure in the pipeline drops to vapour pressure, the above equations are no longer valid, and a special boundary condition should be applied at that section.

Now, having obtained the partial differential equations for water hammer (Eqs. (2.1) and (2.2)), we have to solve them in order to obtain the unit discharge (or velocity) and pressure at any cross section at any time. The equations are non-linear partial differential equations which cannot be solved directly. They can be solved explicitly by a finite difference method based on characteristics. However, before solving the equations, it is advantageous to render them dimensionless.

2.2 Normalization

We can write Eqs. (2.1) and (2.2) in the form:

$$\frac{\partial H}{\partial X} + \frac{\partial Q}{\partial T} + Q^2 = 0 \quad (2.5)$$

and

$$\frac{\partial Q}{\partial X} + \frac{\partial H}{\partial T} = 0 \quad (2.6)$$

where: $H = \eta h$ dimensionless head (2.7a)

$$X = \theta x \quad \text{dimensionless length} \quad (2.7b)$$

$$Q = \phi q \quad \text{dimensionless discharge} \quad (2.7c)$$

$$T = \psi t \quad \text{dimensionless time} \quad (2.7d)$$

Now, we have to solve for the values of η , θ , ϕ , and ψ which convert Eqs. (2.1) and (2.2) into the dimensionless forms given by Eqs. (2.5) and (2.6).

Equation (2.5) can be rewritten:

$$\frac{\partial h}{\partial x} + \frac{\theta}{\eta} \frac{\phi}{\psi} \frac{\partial q}{\partial t} + \frac{\phi^2 \theta}{\eta} q^2 = 0 \quad (2.8)$$

Comparing Eq. (2.8) with Eq. (2.1)

$$\frac{1}{gA} = \frac{\theta \phi}{\eta \psi} \quad (2.9)$$

and

$$\frac{f}{2gDA^2} = \frac{\phi^2 \theta}{\eta} \quad (2.10)$$

Also, Eq. (2.6) can be rewritten:

$$\frac{\partial h}{\partial t} + \frac{\psi \phi}{\eta \theta} \frac{\partial q}{\partial x} = 0 \quad (2.11)$$

Comparing Eq. (2.11) with Eq. (2.2)

$$\frac{a^2}{gA} = \frac{\psi \phi}{\eta \theta} \quad (2.12)$$

Equations (2.10), (2.11), and (2.12) are three equations in four unknowns η , θ , ϕ , and ψ .

If we chose $\phi = \frac{1}{Q_0}$, then dividing Eq. (2.9) by Eq. (2.10)

$$\psi = \frac{fv_0^2}{2gD} \frac{a}{(av_0/g)}$$

Multiplying Eq. (2.9) by Eq. (2.12)

$$\eta = \frac{1}{(av_0/g)}$$

Substituting back in either Eqs. (2.9), (2.10), or (2.12)

$$\theta = \frac{fv_0^2}{2gD} \frac{1}{(av_0/g)}$$

If we substitute: $f' = \frac{fv_0^2}{2gD}$ (2.13)

then:

$$H = \frac{h}{(av_0/g)} \quad (2.14)$$

$$X = \frac{f'x}{(av_0/g)} \quad (2.15)$$

$$Q = \frac{q}{q_0} \quad (2.16)$$

$$T = \frac{f'at}{(av_0/g)} \quad (2.17)$$

v_0 and q_0 are the steady state velocity and discharge, respectively.

2.3 Method of Characteristics Solution

Equations (2.5) and (2.6) can be transformed into total derivative equations^(53,61) as follows:

Multiply Eq. (2.5) by λ and add to Eq. (2.6). After rearrangement:

$$\left[\frac{\partial H}{\partial X} \lambda + \frac{\partial H}{\partial T} \right] + \lambda \left[\frac{\partial Q}{\partial X} \frac{1}{\lambda} + \frac{\partial Q}{\partial T} \right] + \lambda Q^2 = 0 \quad (2.18)$$

H is a function of X and T, i.e. $H = H(X, T)$ and thus

$$\frac{dH}{dT} = \frac{\partial H}{\partial X} \frac{dX}{dT} + \frac{\partial H}{\partial T}$$

If we write:

$$\frac{dX}{dT} = \lambda \quad (2.19)$$

then the first term between brackets in Eq. (2.18) becomes the total derivative $\left(\frac{dH}{dT}\right)$. Q is also a function of X and T, i.e. $Q = Q(X, T)$ and thus

$$\frac{dQ}{dT} = \frac{\partial Q}{\partial X} \frac{dX}{dT} + \frac{\partial Q}{\partial T}$$

If we write

$$\frac{dX}{dT} = \frac{1}{\lambda} \quad (2.20)$$

then, the second term between brackets in Eq. (2.18) becomes the total derivative $\frac{dQ}{dT}$. Comparing Eqs. (2.19) and (2.20)

$$\lambda = \pm 1 \quad . \quad (2.21)$$

Thus, two values of λ , namely, +1 and -1 can convert the two partial differential equations (2.5) and (2.6) into a pair of total derivative equations. These equations are restricted by both Eqs. (2.19) and (2.20). In other words, if we take $\lambda = +1$, and substitute into Eq. (2.18), we get

$$\frac{dH}{dT} + \frac{dQ}{dT} + Q^2 = 0 \quad . \quad (2.22)$$

This equation is applied only along the line

$$\frac{dX}{dT} = +1 \quad . \quad (2.22a)$$

Similarly, using $\lambda = -1$, we get

$$\frac{dH}{dT} - \frac{dQ}{dT} - Q^2 = 0 \quad (2.23)$$

and this equation is applied only along the line

$$\frac{dX}{dT} = -1 \quad . \quad (2.23a)$$

Equations (2.22) and (2.22a) are called the C^+ characteristics equations while Eqs. (2.23) and (2.23a) are called the C^- characteristics equations.

2.4 Solution Plane

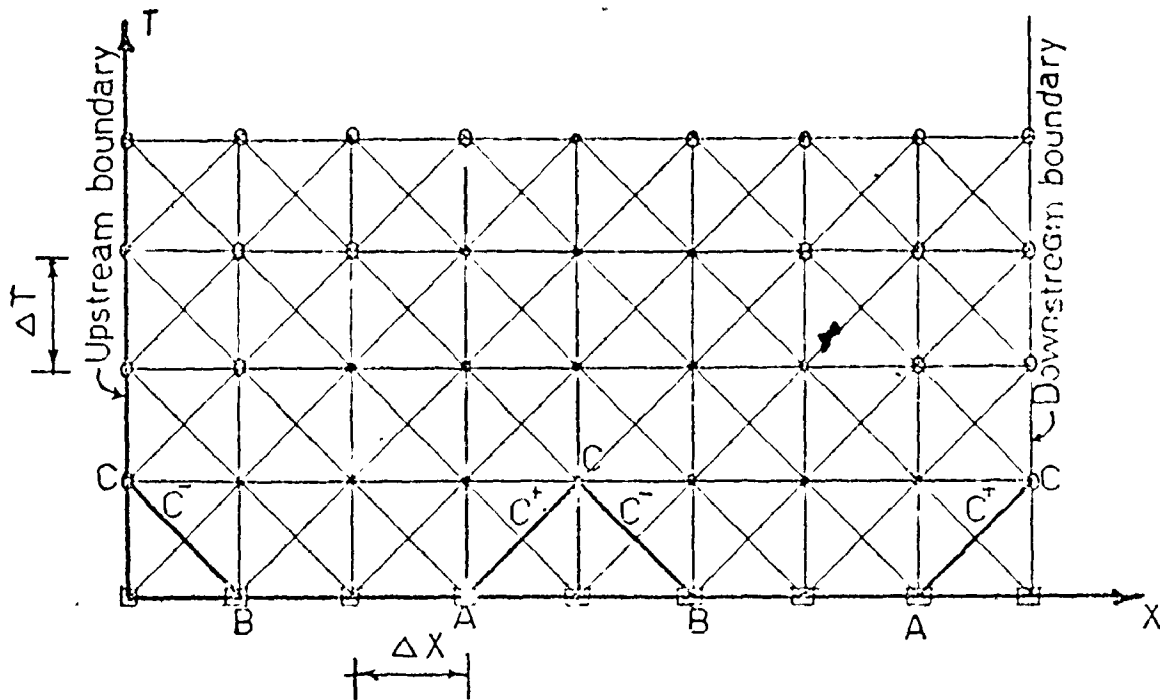


FIG. 2.2: RECTANGULAR GRID FOR SOLUTION OF CHARACTERISTICS EQUATIONS

The solution can be carried out in the X-T plane using the rectangular grid shown in Fig. 2.2. The pipeline is divided into a number of sections N , each ΔX in dimensionless length. The dimensionless time step for the calculation is ΔT , where:

$$\Delta T = \Delta X .$$

Both Eqs. (2.22) and (2.23) contain two unknowns, H and Q . Equation (2.22) is applied only along the C^+ characteristic line (line AC) while Eq. (2.23) is applied only along the C^- characteristic line (line BC). At the intersections of the two characteristics lines both equations are valid. If we know the head and discharge at points A and B, the values at point C can be obtained by solving Eqs. (2.22) and (2.23) simultaneously. At the boundaries, we have only one characteristic line, either C^+ line at the downstream boundary or C^- line at the upstream boundary. Thus, in order to get the solution at the boundaries we must specify one more equation at each boundary, relating H and Q . Referring to Fig. 2.2, if the heads and velocities are known at all sections, we can find their values after time ΔT . If the boundary conditions are known, we continue the solution increasing the time in steps of ΔT .

2.5 Stability

The characteristics method has been proved to be unconditionally stable⁽⁵⁹⁾ as long as

$$\Delta t = \Delta x/a \quad (2.24)$$

or, in the dimensionless form

$$\Delta X = \Delta T \quad (2.25)$$

2.6 Solution For Interior Points

Equation (2.22) can be written:

$$\Delta H + \Delta Q + Q^2 \Delta T = 0 \quad .$$

This equation applies only along the C^+ characteristics line between A and C. In finite difference form:

$$(H_C - H_A) + (Q_C - Q_A) + Q_A |Q_A| \Delta T = 0 \quad . \quad (2.26)$$

We replace Q_A^2 by $Q_A |Q_A|$ to account for negative flow.

Similarly, Eq. (2.23) can be written:

$$\Delta H - \Delta Q - Q^2 \Delta T = 0 \quad .$$

This equation applies only along the C^- characteristics line between B and C. In finite difference form:

$$(H_C - H_B) - (Q_C - Q_B) - Q_B |Q_B| \Delta T = 0 \quad . \quad (2.27)$$

Equations (2.26) and (2.27) can be solved simultaneously for the head and velocity at point C. Adding the two equations:

$$H_C = 0.5[(H_A - H_B) + (Q_A - Q_B) - (Q_A |Q_A| - Q_B |Q_B|) \Delta T] \quad . \quad (2.28)$$

Subtracting the two equations:

$$Q_C = 0.5[(Q_A + Q_B) + (H_A - H_B) - (Q_A |Q_A| + Q_B |Q_B|) \Delta T] \quad (2.29)$$

2.7 Some Simple Boundary Conditions

Consider the simple case of a pipe connecting two reservoirs with difference in elevation shown in Fig. 2.3.

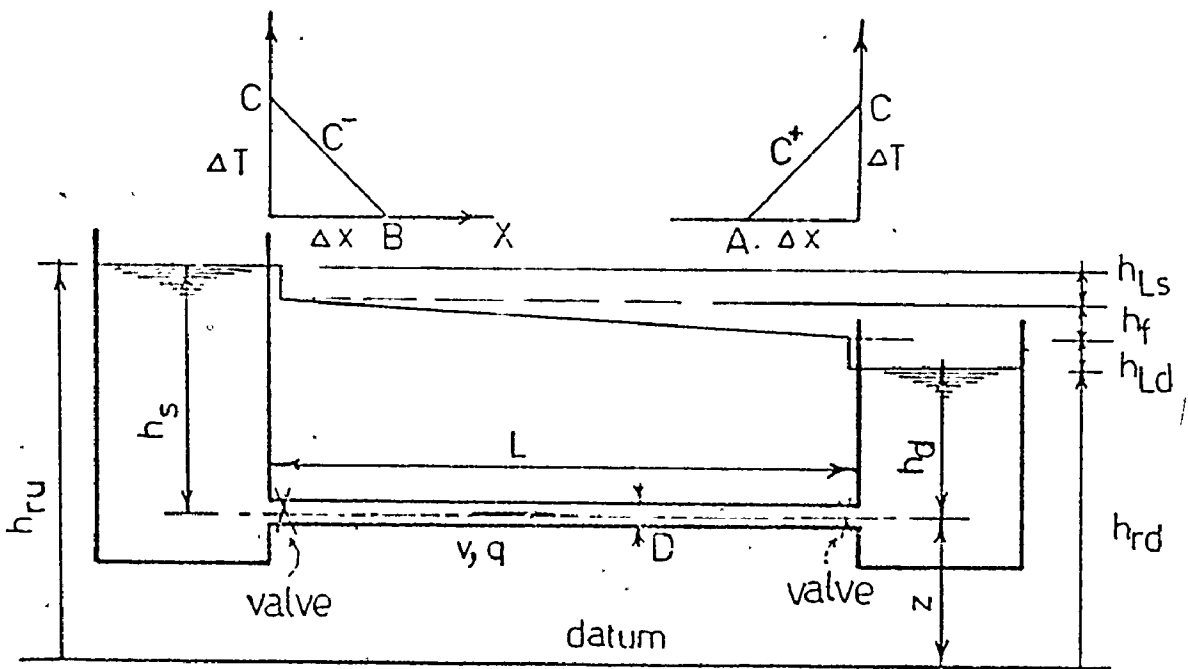


FIG. 2.3: DIAGRAMMATIC SKETCH OF A PIPELINE CONNECTING TWO RESERVOIRS WITH VALVES NEAR THE RESERVOIRS

The elevation of water in the upstream and downstream reservoirs is h_s and h_d respectively, measured from the pipe center line. In general, the water elevation in the upstream and downstream reservoirs is h_{ru} and h_{rd} , respectively, measured from an arbitrary datum, where

$$h_{ru} = h_s + z_u$$

$$h_{rd} = h_d + z_d$$

where z_u and z_d are the elevations of the pipe centerline at the upstream and downstream ends respectively, related to the same reference line. If the pipe outlet is open to the air, then h_d is set equal to zero.

A valve may be placed at either the upstream or the downstream end of the pipe. Valves may be closed instantaneously or gradually. In the case of closure of the downstream valve, a positive pressure wave is created which propagates upstream until it reaches the reservoir where it reflects forming a negative pressure wave.

In case of closure of the upstream valve, a negative pressure wave is created, which propagates downstream until it reaches the reservoir where it reflects forming a positive pressure wave.

If two valves are operated simultaneously at both the upstream and downstream ends, two pressure waves are created, one at the upstream which propagates downstream and the other at the downstream which propagates upstream. The resulting water hammer pressure is due to the combined effect of both waves. The three different cases which can be

considered are discussed as follows:

1. Reservoir at the upstream end, and a valve at the downstream end.
2. Valve at the upstream end, and a reservoir at the downstream end.
3. Valves at both the upstream and downstream ends.

In all the above three cases, the pipe outlet may be open to the air or connected to a reservoir.

Now, steady state dimensionless head loss across the downstream valve,

$$H_{Ld} = \frac{h_{Ld}}{(av_o/g)}$$

and steady state dimensionless head loss across the upstream valve,

$$H_{Ls} = \frac{h_{Ls}}{(av_o/g)}$$

Also, the dimensionless water surface elevations in the upstream and downstream reservoirs are,

$$H_{ru} = \frac{h_{ru}}{(av_o/g)}$$

and

$$H_{rd} = \frac{h_{rd}}{(av_o/g)}$$

respectively. The four different boundary conditions that need to be analysed are:

1. Reservoir at the upstream end.
2. Reservoir at the downstream end.

3. Valve at the upstream end.
4. Valve at the downstream end.

2.7.1 Reservoir at the Upstream End. The C^- characteristics (Eq. (2.27)) can be written:

$$H_C - Q_C - C_1 = 0 \quad (2.30)$$

where

$$C_1 = H_B - Q_B + Q_B |Q_B| \Delta T \quad (2.31)$$

Hence, if the discharge and pressure at B are known, then C_1 can be obtained.

At the reservoir, the head is fixed by the elevation of water.

In other words:

$$h_C = h_{ru} - \frac{v_C^2}{2g}$$

In order to transform this equation into a dimensionless form, divide by $\left(\frac{av_o}{g}\right)$:

$$H_C = H_{ru} - \frac{v_C^2}{2g} \frac{1}{(av_o/g)}$$

but we have $Q_C = \frac{q_C}{q_o} = \frac{v_C}{v_o}$

$$\therefore H_C = H_{ru} - \frac{v_o^2}{2g} \frac{1}{(av_o/g)} Q_C^2$$

Writing $\frac{v_o^2}{2g} \frac{1}{(av_o/g)} = \text{constant} = C_2$ (say), then

$$H_C = H_{ru} - C_2 Q_C^2 \quad (2.32)$$

Solving Eqs. (2.30) and (2.32) simultaneously, we get

$$Q_C^2 + \frac{1}{C_2} Q_C - \frac{H_{ru} - C_1}{C_2} = 0$$

or

$$Q_C = \frac{1}{2C_2} [-1 + \{1 + 4C_2(H_{ru} - C_1)\}^{0.5}] \quad (2.33)$$

Substituting back into Eq. (2.30), we get H_C . If the unit discharge (v) is small, then $\frac{v^2}{2g}$ can be neglected. In this case the head at the upstream is equal to the elevation of water in the reservoir:

$$H_C = H_{ru} \quad (2.34)$$

Q_C can be obtained by direct substitution into Eq. (2.30).

2.7.2 Reservoir at the Downstream End. The C^+ characteristics equation (2.26) can be written:

$$H_C + Q_C - C_3 = 0 \quad (2.35)$$

where

$$C_3 = H_A + Q_A - Q_A |Q_A| \Delta T \quad (2.36)$$

Hence, if the discharge and pressure at A are known, then C_3 can be

obtained.

At the downstream reservoir, we can obtain an equation similar to Eq. (2.32):

$$H_C = H_{rd} + C_2 Q_C^2 \quad (2.37)$$

Solving Eqs. (2.35) and (2.37) simultaneously, we get

$$Q_C^2 + \frac{1}{C_2} Q_C + \frac{H_{rd} - C_3}{C_2} = 0$$

or

$$Q_C = \frac{1}{2C_2} [-1 + \{1 - 4C_2(H_{rd} - C_3)\}^{0.5}] \quad (2.38)$$

Substituting back into Eq. (2.35), we can get H_C . If the velocity is small enough to neglect $\frac{v^2}{2g}$, we get

$$H_C = H_{rd} \quad (2.39)$$

Q_C can be obtained by direct substitution into Eq. (2.35).

2.7.3 Valve at the Upstream End. The steady state discharge through the valve considered as an orifice is given by

$$Q_o = (C_d A_v) \sqrt{2gh_{LS}} \quad (2.40)$$

At any instant, the discharge through the valve is given by

$$q_C = (C_d A_v)_t \sqrt{2g(h_{ru} - h_C)} \quad (2.41)$$

Dividing Eq. (2.41) by Eq. (2.40)

$$\frac{q_C}{q_o} = \frac{(C_d A_v)_t}{(C_d A_v)_o} \sqrt{\frac{h_{ru} - h_C}{h_{Ls}}}$$

or

$$Q_C = \tau_u \sqrt{\frac{H_{ru} - H_c}{H_{Ls}}} \quad (2.42)$$

where τ_u is a known function of time. Equation (2.42) can be written:

$$Q_C^2 = C_4 - C_5 H_C \quad (2.43)$$

where

$$C_4 = \frac{\tau_u^2 H_{ru}}{H_{Ls}}$$

and

$$C_5 = \frac{\tau_u^2}{H_{Ls}}$$

Solving Eq. (2.43) simultaneously with the C^- characteristics (Eq. (2.30))

$$Q_C^2 = C_4 - C_5 (Q_C + C_1)$$

or

$$Q_C = 0.5[-C_5 + \{C_5^2 - 4(C_1 C_5 - C_4)\}^{0.5}] \quad (2.44)$$

Substituting back into Eq. (2.30), we can get H_C .

2.7.4 Valve at the Downstream End. We again seek an equation similar to Eq. (2.42). The flow through the valve is:

$$Q_C = \tau_d \sqrt{\frac{H_C - H_{rd}}{H_{Ld}}} \quad (2.45)$$

where τ_d is a known function of time. Equation (2.45) can be rewritten:

$$Q_C^2 = C_6 H_C - C_7 \quad (2.46)$$

where

$$C_6 = \frac{\tau_d^2}{H_{Ld}}$$

and

$$C_7 = \frac{\tau_d^2 - H_{rd}}{H_{Ld}}$$


Equation (2.46) can be solved simultaneously with the C^+ characteristics equation (2.35) to get:

$$Q_C^2 = C_6 (C_3 - Q_C) - C_7$$

or

$$Q_C = 0.5[-C_6 + \{C_6^2 + 4(C_6 C_3 - C_7)\}^{0.5}] \quad (2.47)$$

H_C can be obtained by direct substitution into Eq. (2.35).



3. WATER HAMMER IN PUMP DISCHARGE LINES

In most cases, it is the pressure occurring as a result of pump stoppage that governs the design of a pump discharge line; since these are the most severe that the pipeline may be exposed to. In many cases it becomes necessary to include pressure-control devices in the pipeline in order to avoid damage. There are generally two different periods of potentially damaging pressures during a transient: a downsurge during pump and fluid deceleration, and an upsurge or overpressure during the reverse phase, especially when the pump reverses its rotation. In addition, complications may arise through vapour pocket collapse.

When the power supply to the pump motor is suddenly cut off, only the kinetic energy of the rotating elements of the motor, pump and the entrained water in the pump is available to continue the forward rotation. However, this energy is small. The pump and discharge decelerate and consequently the pressure on the discharge side drops rapidly. Water hammer waves of subnormal pressure are created and move rapidly up the discharge line to the discharge outlet where a wave reflection occurs. If the moment of inertia of the rotating parts is small, the pressure may drop below the vapour pressure of the liquid and vapour pockets form in the pipe. This phenomena is known as "water column separation". When the water column rejoins again, the vapour cavity collapses resulting in high pressure shock waves. It is recommended that water column separation be avoided because of the destructive effects. The second period of potentially damaging pressure rise occurs during the reversal of flow

through the pump; especially when the pump reverses its rotation and acts as a turbine.

If the pipeline is relatively short with almost all the head used to lift water to a reservoir (gravity loading), high pressure in the discharge side of the pump is possible during the reversal of the pump rotation⁽⁵⁵⁾. If the pipeline is long and most of the pumping head is used to overcome friction (friction loading), the problems arise from the possibility of water column separation⁽⁵⁵⁾. Kinno and Kennedy⁽⁵⁶⁾ noted that if the friction head during the normal operation is greater than about 20% of the total pumping head, the maximum head during flow reversal will not exceed the initial pumping head. In many cases it becomes necessary to provide the pipeline with pressure control devices such as check valves, pressure release valves, surge tanks, discharge tanks, or air vessels. The choice of a certain device (or array of devices) depends upon the hydraulic and physical characteristics of the system.

3.1 Effect of Power Failure

As mentioned earlier, when there is a power outage, the flow decelerates rapidly, since the rotational inertia of the motor, coupling, impellor and entrained water is too small to maintain the flow under the existing head. The pump speed drops rapidly while the discharge is still in the forward direction. As the discharge reduces, a negative pressure wave propagates downstream of the pump in the discharge pipe while a positive pressure wave propagates upstream of the pump in the suction

pipe. The speed of the pump decreases until the pump is unable to deliver any more water against the discharge head. In the absence of a discharge check valve, the flow reverses in direction while the pump is still rotating in the forward direction. This causes greater resistance to the flow which is accompanied by a pressure rise. Then the pump comes to zero speed and starts to reverse rotation acting as a turbine. As the speed increases in the reverse direction, it causes greater resistance to the flow which produces higher pressure at the pump and consequently along the discharge line.

In order to determine the transient hydraulic conditions at the pump and along the pipeline, three effects must be taken into consideration, namely; the pump characteristics, pump and motor inertia, and the water hammer phenomena in the pipe.

3.2 Pump Characteristics

In order to be able to determine a complete history of the transient pressures at the pump and along the pipeline following power failure, it is necessary to have complete characteristics of the pump covering all normal and abnormal operating conditions. As discussed above, following power failure, the pump passes through three different zones. These zones are:

1. Zone of normal pump operation: in which the pump is rotating in the forward direction and the flow is also in the forward direction.
2. Zone of energy dissipation: in which the pump is rotating in the forward direction while the flow is reversed.

3. Zone of turbine operation: In which the pump is working as a turbine, where both pump speed and discharge are reversed.

The three zones are shown in Fig. 3.1.

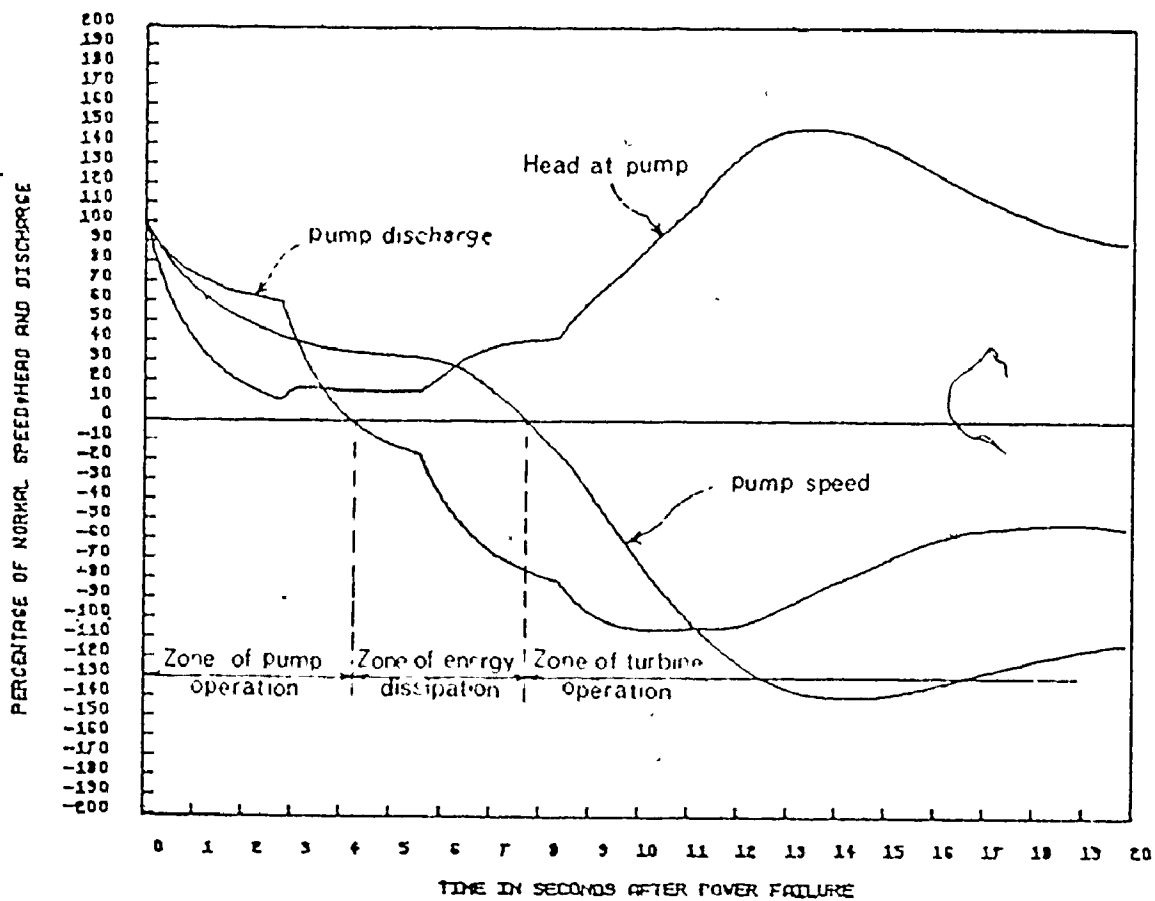


FIG. 3.1: TRANSIENT CONDITIONS FOLLOWING POWER FAILURE AT PUMP MOTOR

Usually, the pump manufacturer supplies curves of the head, brake horsepower, and the efficiency plotted against the discharge for the normal speed of pump operation. From these data it is possible to determine the characteristics of the pump in the zone of normal operation. These data can easily be converted into a family of torque and speed curves on a head-discharge diagram⁽⁴⁸⁾. Data for the zones of energy dissipation and turbine operation must be found in the literature for a pump of approximately the same specific speed as that under study. Unfortunately, it seems that the only data available in the literature are those published by Donsky⁽⁵¹⁾. Tests for three specific speeds: 1800, 7600, and 13500 (gpm units) were the basis for these data. Specific speed of 1800 represents centrifugal pumps which are usually used for relatively high heads. Specific speed of 7600 represents mixed flow pumps which are generally used for relatively medium heads. Specific speed of 13500 represents axial flow pumps which are used for relatively low heads. The pump characteristics are presented in dimensionless ratios of speed, torque, head, and discharge. All of the complete characteristics include the zones of pump operation, energy dissipation, and turbine operation. These curves have been developed by the principle of homologous units. From these curves, the data may be reduced to a few curves of dimensionless-homologous parameters for convenient storage and interpolation for computing⁽⁵⁵⁾. Figures A.1 to A.6 represent these curves, which are presented in tabular forms in Tables A.1, A.2, and A.3 (see Appendix A). The dimensionless homologous ratios plotted and tabulated are:

For heads: $\frac{H'}{\alpha^2}$ against $\frac{Q'}{\alpha}$ or $\frac{H'}{Q'^2}$ against $\frac{\alpha}{Q'}$

For torque: $\frac{\beta}{\alpha^2}$ against $\frac{Q'}{\alpha}$ or $\frac{\beta}{Q'^2}$ against $\frac{\alpha}{Q'}$

where: H' is the total dynamic head divided by the rated head (head at maximum efficiency);

α is the pump speed divided by the rated speed;

Q' is the pump discharge divided by the rated discharge; and

β is the torque divided by the rated torque.

The use of both $\frac{\alpha}{Q'}$ and $\frac{Q'}{\alpha}$ can limit the abscissa values to unity. If $\frac{\alpha}{Q'}$ is greater than unity then we plot $\frac{Q'}{\alpha}$ against $\frac{H'}{\alpha^2}$ (for heads) and $\frac{Q'}{\alpha}$ against $\frac{\beta}{\alpha^2}$ (for torque). If $\frac{\alpha}{Q'}$ is less than unity we plot $\frac{\alpha}{Q'}$ against $\frac{H'}{Q'^2}$ (for heads) and $\frac{\alpha}{Q'}$ against $\frac{\beta}{Q'^2}$ (for torque).

The complete pump characteristics published by Donsky cover only the three specific speeds mentioned above. If the specific speed of the pump being studied is approximately the same as that of the pump characteristics available, the water hammer results will be satisfactory for most engineering purposes⁽⁵¹⁾. Donsky found that the water hammer results determined from the lowest specific speed pump characteristics are generally the most conservative for power failure or shut-down of the pumps.

In 1972, G. O. Thomas⁽⁶³⁾ used the pump characteristics published by Donsky and attempted to develop a method for approximating the characteristics for any specific speed pump using an interpolation procedure. He assumed that any two geometrically similar pumps of the same specific speed will have similar performance characteristics. Thomas' interpolation procedure is unproved and still questionable and requires extreme caution in its application⁽⁶⁴⁾.

3.3 Pump Inertia

When the power to the pump is suddenly cut off, the deceleration of the pump at any instant depends upon the moment of inertia of the rotating parts of the pump, motor, and entrained water, as well as the instantaneous torque exerted by the pump impeller⁽⁴⁹⁾. For a rotating system, the accelerating torque is equal to the product of the mass moment of inertia of the rotating system and the angular acceleration. Following a power failure at the pump motor, the decelerating torque on the rotating system corresponds to the pump torque. If the decelerating torque is taken as positive

$$\begin{aligned} T &= - I \frac{d\omega}{dt} \\ &= - \frac{WR^2}{g} \frac{d\omega}{dt} \end{aligned} \quad (3.1)$$

where: T = the pump input torque;

I = the mass moment of inertia of rotating parts;

ω = the angular velocity of pump; and

WR^2 = rotational inertia of rotating components of pump, motor, and entrained water.

$$\text{But } \omega = \frac{2\pi N}{60}$$

$$\therefore \frac{d\omega}{dt} = \frac{2\pi}{60} \frac{dN}{dt}$$

For a small time interval Δt , Eq. (3.1) can be rewritten

$$T = - \frac{2\pi WR^2}{60g} \frac{\Delta N}{\Delta t} \quad (3.2)$$

Using the ratios:

$$\alpha = \frac{N}{N_R} \quad (3.3)$$

and

$$\beta = \frac{T}{T_R} \quad (3.4)$$

and substituting back into Eq. (3.2)

$$\Delta\alpha = - \beta \frac{30T_R g \Delta t}{\pi WR^2 N_R} \quad (3.5)$$

where T_R can be calculated from

$$T_R = \frac{60\gamma h_R q_R}{2\pi N_R \eta_R} \quad (3.6)$$

where: N_R = the rated speed (speed at rated conditions);

q_R = the rated discharge;

T_R = the rated torque;

h_R = the rated head; and

η_R = the pump efficiency at rated conditions.

Combining Eqs. (3.5) and (3.6)

$$\Delta\alpha = - \beta \frac{900\gamma h_R q_R}{\pi WR^2 N_R^2 \eta_R} \Delta t \quad (3.7)$$

Equation (3.7) is used to compute the speed change of a failing pump

during time interval Δt .

3.4 Pump Analysis

In this section, equations are derived describing the conditions at the pump resulting from power failure or pump shut-down. The pump (or a number of pumps in parallel) can be connected directly to the suction reservoir or to both suction and delivery pipes. The equations account for an arbitrary valve closure at the pump discharge side. Again, the equations are derived in dimensionless form.

3.4.1 Pump Connected to a Reservoir. In this case the suction pipe is very short and can usually be neglected. Consider Fig. 3.2 which represents a pipeline connecting two reservoirs A and B. A pump is connected to the lower reservoir A. The pump is used to deliver a steady state discharge q_0 to the downstream reservoir B. In case of interruption of power to the pump, a negative pressure wave is created which propagates downstream until it reaches the downstream reservoir B where it reflects negatively forming a positive pressure wave. Usually, it is recommended that a discharge valve or a check valve be placed on the discharge side of the pump. This prevents reversal of the pump which is often accompanied by high pressure at the pump and along the pipeline.

3.4.1.1 Single Pump Without Discharge Valve. In this case, the C^- characteristics (Eq. (2.30)) is available

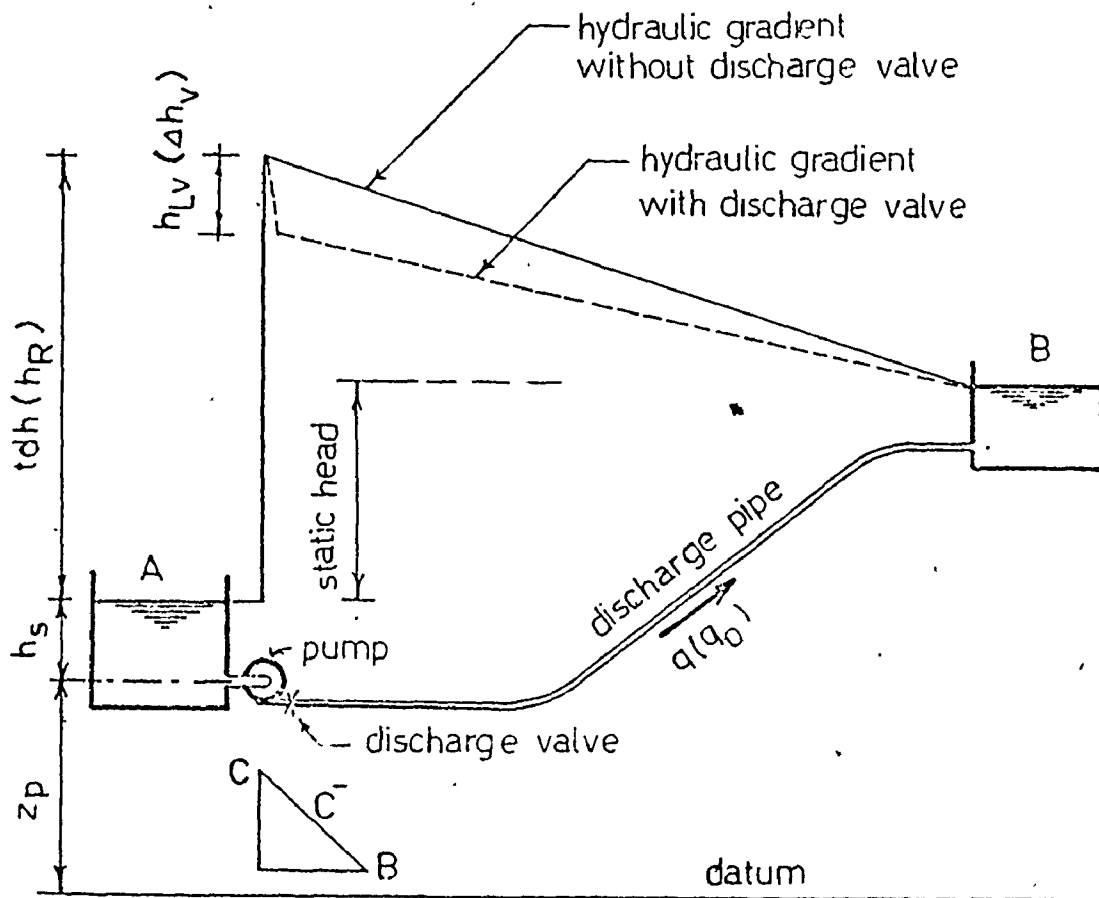


FIG. 3.2: DIAGRAMMATIC SKETCH OF A PUMP-DISCHARGE LINE WITH THE PUMP(S) CONNECTED TO THE SUCTION RESERVOIR

$$H_C = Q_C + C_1$$

This equation relates the discharge and the pressure head in the pipeline at the delivery side of the pump. At any instant after power failure we can use the pump head and discharge relations (i.e., $\frac{Q'}{\alpha}$ and $\frac{H'}{2}$; or $\frac{\alpha}{Q'}$ and

$\frac{H'}{Q'^2}$) provided that the pump speed is known. If $\frac{\alpha}{Q'}$ is greater than unity, then we use the $\frac{Q'}{\alpha}$ and $\frac{H'}{\alpha^2}$ curves. These curves can be locally approximated by a parabola of the second degree:

$$\frac{H'_C}{\alpha^2} = b_1 + b_2 \left(\frac{Q'_C}{\alpha}\right) + b_3 \left(\frac{Q'_C}{\alpha}\right)^2 \quad (3.8)$$

b_1 , b_2 , and b_3 are constants which are determined by fitting a parabola through three adjacent points on the appropriate head-discharge curve.

But

$$h_C = H_C(av_o/g)$$

and

$$tdh = H'_C h_R$$

h_C is measured from the datum, while tdh is the total dynamic head of the pump which is measured in this case from the water surface in the suction reservoir. If the elevation of the pump related to the datum is z_p :

$$h_C = tdh + h_s + z_p \quad (3.9)$$

or

$$H_C(av_o/g) = H'_C h_R + h_s + z_p$$

or

$$H'_C = H_C \frac{(av_o/g)}{h_R} - \frac{h_s}{h_R} - \frac{z_p}{h_R}$$

If we write the Joukowski head $(av_o/g) = H_j$

$$H'_C = H_C \frac{H_j}{h_R} - \frac{h_s}{H_j} \frac{H_j}{h_R} - \frac{z_p}{H_j} \frac{H_j}{h_R} = (H_C - H_s - Z_{pn}) \frac{H_j}{h_R} \quad (3.9a)$$

H_s is the normalized static suction head (the static suction head divided by (av_o/g)) and Z_{pn} is the elevation of the pump divided by (av_o/g) .

We also have:

$$q_C = Q'_C q_R$$

and

$$q_C = Q_C q_o$$

Then

$$\begin{aligned} Q'_C &= Q_C (q_o/q_R) \\ &= Q_C q_{rr} \end{aligned} \quad (3.10)$$

If the pump before power failure is working at rated conditions

$$q_o = q_R \quad (3.10a)$$

and

$$Q'_C = Q_C \quad (3.10b)$$

Equation (3.8) can be written in the form

$$H'_C = b_1 \alpha^2 + b_2 \alpha Q'_C + b_3 Q_C'^2$$

or

$$(H_C - H_s - Z_{pn}) \frac{H_C}{h_R} = b_1 \alpha^2 + b_2 \alpha \left(\frac{q_o}{q_R}\right) Q_C + b_3 \left(\frac{q_C}{q_R}\right)^2 Q_C^2$$

Solving this equation with Eq. (2.30)

$$Q_C = \frac{1}{2b_3q_{rr}^2} \left[\left(\frac{H_j}{h_R} - b_2\alpha q_{rr} \right) - \left(b_2q_{rr}\alpha \frac{H_j}{h_R} \right)^2 - 4b_3q_{rr}^2 \left[b_1\alpha^2 + \left(Z_{pn} + H_s - C_1 \right) \frac{H_j}{h_R} \right]^{0.5} \right] \quad (3.11)$$

Equation (3.11) can be used as long as $\frac{\alpha}{Q_r}$ is greater than 1.0. If $\frac{\alpha}{Q_r}$ is less than 1.0, then we use the $\frac{\alpha}{Q_r}$ and $\frac{H'}{Q_r^2}$ relations. Using the appropriate curve, depending on the running conditions of the pump (normal, energy dissipation or turbine zone), we again fit a curve of the form

$$\frac{H'_C}{Q_C'^2} = a_1 + a_2 \left(\frac{\alpha}{Q_r} \right) + a_3 \left(\frac{\alpha}{Q_r} \right)^2 \quad (3.12)$$

Using Eq. (3.12) instead of Eq. (3.8) and following the same procedures, we can get a formula for discharge in a similar form:

$$Q_C = \frac{1}{2a_1q_{rr}^2} \left[\left(\frac{H_j}{h_R} - a_2\alpha q_{rr} \right) - \left(a_2q_{rr}\alpha - \frac{H_j}{h_R} \right)^2 - 4a_1q_{rr}^2 \left[a_3\alpha^2 + \left(Z_{pn} + H_s - C_1 \right) \frac{H_j}{h_R} \right]^{0.5} \right] \quad (3.13)$$

Substituting back into Eq. (2.30), we can get H_C .

3.4.1.2 Pump With a Discharge Valve. A discharge valve may be placed at the pump discharge side. It is used to prevent the flow reversal through the pump. In Fig. 3.2, the dotted line represents the hydraulic grade line when a discharge valve is used.

Assume that the head loss across the valve at steady state conditions is Δh_v , then

$$q_o = (c_{d^A_v})_o \sqrt{2g\Delta h_v} \quad (3.14)$$

At any time, the head loss across the valve is h_{Lv} , then:

$$q_C = (c_{d^A_v})_t \sqrt{2gh_{Lv}} \quad (3.15)$$

Dividing Eq. (3.15) by Eq. (3.14)

$$\frac{q_C}{q_o} = \tau \sqrt{\frac{h_{Lv}}{\Delta h_v}}$$

where $\tau = \frac{(c_{d^A_v})_t}{(c_{d^A_v})_o}$ which is a known function of time. If we write

$$H_{Lv} = \frac{h_{Lv}}{(av_o/g)}$$

and

$$\Delta H_v = \frac{\Delta h_v}{(av_o/g)}$$

then $\frac{q_C}{q_o} = \tau \sqrt{\frac{H_{Lv}}{\Delta H_v}}$

or

$$H_{Lv} = \frac{\Delta H_v}{\tau^2} \frac{q_C^2}{q_o^2}$$

or

$$H_{Lv} = \frac{\Delta H_v}{\tau^2} Q_C |Q_C| \quad (3.16)$$

Note that $Q_C |Q_C|$ is used instead of Q_C^2 to account for the case when the flow is reversed. We also have

$$h_C = t d h + h_s + z_p - h_{Lv} \quad (3.17)$$

which is similar to Eq. (3.9).

Equation (3.17) leads to

$$H'_C = (H_C - H_s - Z_{pn} + H_{Lv}) \frac{H_j}{h_R} \quad (3.18)$$

Substituting from Eqs. (3.16) and (3.18) into Eq. (3.8)

$$(H_C - H_s - Z_{pn} + \frac{\Delta H_v}{\tau^2} Q_C |Q_C|) \frac{H_j}{h_R} = b_1 \alpha^2 + b_2 \alpha q_{rr} Q_C + b_3 q_{rr}^2 Q_C^2 \quad (3.19)$$

Equations (2.35) and (3.19) can be solved for Q_C and H_C

$$Q_C = \frac{1}{2[b_3 q_{rr}^2 - \frac{\Delta H_v}{\tau^2} \frac{H_j}{h_R}]} \left[\left(\frac{H_j}{h_R} - b_2 \alpha q_{rr} \right) - \left\{ \left(\frac{H_j}{h_R} - b_2 \alpha q_{rr} \right)^2 - 4 \left(b_3 q_{rr}^2 - \frac{\Delta H_v}{\tau^2} \frac{H_j}{h_R} \right) [b_1 \alpha^2 + (Z_{pn} + H_s - C_1) \frac{H_j}{h_R}] \right\}^{0.5} \right] \quad (3.20)$$

Equation (3.20) is used when the flow is positive, i.e., in the zone of normal pump operation. If the flow is reversed, then $Q_C |Q_C|$ becomes negative and this leads to:

$$Q_C = \frac{1}{2[b_3 q_{rr}^2 + \frac{\Delta H_v}{\tau^2} \frac{H_j}{h_R}]} \left[\left(\frac{H_j}{h_R} - b_2 \alpha q_{rr} \right) - \left\{ \left(\frac{H_j}{h_R} - b_2 \alpha q_{rr} \right)^2 - 4 \left(b_3 q_{rr}^2 + \frac{\Delta H_v}{\tau^2} \frac{H_j}{h_R} \right) [b_1 \alpha^2 + (Z_{pn} + H_s - C_1) \frac{H_j}{h_R}] \right\}^{0.5} \right] \quad (3.21)$$

Equation (3.21) is used when the flow is reversed, i.e., in the zones of energy dissipation and turbine operation.

If a check valve is used so that no flow reversal is permitted,

Eq. (3.20) only is used.

Equations (3.20) and (3.21) can be used as long as $\frac{\alpha}{Q_r}$ is greater than 1.0. If $\frac{\alpha}{Q_r}$ is less than 1.0, then Eq. (3.12) is used instead of Eq. (3.8) which leads to

$$Q_C = \frac{1}{2[a_1 q_{rr}^2 - \frac{\Delta H_v}{\tau} \frac{H_j}{h_R}]} \left[\left(\frac{H_j}{h_R} - a_2 \alpha q_{rr} \right) - \left\{ \left(\frac{H_j}{h_R} - a_2 \alpha q_{rr} \right)^2 - 4 \left(a_1 q_{rr}^2 - \frac{\Delta H_v}{\tau} \frac{H_j}{h_R} \right) \left[a_3 \alpha^2 + (Z_{pn} + H_s - C_1) \frac{H_j}{h_R} \right] \right\}^{0.5} \right] \quad (3.22)$$

Equation (3.22) is used for the zone of normal pump operation where the flow is positive. For the zones of energy dissipation and turbine operation, the head loss across the valve is negative and this leads to

$$Q_C = \frac{1}{2[a_1 q_{rr}^2 + \frac{\Delta H_v}{\tau} \frac{H_j}{h_R}]} \left[\left(\frac{H_j}{h_R} - a_2 \alpha q_{rr} \right) - \left\{ \left(\frac{H_j}{h_R} - a_2 \alpha q_{rr} \right)^2 - 4 \left(a_1 q_{rr}^2 + \frac{\Delta H_v}{\tau} \frac{H_j}{h_R} \right) \left[a_3 \alpha^2 + (Z_{pn} + H_s - C_1) \frac{H_j}{h_R} \right] \right\}^{0.5} \right] \quad (3.23)$$

H_C can be obtained from Eq. (2.35). If no reversed flow is permitted, then Eq. (3.23) is no longer valid.

If the discharge valve is omitted, then ΔH_v is set equal to zero. In this case, Eqs. (3.20) and (3.21) are reduced to one equation which is exactly the same as Eq. (3.11). Also, Eqs. (3.22) and (3.23) are reduced to one equation which is exactly the same as Eq. (3.13). In other words, Eqs. (3.20) or (3.21) and (3.22) or (3.23) can be used when the pump is connected directly to the suction reservoir whether a discharge valve is used or not.

3.4.1.3 Identical Pumps in Parallel. If several identical pumps are placed in parallel to supply a common discharge line, then the flow in the pipeline is the summation of the individual discharges. If the pump discharge is q'_C , then

$$q_C = nq'_C$$

where q_C is the discharge in the pipe, and n is the number of pumps. But

$$q_C = Q_C q_o$$

and

$$q'_C = Q'_C q_R$$

Then

$$Q'_C = \left(\frac{q_o}{nq_R}\right) Q_C \quad (3.24)$$

Following the same procedures as for the case of a single pump and using Eq. (3.24) instead of Eq. (3.10), we get the same equation for discharge with the exception that

$$q_{rr} = \frac{q_o}{nq_R} \quad (3.25)$$

If the pumps are running at rated conditions:

$$q_o = nq_R$$

and q_{rr} becomes equal to unity. If all the pumps are provided with

identical discharge valves which operate in the same manner, the equations for discharge will not differ from the case of a single pump except for q_{rr} which is then given by Eq. (3.25).

3.4.2 Pump In-Line. Consider Fig. 3.3 which represents a pipeline connecting two reservoirs A and B. A pump is (or a number of pumps in

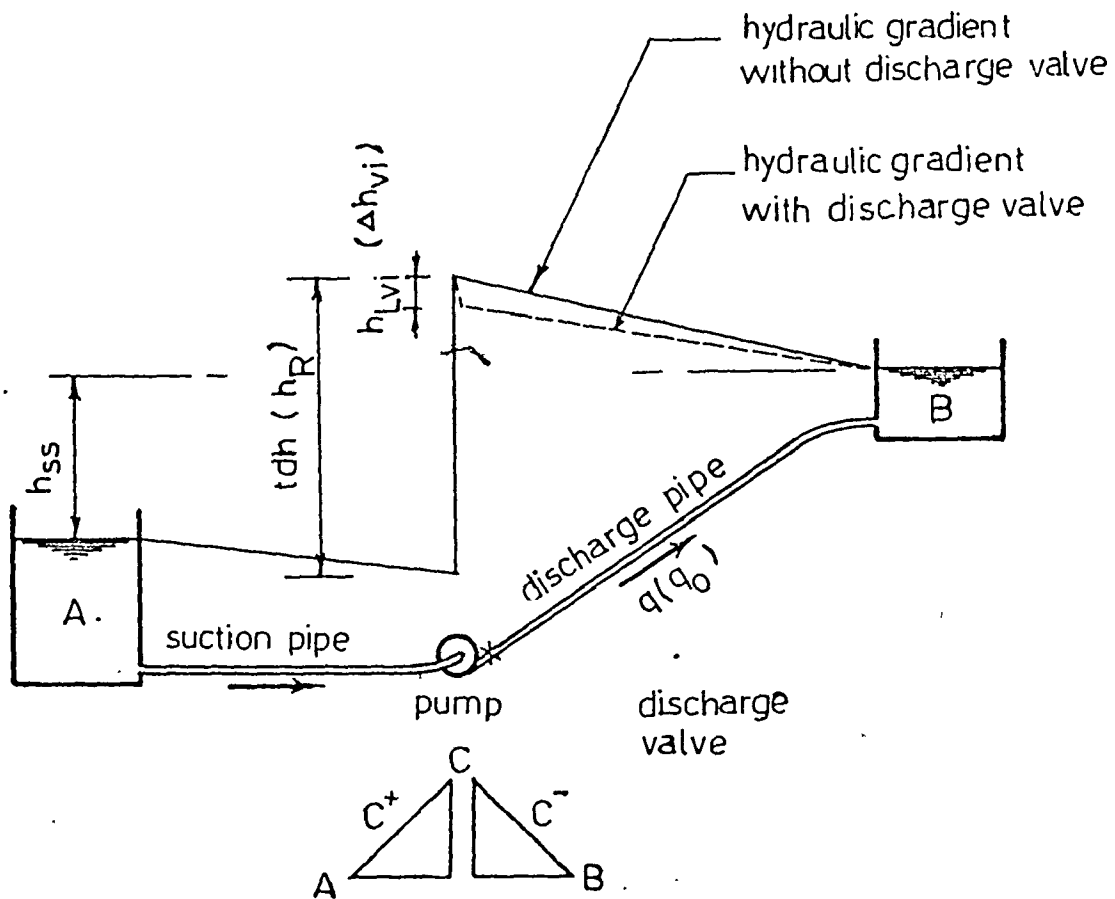


FIG. 3.3: DIAGRAMMATIC SKETCH OF A PUMP-DISCHARGE LINE WITH THE PUMP(S) CONNECTED TO SUCTION AND DELIVERY PIPES

parallel are) connected to suction and discharge pipes which in turn are connected to reservoirs A and B; respectively. The pump delivers a steady state discharge q_0 to reservoir B. In case of pump stoppage, negative and positive pressure waves propagate upstream and downstream; respectively, where they reflect at the reservoirs. Check valves may be placed at the pumps to prevent pump reversal which is usually accompanied by high pressures in the discharge line.

3.4.2.1 Pump In-Line Without Discharge Valve. The two characteristics (Eqs. (2.35) and (2.30)) are:

$$C^+ : H_{CL} + Q_C - C_3 = 0$$

$$C^- : H_{CR} - Q_C - C_1 = 0$$

where: H_{CL} is the head at the suction side of the pump (h_{CL}) divided by (av_0/g) ; and

H_{CR} is the head at the delivery side of the pump (h_{CR}) divided by (av_0/g) .

We also have:

$$h_{CR} - h_{CL} = tdh$$

or

$$(H_{CR} - H_{CL}) \frac{H_1}{h_R} = H' \quad (3.26)$$

where H' is the total dynamic head divided by the rated head.

Subtracting Eq. (2.30) from Eq. (2.35)

$$(H_{CR} - H_{CL}) - 2Q_C + C_3 - C_1 = 0$$

and substituting back into Eq. (3.26)

$$H' = (2Q_C - C_3 + C_1) \frac{H_j}{h_R}$$

Substituting back into Eq. (3.8) and using Eq. (3.10)

$$(2Q_C - C_3 + C_1) \frac{H_j}{h_R} = b_1 \alpha^2 + b_2 q_{rr} \alpha Q_C + b_2 q_{rr}^2 Q_C^2$$

Solving for Q_C

$$Q_C = \frac{1}{2b_3 q_{rr}} \left[\left(2 \frac{H_j}{h_R} - b_2 q_{rr} \alpha \right) - \left\{ \left(2 \frac{H_j}{h_R} - b_2 q_{rr} \alpha \right)^2 - 4b_3 q_{rr}^2 \left[b_1 \alpha^2 + (C_3 - C_1) \frac{H_j}{h_R} \right] \right\}^{0.5} \right] \quad (3.27)$$

Equation (3.27) can be used as long as $\frac{\alpha}{Q_C}$ is greater than 1.0. If $\frac{\alpha}{Q_C}$ is less than 1.0, then we use Eq. (3.12) instead of Eq. (3.8), which leads to

$$Q_C = \frac{1}{2a_1 q_{rr}} \left[\left(2 \frac{H_j}{h_R} - a_2 q_{rr} \alpha \right) - \left\{ \left(2 \frac{H_j}{h_R} - a_2 q_{rr} \alpha \right)^2 - 4a_1 q_{rr}^2 \left[a_3 \alpha^2 + (C_3 - C_1) \frac{H_j}{h_R} \right] \right\}^{0.5} \right] \quad (3.28)$$

H_{CL} and H_{CR} can be determined by substitution into Eqs. (2.35) and (2.30).

If several identical pumps in parallel are used, the formula for discharge will be the same, except that

$$q_{rr} = \frac{q_o}{nq_R}$$

3.4.2.2 Pump In-Line With Discharge Valve. Assume that Δh_{vi} is the steady state head loss across the valve, and h_{Lvi} is the head loss at any instant. We can derive an equation similar to Eq. (3.16):

$$H_{Lvi} = \frac{\Delta H_{vi}}{\tau} Q_C |Q_C| \quad (3.29)$$

where

$$H_{Lvi} = \frac{h_{Lvi}}{(av_o/g)}$$

and

$$\Delta H_{vi} = \frac{\Delta h_{vi}}{(av_o/g)}$$

We also have

$$h_{CR} - h_{CL} + h_{Lvi} = t dh$$

which leads to

$$(H_{CR} - H_{CL} + H_{Lvi}) \frac{H_i}{h_R} = H' \quad (3.30)$$

Using Eqs. (3.8), (3.29), (3.30), and the two characteristics equations for the pipeline (Eqs. (2.30) and (2.35)), we can solve for Q_C , H_{CL} and H_{CR}

$$Q_C = \frac{1}{2(b_3 q_{rr}^2 - \frac{\Delta H_{vi}}{\tau^2} \frac{H_j}{h_R})} \left[\left(2 \frac{H_j}{h_R} - b_2 q_{rr} \alpha \right) - \left\{ \left(2 \frac{H_j}{h_R} - b_2 q_{rr} \alpha \right)^2 - 4 \left(b_3 q_{rr}^2 - \frac{\Delta H_{vi}}{\tau^2} \frac{H_j}{h_R} \right) [b_1 \alpha^2 + (C_3 - C_1) \frac{H_j}{h_R}] \right\}^{0.5} \right] \quad (3.31)$$

Equation (3.31) can be used for the zone of normal pump operation. In the energy dissipation and turbine operation zones the flow is negative and consequently the head loss across the valve becomes negative:

$$Q_C = \frac{1}{2(b_3 q_{rr}^2 + \frac{\Delta H_{vi}}{\tau^2} \frac{H_j}{h_R})} \left[\left(2 \frac{H_j}{h_R} - b_2 q_{rr} \alpha \right) - \left\{ \left(2 \frac{H_j}{h_R} - b_2 q_{rr} \alpha \right)^2 - 4 \left(b_3 q_{rr}^2 + \frac{\Delta H_{vi}}{\tau^2} \frac{H_j}{h_R} \right) (b_1 \alpha^2 + (C_3 - C_1) \frac{H_j}{h_R}) \right\}^{0.5} \right] \quad (3.32)$$

Equations (3.31) and (3.32) are valid as long as $\frac{\alpha}{Q_r}$ is greater than 1.0. If $\frac{\alpha}{Q_r}$ is less than 1.0, then Eq. (3.12) is used instead of Eq. (3.8), which leads to

$$Q_C = \frac{1}{2(a_1 q_{rr}^2 - \frac{\Delta H_{vi}}{\tau^2} \frac{H_j}{h_R})} \left[\left(2 \frac{H_j}{h_R} - a_2 q_{rr} \alpha \right) - \left\{ \left(2 \frac{H_j}{h_R} - a_2 q_{rr} \alpha \right)^2 - 4 \left(a_1 q_{rr}^2 - \frac{\Delta H_{vi}}{\tau^2} \frac{H_j}{h_R} \right) [a_3 \alpha^2 + (C_3 - C_1) \frac{H_j}{h_R}] \right\}^{0.5} \right] \quad (3.33)$$

or

$$Q_C = \frac{1}{2(a_1 q_{rr}^2 + \frac{\Delta H_{vi}}{\tau^2} \frac{H_j}{h_R})} \left[\left(2 \frac{H_j}{h_R} - a_2 q_{rr} \alpha \right) - \left\{ \left(2 \frac{H_j}{h_R} - a_2 q_{rr} \alpha \right)^2 - 4 \left(a_1 q_{rr}^2 + \frac{\Delta H_{vi}}{\tau^2} \frac{H_j}{h_R} \right) [a_3 \alpha^2 + (C_3 - C_1) \frac{H_j}{h_R}] \right\}^{0.5} \right] \quad (3.34)$$

Equation (3.33) is valid for the zone of normal pump operation while Eq. (3.34) is used for the zones of energy dissipation and turbine operation.

Once Q_C is known, H_{CL} and H_{CR} can be obtained by direct substitution into Eqs. (2.35) and (2.30).

If the discharge valve is omitted, then ΔH_{vi} is set equal to zero. In this case, Eqs. (3.31) and (3.32) are reduced to one equation which is exactly the same as Eq. (3.27). Also Eqs. (3.33) and (3.34) are reduced to one equation which is exactly the same as Eq. (3.28). In other words, Eqs. (3.31) or (3.32) and (3.33) or (3.34) can be used when the pump is (or pumps in parallel are) connected to suction and discharge pipes whether a discharge valve is used or not.

3.5 Pipeline Protection Against Water Hammer

In pipelines where dangerous water hammer pressure transients are expected, a protective device (or combination of devices) should be used. The most common protective devices are surge tanks, one-way surge tanks (discharge tanks), in-line valves, and air chambers. It may also be possible to protect pump-discharge lines against severe water hammer transients by increasing the inertia of the rotating elements: pump, motor, and entrained water. In this section (all of section 3.5) equations are derived for in-line valves, surge tanks, discharge tanks, and air chambers. All equations are derived in dimensionless form.

3.5.1 Valve In-Line. Referring to Fig. 3.4, Δh_o is the steady state

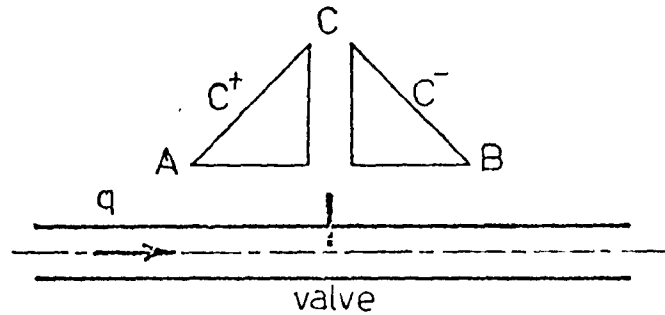


FIG. 3.4: IN-LINE VALVE

drop in hydraulic grade across the valve, which can be written in the dimensionless form

$$\Delta H_o = \frac{\Delta h_o}{(av_o/g)} .$$

The steady state discharge through the valve considered as an orifice is given by

$$q_o = Av_o = (C_{d v_o} A_o) \sqrt{2g\Delta h_o} \quad (3.35)$$

At any instant, the flow through the valve is given by:

$$q_{CR} = q_{CL} = q_C = (C_{d v_t} A_o) \sqrt{2g(h_{CL} - h_{CR})} . \quad (3.36)$$

Dividing Eq. (3.36) by Eq. (3.35)

$$\frac{q_C}{q_0} = \tau_I \sqrt{\frac{h_{CL} - h_{CR}}{\Delta h_0}}$$

or in dimensionless form:

$$Q_C = \tau_I \sqrt{\frac{H_{CL} - H_{CR}}{\Delta H_0}} \quad (3.37)$$

where τ_I is a known function of time

$$Q_C^2 = \frac{\tau_I^2}{\Delta H_0} (H_{CL} - H_{CR}) \quad (3.37a) \quad \checkmark$$

Equations (2.35) and (2.30) can be rewritten

$$C^+ : H_{CL} + Q_C - C_3 = 0 \quad (3.38)$$

and

$$C^- : H_{CR} - Q_C - C_1 = 0 \quad (3.39)$$

Substituting from Eqs. (3.38) and (3.39) into Eq. (3.37a)

$$Q_C^2 = \frac{\tau_I^2}{\Delta H_0} (C_3 - C_1 - 2Q_C)$$

or

$$Q_C^2 + C_8 Q_C + C_9 = 0 \quad (3.40)$$

where $C_8 = \frac{2\tau_I^2}{\Delta H_0}$

$$\text{and } C_9 = \frac{\tau_I^2}{\Delta H_o} (C_1 - C_3) .$$

Solving Eq. (3.40)

$$Q_C = 0.5[-C_8 + (C_8^2 - 4C_9)^{0.5}] . \quad (3.41)$$

The +ve sign is used because the flow is positive as given by Eq. (3.36).

For negative flow, the discharge through the valve is given by

$$q_C = -(C_{dV} A_v)_t \sqrt{2g(h_{CR} - h_{CL})}$$

and an equation similar to Eq. (3.41) can be obtained

$$Q_C = 0.5[C_8 - (C_8^2 + 4C_9)^{0.5}] . \quad (3.42)$$

The negative sign is used because the flow is negative. It is possible for Eq. (3.42) to yield a negative answer only if C_9 is positive, i.e., $C_1 - C_3 > 0$, and thus Eq. (3.42) is used only when C_1 is greater than C_3 .

Similarly, it is possible for Eq. (3.41) to yield a positive value only when C_9 is negative, i.e., when $C_1 - C_3 < 0$, and thus Eq. (3.41) is used only when C_1 is less than C_3 . When $C_1 = C_3$, Q_C is equal to zero.

H_{CL} and H_{CR} can be obtained by substitution into Eqs. (3.38) and (3.39), respectively.

3.5.2 Surge Tanks. The surge tank acts as a balancing tank for the flow variation that may occur in a pipeline. The top of the tank is exposed to atmospheric

pressure while its bottom is connected to the pipeline. Its function is to add water to the pipe in case of a head drop, or withdraw water in case of pressure rise. The height of the tank must, at least, be equal to the maximum head expected to occur at the tank site. This limits the use of a surge tank to protect pump discharge lines because if it is placed near the pump, then its height may become impractical. On the other hand, if it is placed at high peaks in the pipe where the pipeline profile is closer to the hydraulic grade line, it cannot protect the pipeline between the tank and the pump. In this case we have to find some other means to serve that purpose. The surge tank can be used effectively at the head of turbine penstocks. It has the advantages that no maintenance or operating costs are required as the operation does not require any mechanical elements. However, if the pipeline lies in a cold weather area, then precautions should be taken against freezing.

Referring to Fig. 3.5 which represents a diagrammatic sketch of a simple surge tank connected to a pipeline, if we neglect the dynamic effects between sections 1 and 2, then:

$$z = h_{CL} = h_{CR} = h_C$$

or, in dimensionless form

$$Z = H_{CL} = H_{CR} = H_C \quad (3.43)$$

where $Z = \frac{z}{(av_o/g)}$ and $H_C = \frac{h_C}{(av_o/g)}$. Equations (3.38) and (3.39) become,

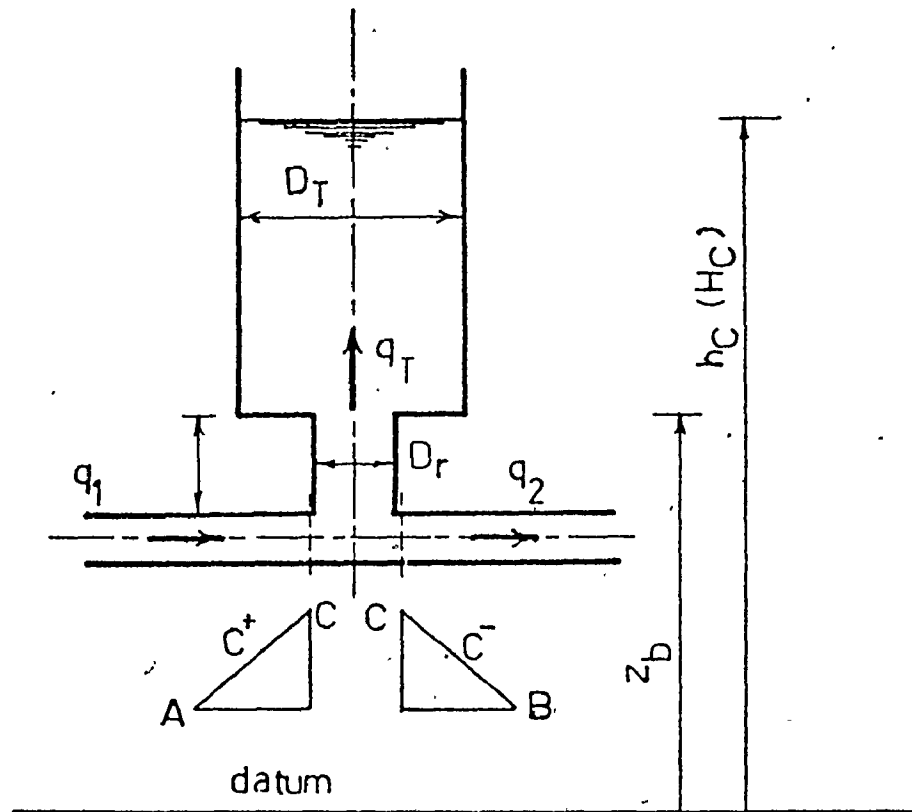


FIG. 3.5: SCHEMATIC FOR SIMPLE SURGE TANK

$$C^+ : H_C + Q_{C1} - C_3 = 0 \quad (3.44)$$

$$C^- : H_C - Q_{C2} - C_1 = 0 \quad (3.45)$$

The continuity equation at the junction between the pipe and the tank:

$$Q_{TC} = Q_{C1} - Q_{C2} \quad (3.46)$$

where: $Q_{TC} = q_{TC}/q_o$, and q_{TC} is the discharge into the tank after time interval Δt .

The head in the tank h_C after time Δt can be calculated from:

$$h_C = h + \frac{q_T + q_{TC}}{2} \frac{\Delta t}{A_T} \quad (3.47)$$

where A_T is the cross sectional area of the tank, h is the initial head in the tank, and q_T is the discharges into the tank at the beginning of the time interval Δt .

Equation (3.47) can be transformed into the dimensionless form:

$$H_C = H + \left(\frac{Q_T + Q_{TC}}{2} \right) \frac{q_o \Delta t}{(av_o/g)A_T} \quad (3.48)$$

If, at any time, the water surface in the tank falls below Z_b ; where $Z_b = z_b/(av_o/g)$, then we have to use the cross sectional area of the riser (A_R) instead of A_T in Eq. (3.48).

$$H_C = H + \left(\frac{Q_T + Q_{TC}}{2} \right) \frac{q_o \Delta t}{(av_o/g)A_R} \quad (3.49)$$

If we substitute

$$\frac{q_o \Delta t}{2(av_o/g)A_T} = C_{10} \text{ (say)}$$

then we get

$$H_C = H + (Q_T + Q_{TC}) C_{10} \quad (3.50)$$

Equations (3.44), (3.45), (3.46), and (3.50) can be solved for the four unknowns H_C , Q_{C1} , Q_{C2} , and Q_{TC} . Subtracting Eq. (3.44) from Eq. (3.45)

$$Q_{C1} = C_3 - C_1 - Q_{C2} \quad (3.51)$$

Substituting back into Eq. (3.46):

$$Q_{TC} = C_3 - C_1 - 2Q_{C2} \quad (3.52)$$

Combining Eqs. (3.50) and (3.52)

$$H_C = H + (Q_T + C_3 - C_1 - 2Q_{C2})C_{10}$$

and substituting back from Eq. (3.45), we obtain

$$Q_{C2} + C_1 = H + (Q_T + C_3 - C_1 - 2Q_{C2})C_{10}$$

or

$$Q_{C2} = [(H - C_1) + (Q_T + C_3 - C_1)C_{10}] / [1 + 2C_{10}] \quad (3.53)$$

Q_{C1} , Q_{TC} , and H_C can be obtained by direct substitution into Eqs. (3.51), (3.46), and either Eqs. (3.44) or (3.45); respectively.

The solution can be repeated for each time increment until the required time is reached.

3.5.3 One-Way Surge Tanks or Discharge Tanks. In situations where the pipeline profile is considerably lower than the hydraulic grade line, the

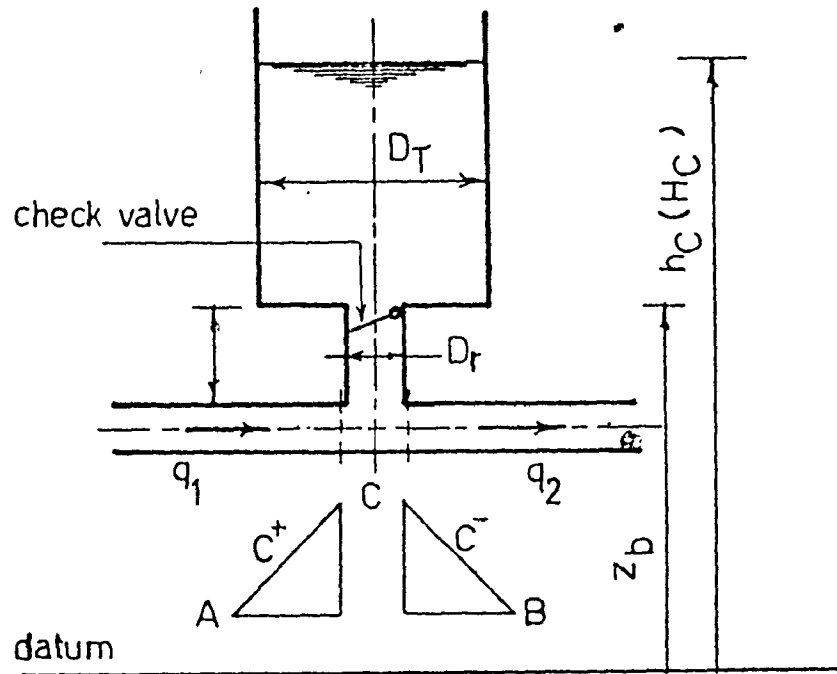


FIG. 3.6: SCHEMATIC FOR ONE-WAY SURGE TANK

use of a surge tank becomes impractical. In this case we can use a one-way surge tank (discharge tank). The tank is connected to the pipeline via a reflux valve (or check valve); (see reference 57 for typical arrangements). Figure 3.6 represents a diagrammatic sketch of a discharge tank connected to the pipeline. The tank water surface is subject, to atmospheric pressure, but still below the hydraulic grade line. Under normal operating conditions, the reflux valve remains closed and the tank

is separated from the pipeline.

If, at any time, the pressure at the tank site drops below the elevation of the water surface in the tank, the check valve opens and the tank discharges water into the pipe. A small-bore inlet pipe bypassing the reflux valve with a float valve at the tank should be installed to refill the tank slowly⁽⁵⁷⁾. If the pressure at the tank site rises above the water surface elevation in the tank, the check valve closes and the tank is again separated from the pipeline. It may be necessary⁽⁶⁵⁾ to prevent reverse motion of the water column which would cause water hammer overpressure. This could be achieved by installing a reflux valve in the line. It is often convenient⁽⁵⁷⁾ to situate a number of discharge tanks at successively higher peaks along the pipeline, with in-line reflux valves installed at various positions along the pipeline. The optimum locations of discharge tanks and in-line reflux valves has to be determined by trial analysis.

We can use the same equations derived for the surge tank for the discharge tank. These equations can be applied as long as the pressure in the pipe below the tank is less than the elevation of water surface in the tank.

If, at any time, the pressure in the pipe below the tank rises so that it exceeds the elevation of water in the tank, the check valve closes and the tank is separated from the pipeline. In this case we can apply Eqs. (2.28) and (2.29) to determine the heads and discharges in the pipe at the tank site.

3.5.4 Air Chambers or Pressure Vessels. If the profile of a pipeline is not high enough to use a surge tank or discharge tank to protect the pipeline, it may be possible to force water into the low pressure zone by means of compressed air in a vessel. Figure 3.7 represents a diagrammatic sketch of an air chamber connected to the pipe. The pressure in the vessel, will gradually decrease as water is released until the pressure in the vessel equals that in the adjacent line. At this stage the decelerating water column will tend to reverse. The vessel capacity should be sufficient to ensure no air escapes into the pipeline, and should exceed the maximum air volume required⁽⁶⁵⁾. The air in the vessel will dissolve in the water to some extent and has to be replenished by means of a compressor⁽⁶⁵⁾. A float switch should be set to automatically switch the compressor on when the water level rises above a certain level. A second switch, below the first should switch the compressor off again. An emergency level switch could be installed to switch the pump off if the air volume or water volume was dangerously low. A glass tube for observing the water level should be mounted on the side of the vessel. Air vessels are normally installed at the pumping station in order to protect the whole pipeline.

Assume that the gas follows the polytropic relation:

$$h_g^* V^{n'} = C \quad (3.55)$$

where: h_g^* is the absolute head;
 V is the gas volume;
 n' is the polytropic exponent; and

C is a constant.

If h_{bar} is the barometer reading, then, referring to Fig. 3.7, we have:

$$h_g^* = h + h_{\text{bar}} - z_w - z \quad (3.56)$$

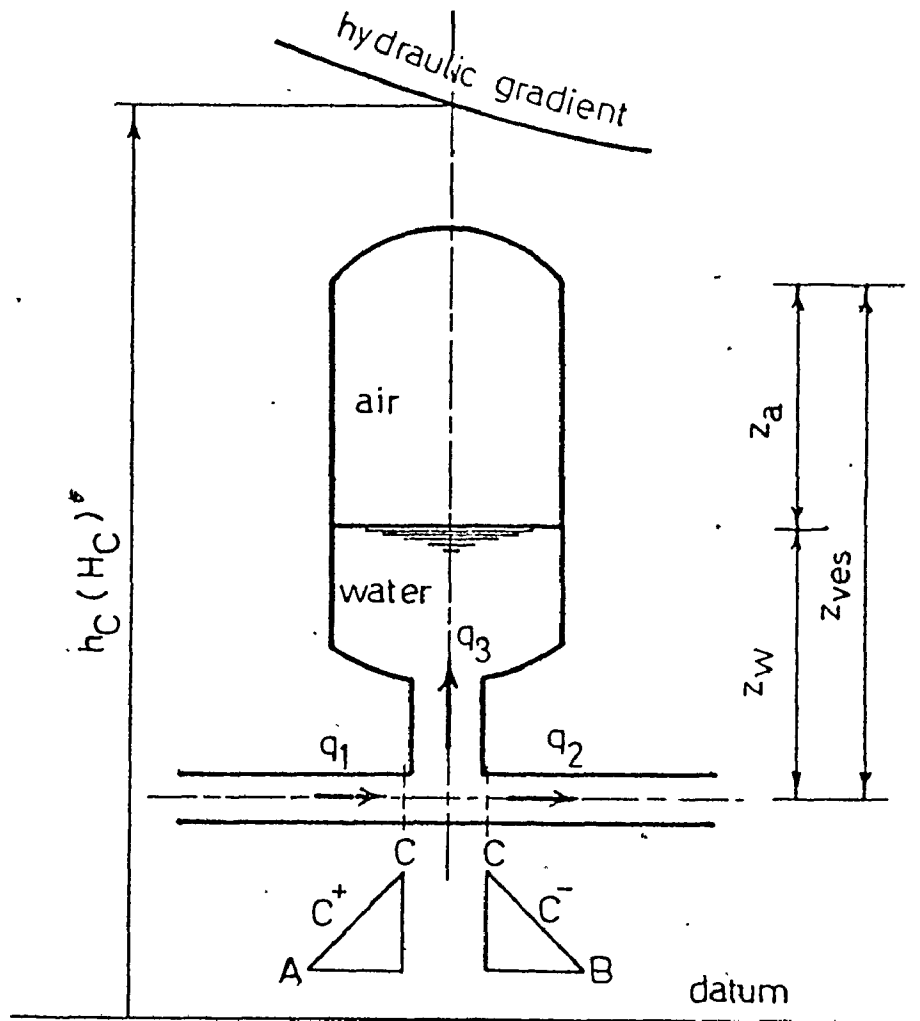


FIG. 3.7: SCHEMATIC FOR PRESSURE VESSEL

Differentiating Eq. (3.55) with respect to time

$$\frac{dh_g^*}{dt} = - \frac{nC}{v^{n+1}} \frac{dV}{dt} \quad (3.57)$$

But we have

$$\frac{dV}{dt} = - \frac{q_3 + q_{C3}}{2} \quad (3.58)$$

Combining Eqs. (3.57) and (3.58)

$$\frac{dh_g^*}{dt} = \frac{nC}{v^{n+1}} \left(\frac{q_3 + q_{C3}}{2} \right)$$

In finite difference form.

$$(h_C - z_{Cw}) - (h - z_w) = \frac{nC}{v^{n+1}} \left(\frac{q_3 + q_{C3}}{2} \right) \Delta t$$

or in dimensionless form

$$H_C - Z_{Cw} - H + Z_w = \frac{nC}{v^{n+1}} \left(\frac{Q_3 + Q_{C3}}{2} \right) \frac{q_o \Delta t}{(av_o/g)}$$

or

$$H_C = C_{11} Q_{C3} + Z_{Cw} + C_{12} \quad (3.59)$$

where:

$$C_{11} = \frac{nC q_o \Delta t}{2v^{n+1} (av_o/g)}$$

and

$$C_{12} = C_{11} Q_3 + H - Z_w$$

We also have

$$z_{Cw} = z_w + \frac{q_3 + q_{C3}}{2} \frac{\Delta t}{A_{ves}}$$

or in dimensionless form

$$z_{Cw} = z_w + \frac{Q_3 + Q_{C3}}{2} \frac{q_o \Delta t}{(a\hat{v}_o/g)A_{ves}}$$

or

$$z_{Cw} = z_w + C_{13}(Q_3 + Q_{C3}) \quad (3.60)$$

where

$$C_{13} = \frac{q_o \Delta t}{2(a\hat{v}_o/g)A_{ves}}$$

The continuity equation at the bottom of the air vessel is

$$Q_{C3} = Q_{C1} - Q_{C2} \quad (3.61)$$

Equations (3.59), (3.60), and (3.61), together with the C^+ and C^- characteristics equations ((3.44) and (3.45)) can be solved simultaneously to find the five unknowns Q_{C1} , Q_{C2} , Q_{C3} , H_C , and z_{Cw} ; as follows:

Adding Eqs. (3.44) and (3.45):

$$2H_C + (Q_{C1} - Q_{C2}) - (C_1 + C_3) = 0$$

and substituting from Eq. (3.61)

$$2H_C + Q_{C3} - (C_1 + C_3) = 0 \quad (3.62)$$

Combining Eqs. (3.59) and (3.60):

$$H_C - C_{11}Q_{C3} - C_{12} = Z_w + C_{13}(Q_3 + Q_{C3}) \quad (3.63)$$

Combining Eqs. (3.62) and (3.63):

$$0.5(C_1 + C_3 - Q_{C2}) - C_{11}Q_{C3} - C_{12} = Z_w + C_{13}(Q_3 + Q_{C3})$$

or

$$Q_{C3}(C_{11} + C_{13} + 0.5) = 0.5(C_1 + C_3) - C_{12} - C_{13}Q_3 - Z_w$$

or

$$Q_{C3} = [0.5(C_1 + C_3) - C_{12} - C_{13}Q_3 - Z_w] / [C_{11} + C_{13} + 0.5] \quad (3.64)$$

H_C , Q_{C1} , Q_{C2} , and Z_{Cw} can be obtained by direct substitution into Eqs. (3.62), (3.44), (3.45), and (3.60); respectively.

If the static head difference between the water surface in the air chamber and the center line of the pipe below the chamber is neglected, then we can get a simpler equation. In this case, Eq. (3.56) is reduced to

$$h_g^* = h + h_{bar} - z \quad (3.65)$$

and Eq. (3.59) is reduced to

$$H_C = C_{11}(Q_3 + Q_{C3}) + H \quad (3.66)$$

Solving Eqs. (3.62) and (3.66) simultaneously

$$Q_{C3} = [0.5(C_1 + C_3) - C_{11}Q_3 - H] / [C_{11} + 0.5] \quad (3.67)$$

H_C , Q_{C1} , and Q_{C2} can be obtained by direct substitution into Eqs. (3.66), (3.44), and (3.45); respectively.

4. DEVELOPMENT OF THE COMPUTER MODEL

The structure of the program is shown schematically in Fig. 4.1. The program is divided into sub-programs, each of which serves the purpose indicated in Fig. 4.1. This increases the flexibility of the program by allowing boundary conditions to be added easily as required. In the present computer model, the pipeline diameter and pipe roughness may not vary from one section to the other.

4.1 Representation of the Pipeline Profile

The pipeline is divided into N sections. The length of each section (Δx) is usually taken constant. If L is the length of the pipeline, then the number of sections $N = L/\Delta x$ and the number of stations equals $(N+1)$. The pipeline elevation at each station is supplied to the computer program as input data. As the distance between stations decreases, the number of sections increases with the result that computation time and cost also increase. The most important points along the profile are the highest points, where the pressure may reach a negative value with the possibility of water column separation; and the lowest points where surges may exceed design heads. These points should be represented in the computer model, even if they are not at the stations. This necessitates moving critical points on the pipeline to

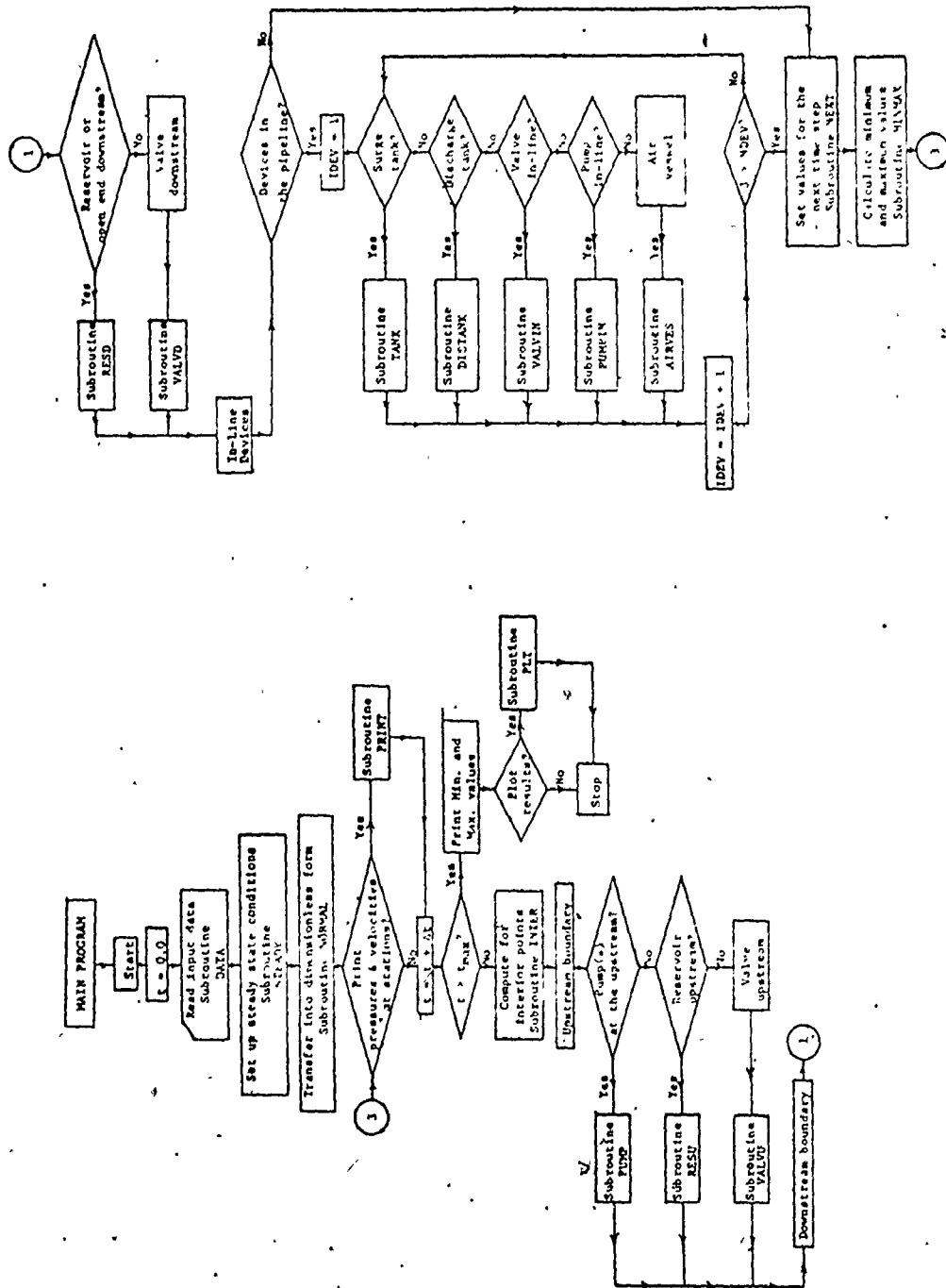


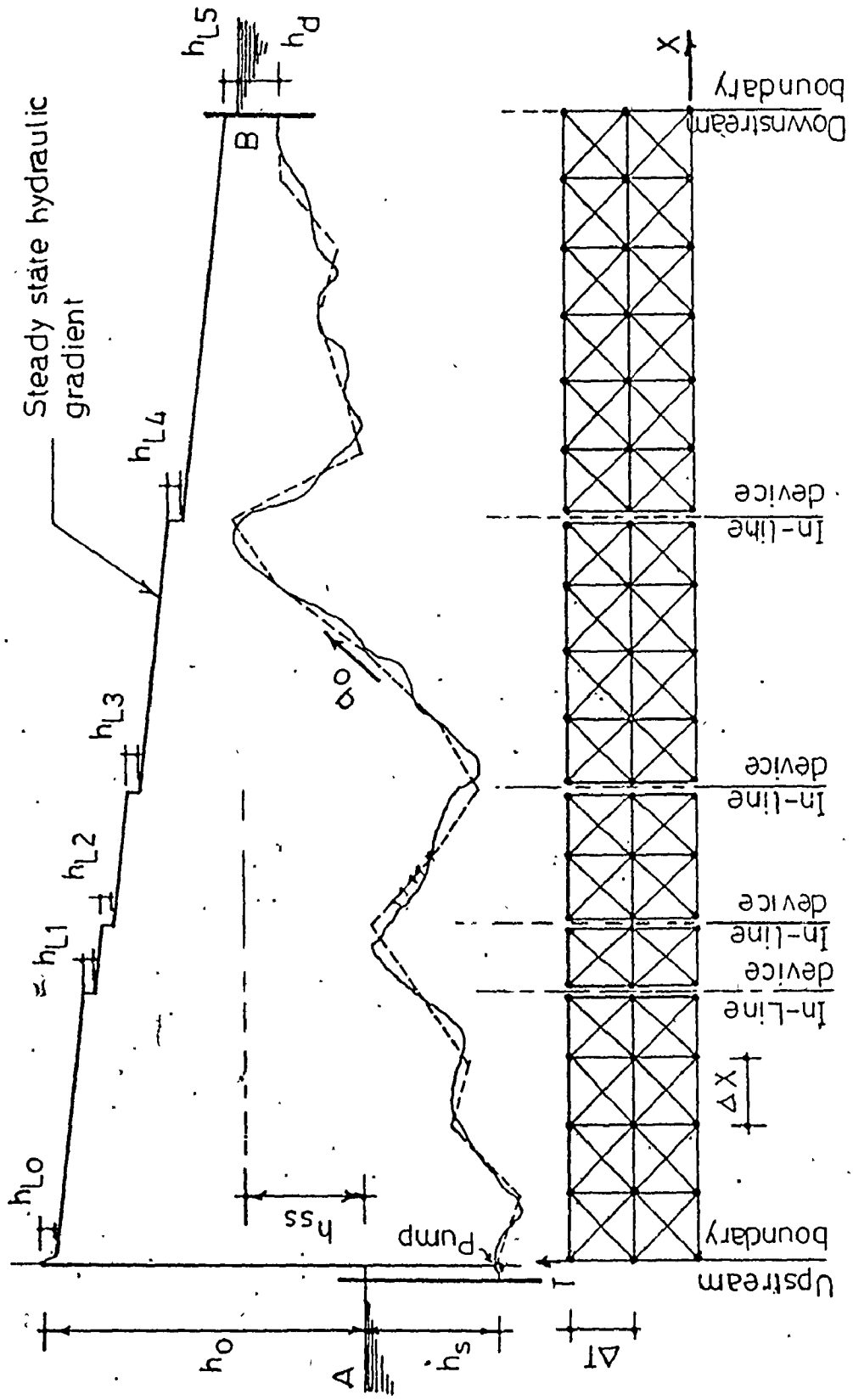
FIG. 4.1: FLOW CHART

the nearest stations, especially the higher points. This provides a better representation of the pipeline than disregarding conspicuous points on the pipeline. However, we should note that the hydraulic gradient for any pipeline is independent of the pipeline profile, except at high points where water column separation is probable.

4.2 General Method

The pipeline shown in Fig. 4.2 connects two reservoirs A and B. A pump is (or a number of pumps in parallel are) used to deliver a steady state discharge q_0 from the lower reservoir A to the higher reservoir B. The suction pipe is so short that it can be neglected. The static head is h_{ss} ; head on suction h_s ; and head on delivery h_d . In the pipeline we have a number of surge control devices. The pipeline is divided into N sections at equal distances Δx . Once again we assume that each device is placed at a station. If in the real pipeline, the device is not placed at a station, then we have to move it slightly to the nearest station. In the computer program we have to supply the number of devices (NDEV) as input data through Subroutine (DATA). Then we have to supply the number of sections between devices N_{si} where $i = 1, 2, \dots, (NDEV+1)$. At each device we have to supply the pipeline elevation twice because we have two nodes there; one at the upstream side of the device and the other at the downstream side.

The program can accept a large number of devices, which can be placed anywhere in the pipeline (a device may be placed at each station).



$$N_{S1} = 4 \quad N_{S2} = 1 \quad N_{S3} = 2 \quad N_{S4} = 4 \quad N_{S5} = 6$$

FIG. 4.2: A HYPOTHETICAL PIPELINE TO ILLUSTRATE THE GENERAL METHOD

The user must specify the devices in the pipeline starting from the upstream end and moving downstream. There is no restriction on the devices or their order.

First, we have to set up the steady state conditions for the given situation. The elevation of the hydraulic grade line at all stations is fixed; as shown in Fig. 4.2: where h_{L0} is the steady state head loss across the discharge valve (if any) at the pump. If no discharge valves are placed at the pump, then h_{L0} is set equal to zero. Also the head loss at the devices h_{Li} where $i = 1, 2, \dots, NDEV$; should be considered when fixing the hydraulic grade line. If the losses at the devices are negligible, then their values are set equal to zero. Having obtained the initial conditions at all stations the solution can be carried out in the X-T plane using a rectangular grid and the explicit method of characteristics as discussed in Chapter 2. We solve first for interior points to find the heads and discharges at the stations between devices, then for the boundary conditions at the upstream and downstream ends. Next we solve for the boundary conditions at the in-line devices. Having done that, the heads and velocities (or discharges) at all stations are known at the end of time interval ΔT . Starting again from these conditions, we similarly obtain the heads and discharges after another time interval ΔT . We continue the solution in this way until the required time for the calculation is reached.

The results can be printed out after each time step giving the heads and velocities at all stations, if desired. Maximum and minimum heads at all stations during the transients can also be printed out. Time of flow reversal, pump speed reversal, and maximum reverse speed of

the pump can be obtained. The time history of pump discharge, pump speed, and head at any station in the pipeline can also be obtained on computer plots; at present accurate to 0.001".

If, in the pipeline, there are no surge control devices, then we input $N_{s1} = N_{s2} = N$; the total number of sections and we are left with only the upstream and downstream boundaries.

If the pump is (or pumps are) connected to suction and delivery pipes, then nothing will be changed except the initial hydraulic grade line. The pump is treated as an internal boundary condition in Subroutine (PUMPIN).

4.3 The Pump

The main objective of the computer program is to compute the transient pressures that follow pump shutdown. The events that follow pump shutdown, the complete pump characteristics, and the pump inertia equation were discussed in Chapter 3 where the boundary condition for the pump was derived. In the computer program, a check valve or gate valve can be placed at the discharge side of the pump or they can be omitted.

At the instant of power failure at the pump motor, the pump speed (α) and discharge (q) are known. The pump starts to decelerate. The first step is to calculate the change in speed ($d\alpha$) during the time interval Δt using the inertia equation (Eq. (3.7)). We start with estimating the torque (β) at the instant of power failure by parabolic

interpolation using the appropriate curve in Figs. (A.1) for centrifugal pump, (A.3) for mixed flow pumps, or (A.5) for axial flow pumps using Subroutine (LESQ). The pump speed change is estimated through Subroutine (SPEED). We assume that the torque (β) remains constant during the time increment Δt . Using the inertia equation, the change in pump speed ($d\alpha_1$) during the time interval Δt is obtained. Adding $d\alpha_1$ to the previous speed (α) yields the new pump speed (α_1). Using this value in the main Subroutine (PUMP), we obtain the new discharge after time Δt , using the appropriate curve in Figs. (A.2) for centrifugal pumps, (A.4) for mixed flow pumps, or (A.6) for axial flow pumps and either Eqs. (3.20) or (3.22) if the suction pipe is so short that it can be neglected; or either Eqs. (3.31) or (3.33) if the pump is connected to suction and delivery pipes. Actually, the torque is not constant during the time interval Δt . To account for that error, we start again considering the new pump speed and discharge. Then we calculate (α_1/q_r) , where q_r is the ratio between pump discharge at any time and the rated pump discharge. Using the appropriate curve in Figs. A.1, A.3, or A.5 as discussed before, we estimate the new torque (β). Having obtained the torque, we again assume that it is constant during next time interval Δt . We then calculate the change in pump speed ($d\alpha_2$), and set the change in pump speed equal to the average of the two values:

$$d\alpha = 0.5(d\alpha_1 + d\alpha_2)$$

Thus we can more accurately estimate the new pump speed by adding $d\alpha$ to the initial pump speed α . We can then use the appropriate equation

((3.20), (3.22), (3.31), or (3.33)) to calculate the new discharge at the end of the time interval.

We repeat this procedure starting from the new conditions until the required time is reached. If the discharge is reversed while the pump is still rotating in the forward direction (zone of energy dissipation), the calculations will continue in the same way except that we have to use the pump characteristics for the energy dissipation zone. Once the pump speed reverses (zone of turbine operation), then we have to use the pump characteristics for that zone. To estimate the discharge when the pumps are operating in either the energy dissipation or turbine operation zones, we have to use either Eqs. (3.21) or (3.23) instead of Eqs. (3.20) and (3.22) when the suction pipe is neglected and either Eqs. (3.32) or (3.34) instead of Eqs. (3.31) and (3.32) when the pump is connected to both suction and discharge pipes.

If the discharge valve is completely closed during the water hammer transients, then the pump is separated from the calculations and we have to set the discharge at the pump equal to zero.

5. VALIDATION OF THE COMPUTER MODEL

The computer program has been used for different pipelines, where water hammer is caused by either (a) valve operation or (b) power failure at pump motors (with emphasis on case b). Different boundary conditions are checked against field tests whenever published data were available. In other situations, comparison with the graphical method of solution is presented. Water hammer charts by Parmakian⁽⁴⁹⁾, Kinno and Kennedy⁽⁵⁶⁾, and those by Evans and Crawford⁽⁵²⁾ are also used to check the computer results whenever relevant (the air chamber will be checked later in Chapter 6). When data were not available, the computer results are investigated and shown to be valid. The effects of valve operation at the pump, pump and motor inertia, and friction losses on the water hammer transients are also investigated. Computer plots are shown to be useful in presenting the results.

5.1 Water Hammer Due to Valve Operation

The program deals primarily with pump discharge lines, yet it can also compute water hammer transients resulting from arbitrary valve operation. Valves closure may be instantaneous or gradual.

5.1.1 Valve Operation at the Downstream End of a Pipe. Consider the simple case of a pipe connected to a reservoir at the upstream end with a

valve placed at the downstream end to control flow. Any movement of the valve to reduce (or increase) the flow is accompanied by a pressure rise (or pressure drop). For closure, a positive pressure wave is created at the valve which travels upstream at the velocity of sound (a) where it reflects negatively at the reservoir. This wave then travels downstream where it now reflects positively and travels upstream again. If the pipe is frictionless, this sequence will continue for an infinite time. Friction resistance in the pipe will attenuate the resulting pressure amplitudes; the higher the pipe friction, the more rapid is the damping.

5.1.1.1 Sudden Valve Closure. The pressure rise resulting from sudden valve closure can be estimated from the Joukowski Law ($h = av_0/g$).

Using the data for the pipeline in Fig. 5.1, the pressure rise due to sudden valve closure is 1000.0 ft. The time required by the pressure wave to reach the upstream reservoir (L/a) is equal to 1.0 second.

Figure 5.1 presents the transient pressure distribution at four different sections along the pipeline, as obtained from the computer program. The pressures and the wave travel times are in agreement (a description of wave phenomena due to sudden valve closure can be found elsewhere (49)).

In Fig. 5.1 the pipeline was assumed frictionless.

5.1.1.2 Gradual Valve Closure. Figure 5.2 represents a pipeline similar to that shown in Fig. 5.1. Figure 5.3 presents the pressure transients adjacent to the valve and at the midlength of the pipe resulting from the gradual valve closure shown in Fig. 5.4. Superimposed on the results obtained from the computer program are those obtained from an analytical

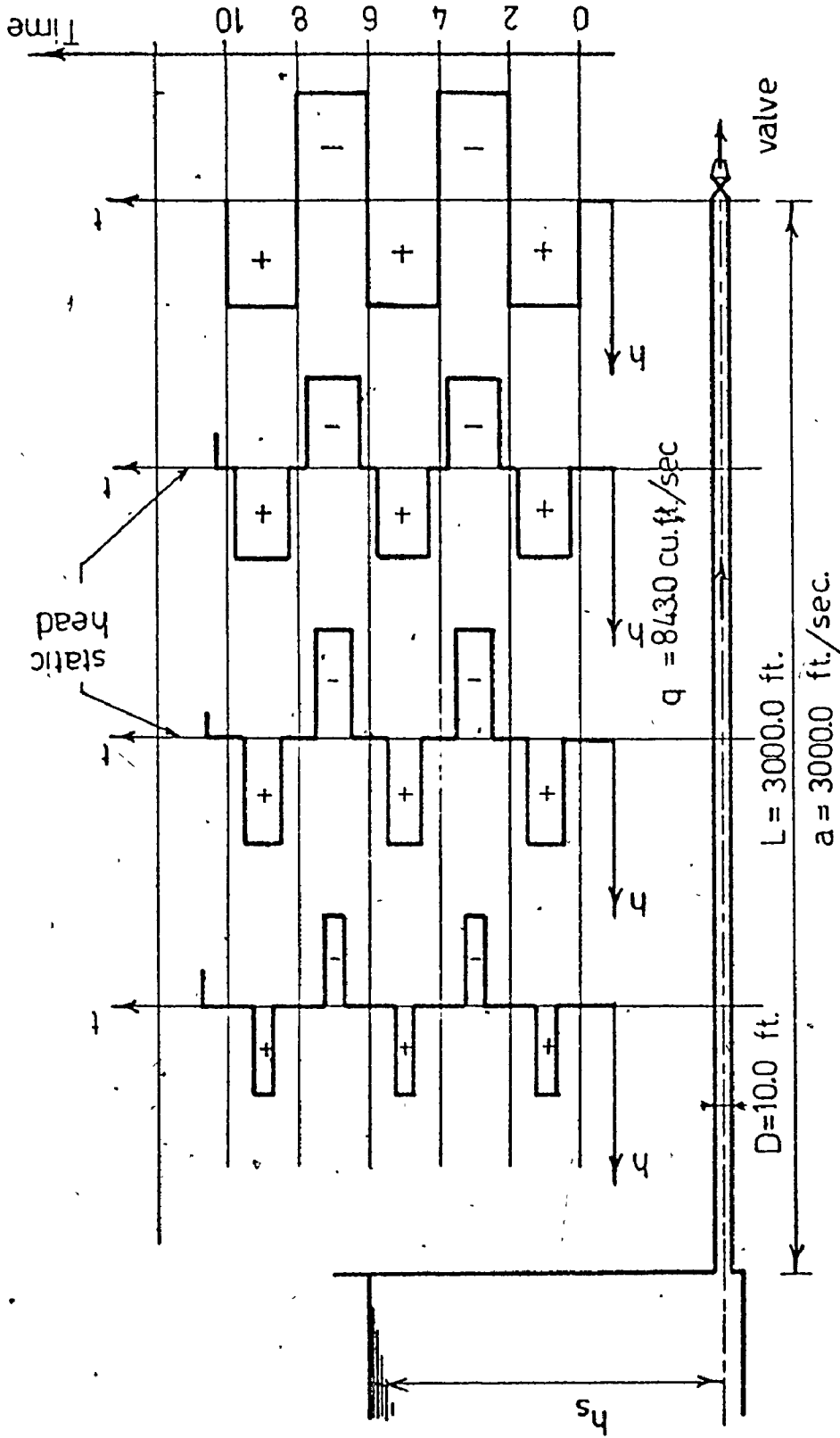


FIG. 5.1: PRESSURE DISTRIBUTION ALONG PIPE DUE TO SUDDEN VALVE CLOSURE

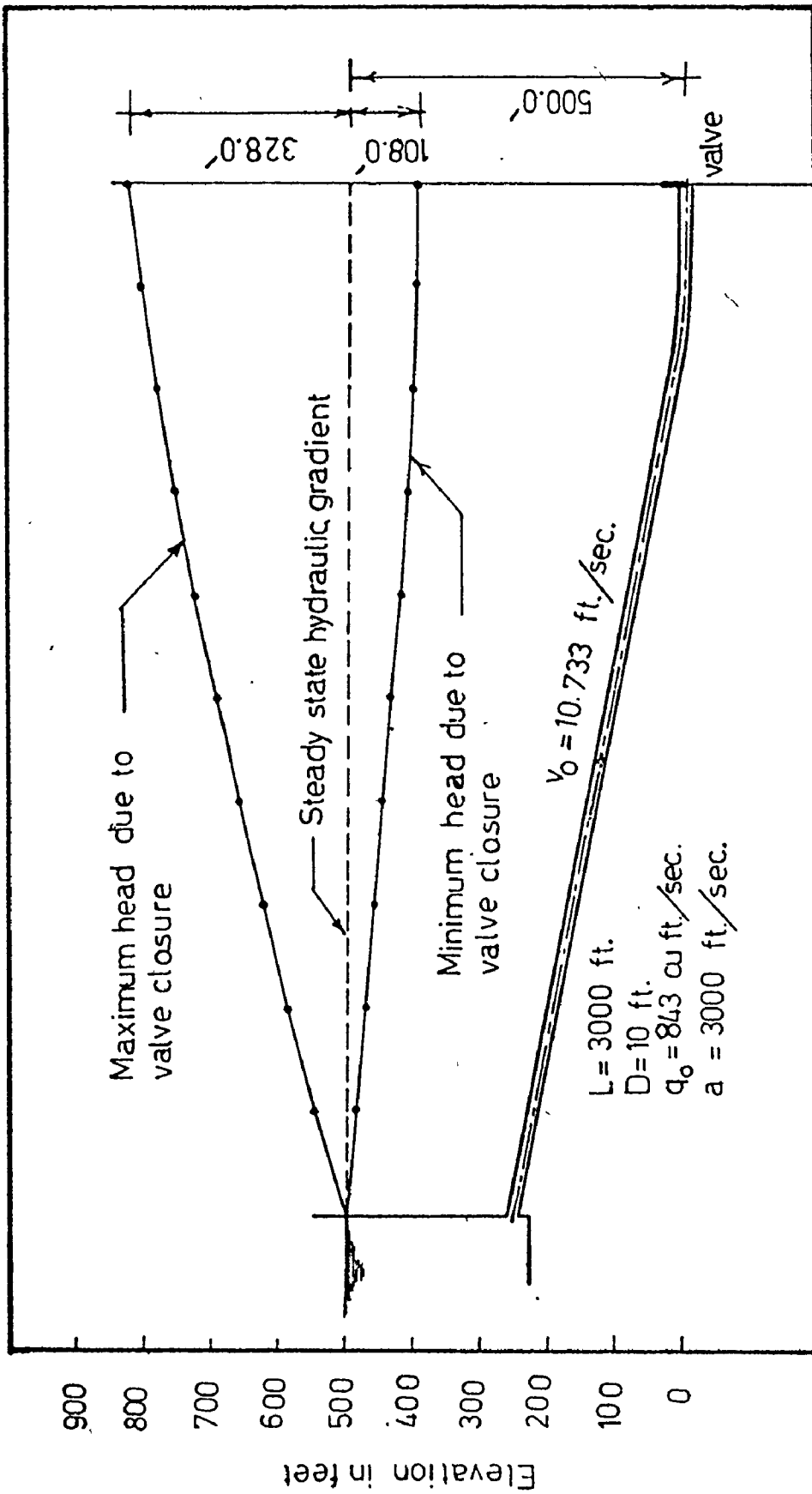


FIG. 5.2: MAXIMUM AND MINIMUM PRESSURES ALONG THE PIPE DUE TO GRADUAL VALVE CLOSURE AT THE DOWNSTREAM END

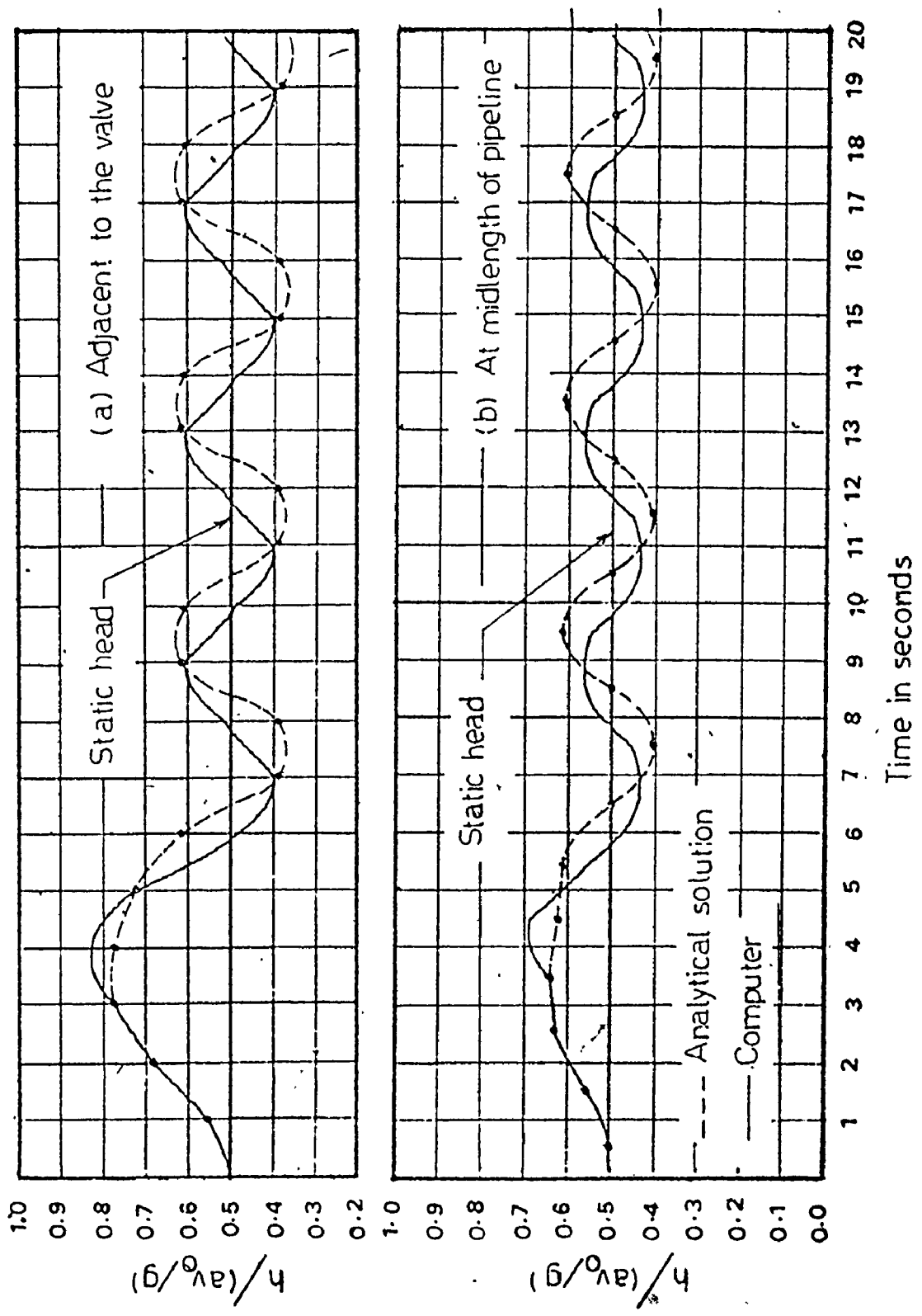


FIG. 5.3: PRESSURE TRANSIENTS DUE TO GRADUAL VALVE CLOSURE -
COMPARISON WITH AN ANALYTICAL SOLUTION

solution⁽⁴⁹⁾. The agreement is excellent for the early stages of closure, but a slight discrepancy appears at the late stages of closure. We note here that an accurate determination of the instantaneous gate position is critical in computing the resulting water hammer pressures. In the analytical solution⁽⁴⁹⁾, τ was taken at time intervals of 1.0 second, while in the computer program, the time step for the calculation was set at 0.1 second and τ was estimated at each time step by parabolic interpolation. This may account for the discrepancy between the results. In addition, Fig. 5.2 presents the resulting envelopes of maximum and minimum pressures along the pipeline. In the above analysis,

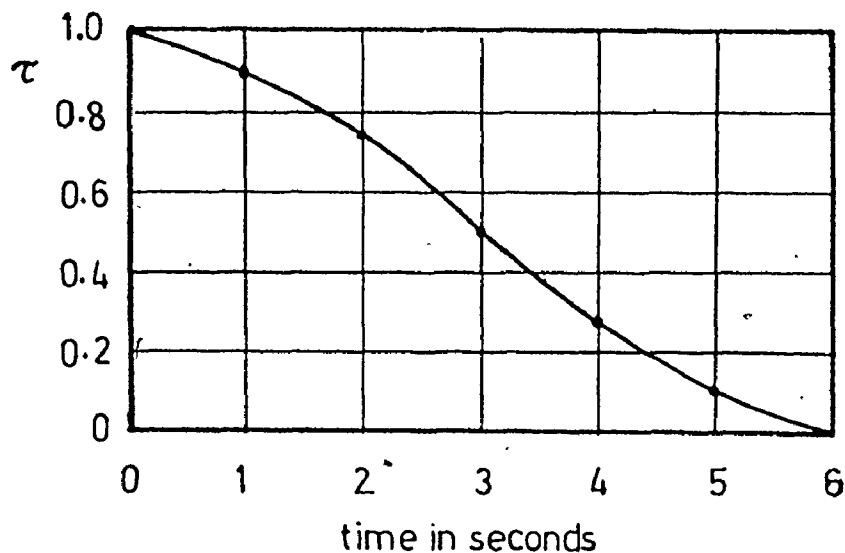


FIG. 5.4: VALVE CLOSURE TIME RELATIONSHIP

pipe friction is small. For the data presented in Fig. 5.2, the wave travel time (L/a) is 1.0 second. This means that the period of the

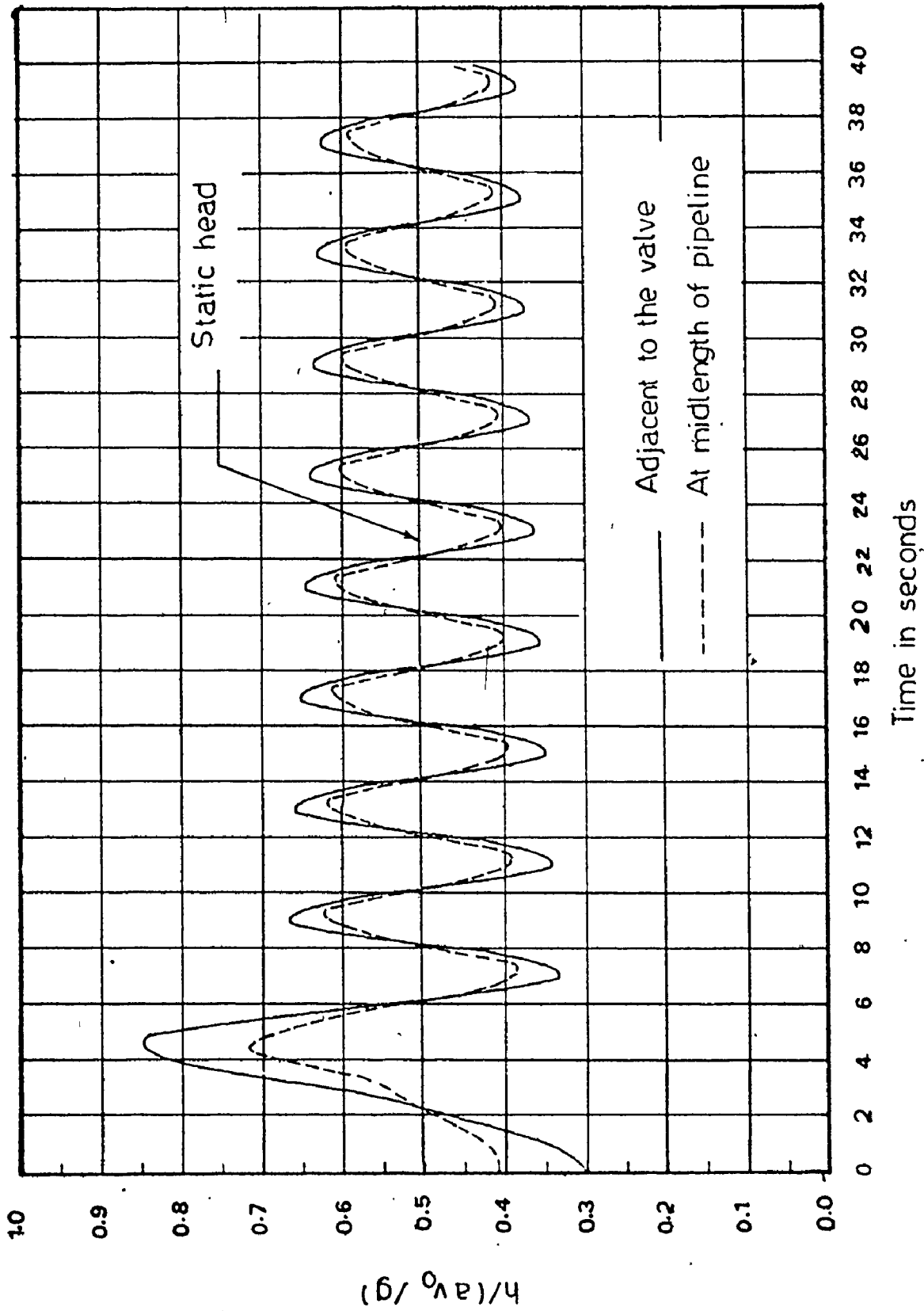


FIG. 5.5: EFFECT OF FRICTION ON THE PRESSURE TRANSIENTS DUE TO GRADUAL VALVE CLOSURE AT THE DOWNSTREAM END OF A PIPE

pressure wave (peak to peak) is 4.0 seconds which agrees with Fig. 5.3. Figure 5.5 presents the pressure variations at the valve and at the midlength of the pipe for the same pipe and valve closure, but with a steady state head loss 30% of the static head. The effect of friction on damping can be observed.

5.1.2 Valve Operation at the Upstream End of a Pipe. Figure 5.6 represents a pipeline connecting two reservoirs with a valve adjacent to the upstream reservoir. When the valve is closed, a negative pressure wave is created, which reflects negatively when it reaches the downstream reservoir. Figure 5.7 depicts the pressure transients adjacent to the valve and at the midlength of the pipe. For the data and valve closure shown in Fig. 5.6, the pressure in the pipe, adjacent to the valve drops to a value of -32.0 ft of water. This pressure is close to the vapour pressure of water. If the steady state discharge is increased, the possibility of water column separation, starting at the valve, is high. The envelopes of maximum and minimum pressure along the pipe are plotted in Fig. 5.6. For the data presented, $L/a = 1.0$ second, and wave period is 4.0 seconds which agrees with Fig. 5.7.

5.1.3 Surge Tank Near the Downstream Valve. In this section, the results for surge tanks obtained from the computer program are proved to be valid. Consider the simple surge tank installation shown in Fig. 5.8 where the initial flow through the control gate is cut off rapidly. The surge tank oscillations due to the water hammer pressure waves are presented in Fig. 5.9. The amplitudes of the oscillations attenuate rapidly due

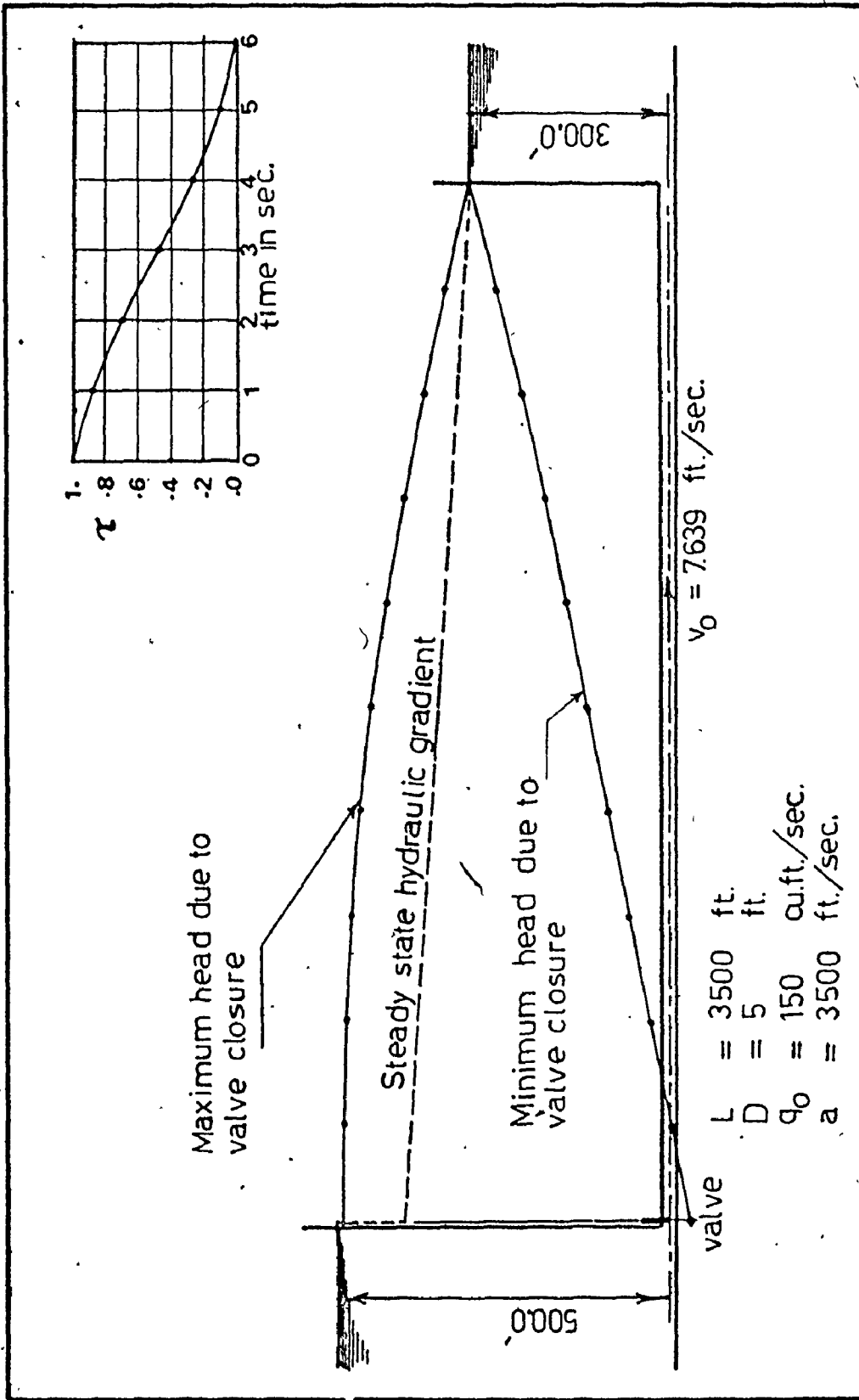


FIG. 5.6: MAXIMUM AND MINIMUM PRESSURES ALONG THE PIPE DUE TO GRADUAL VALVE CLOSURE AT THE UPSTREAM END

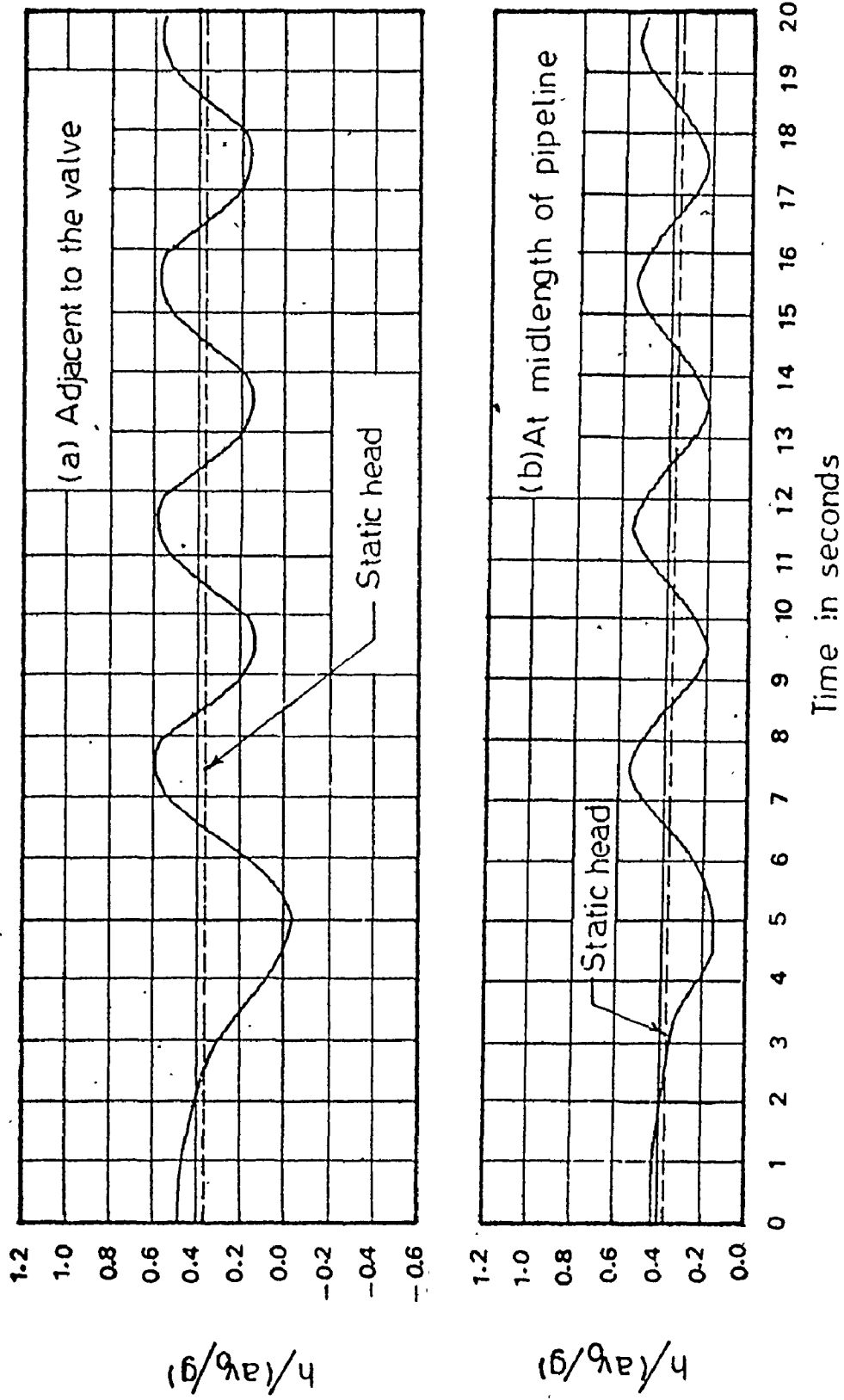


FIG. 5.7: PRESSURE TRANSIENTS DUE TO GRADUAL VALVE CLOSURE AT THE UPSTREAM END OF A PIPE

to friction effects. In Fig. 5.8, the envelopes of maximum and minimum pressure along the pipeline are plotted. A comparison with Fig. 5.2, where no surge tanks were used, shows the effect of the surge tank on reducing the pressures along the pipeline.

Parmakian⁽⁴⁹⁾ presented charts that can be used to determine the surge resulting from an instantaneous stoppage of the flow at either a turbine or pump installation. These charts can be used for the determination of the maximum surge at the tank. Referring to the surge tank installation shown in Fig. 5.8: S is the maximum surge measured from the operating level, and h_f is the pipe losses between the surge tank and the reservoir. In the charts, Parmakian uses

$$\begin{aligned} h_{f1} &= h_f + \frac{v^2}{2g} \\ &= 51.3 + \frac{(10.733)^2}{2 \times 32.2} = 53.0 \text{ ft} \end{aligned}$$

and this gives

$$\frac{S}{h_{f1}} = 2.3 \text{ ,}$$

and the upsurge becomes

$$S_{\text{charts}} = 2.3 \times 53 = 122.0 \text{ ft .}$$

From the computer program

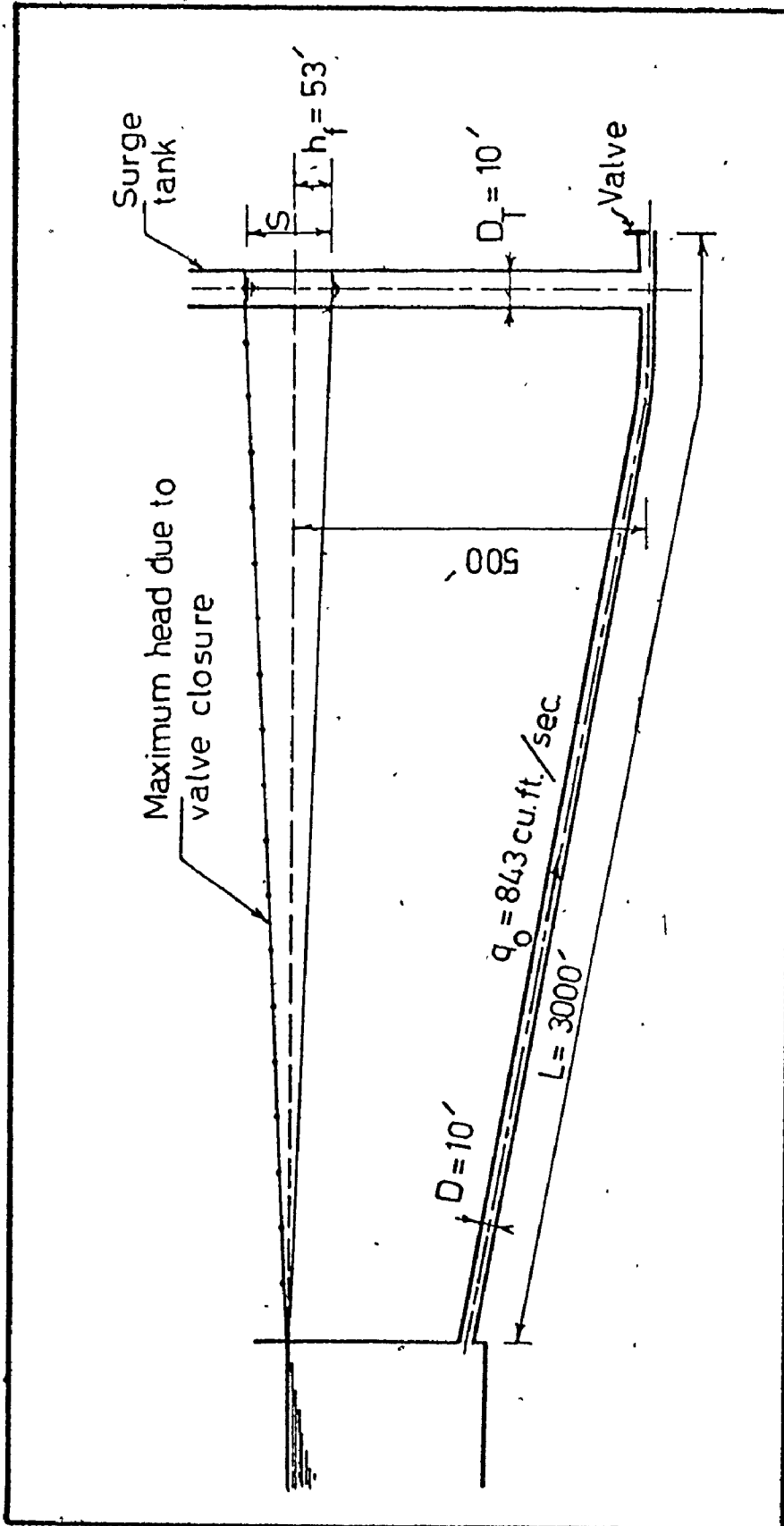


FIG. 5.8: EFFECT OF SURGE TANK ON REDUCING THE TRANSIENT PRESSURES ALONG THE PIPELINE

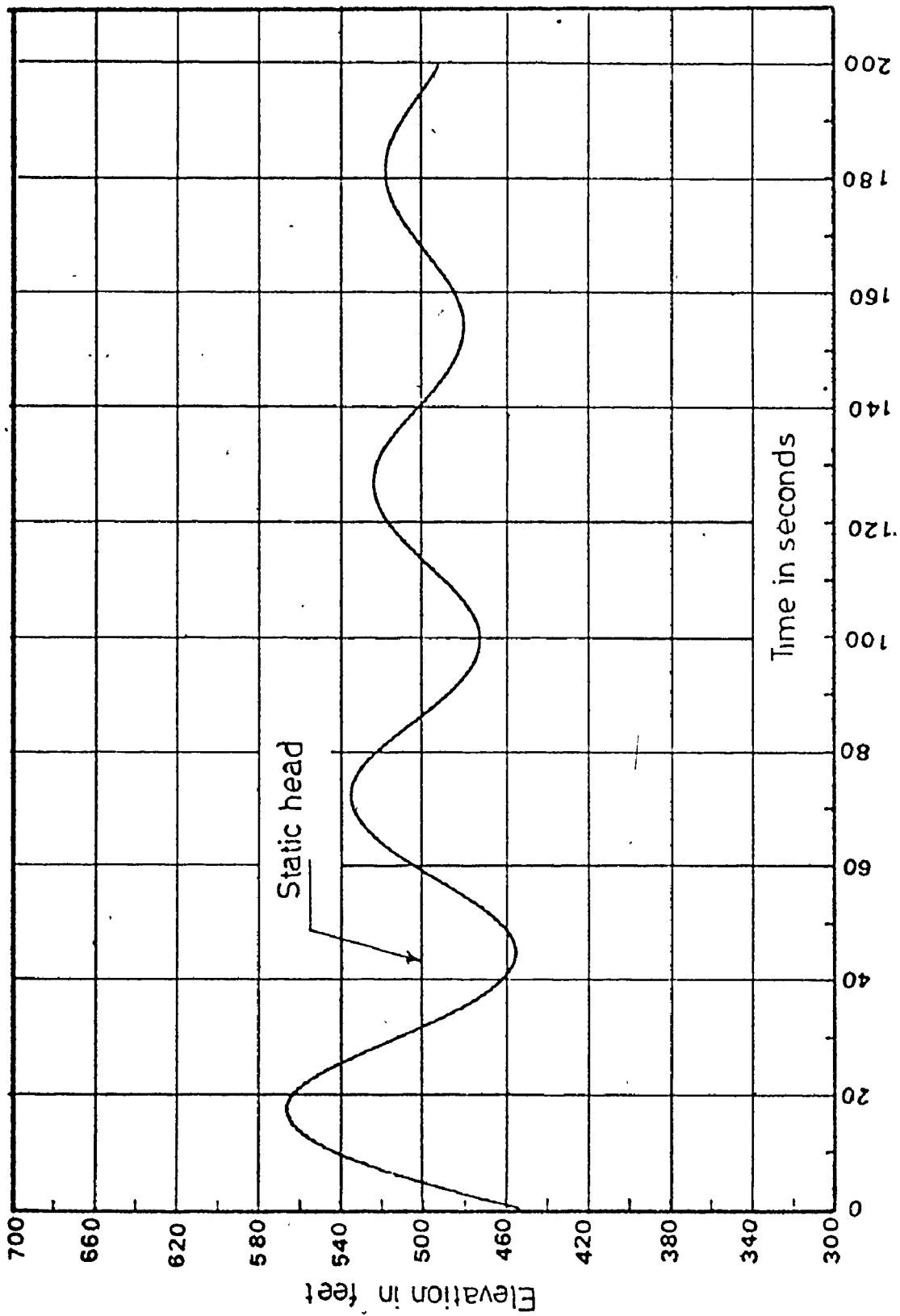


FIG. 5.9: SURGE LEVELS IN A SIMPLE SURGE TANK

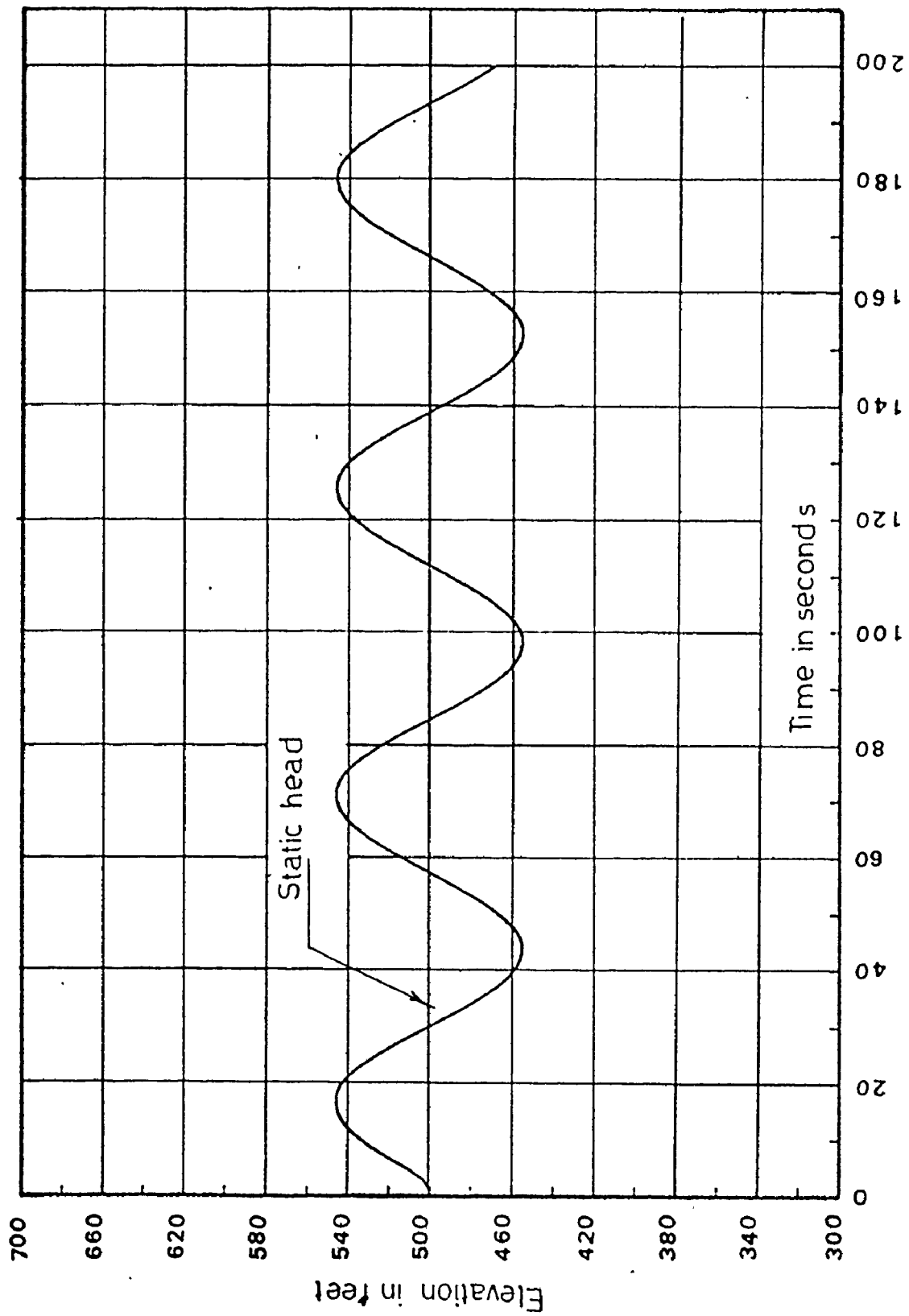


FIG. 5.10: SURGE LEVELS IN A SIMPLE SURGE TANK; WITH PIPE FRICTION NEGLECTED

$$S_{\text{program}} = 121.30 \text{ ft}$$

If the pipeline is frictionless, the surge tank oscillations will continue for an infinite time. Figure 5.10 represents such oscillations for the same installation shown in Fig. 5.8, but with pipe friction neglected.

5.2 Water Hammer Due to Pump Shut-Down

In this section, various pump discharge lines are considered with the pump(s) connected directly to the suction reservoir or through a suction pipe. At the pump discharge side there may be (a) a check valve, which closes rapidly at the instant of flow reversal at the pump; (b) a butterfly discharge valve, which closes gradually upon power failure in a prescribed manner; or (c) no valves at the pumps.

5.2.1 Pumps Without Any Discharge or Check Valves Connected Directly to the Suction Reservoir. Parmakian⁽⁴⁸⁾ used the graphical

solution to compute the pressure surges in the pump-discharge line, shown in Fig. 5.11 subsequent to power failure at all three pump motors. The pumps are not provided with any discharge or check valves. Data relevant to water hammer calculation used in Parmakian's solution are as follows:

Length of pump discharge line	L = 3940 ft
Diameter of discharge line	D = 32 in

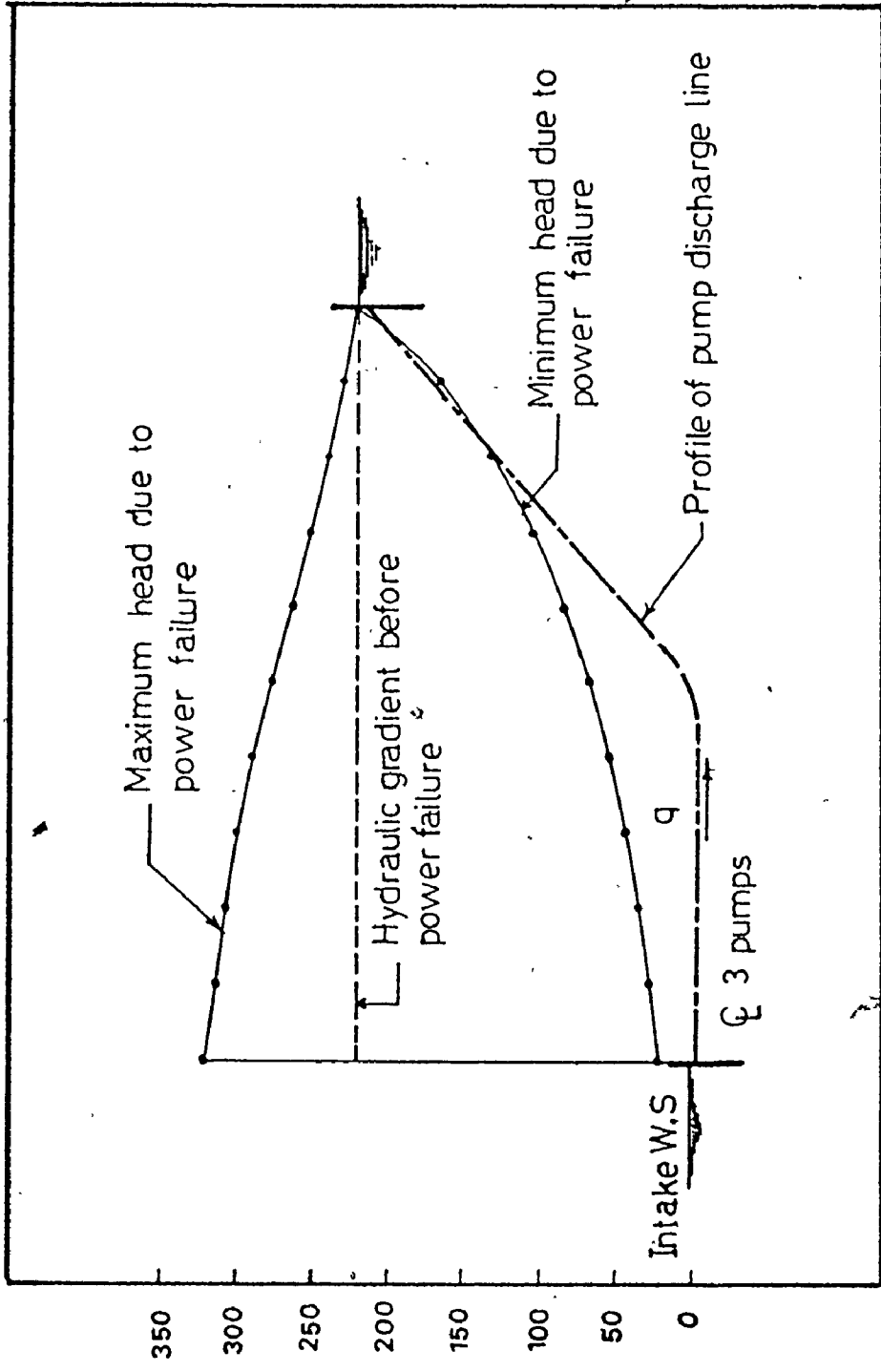
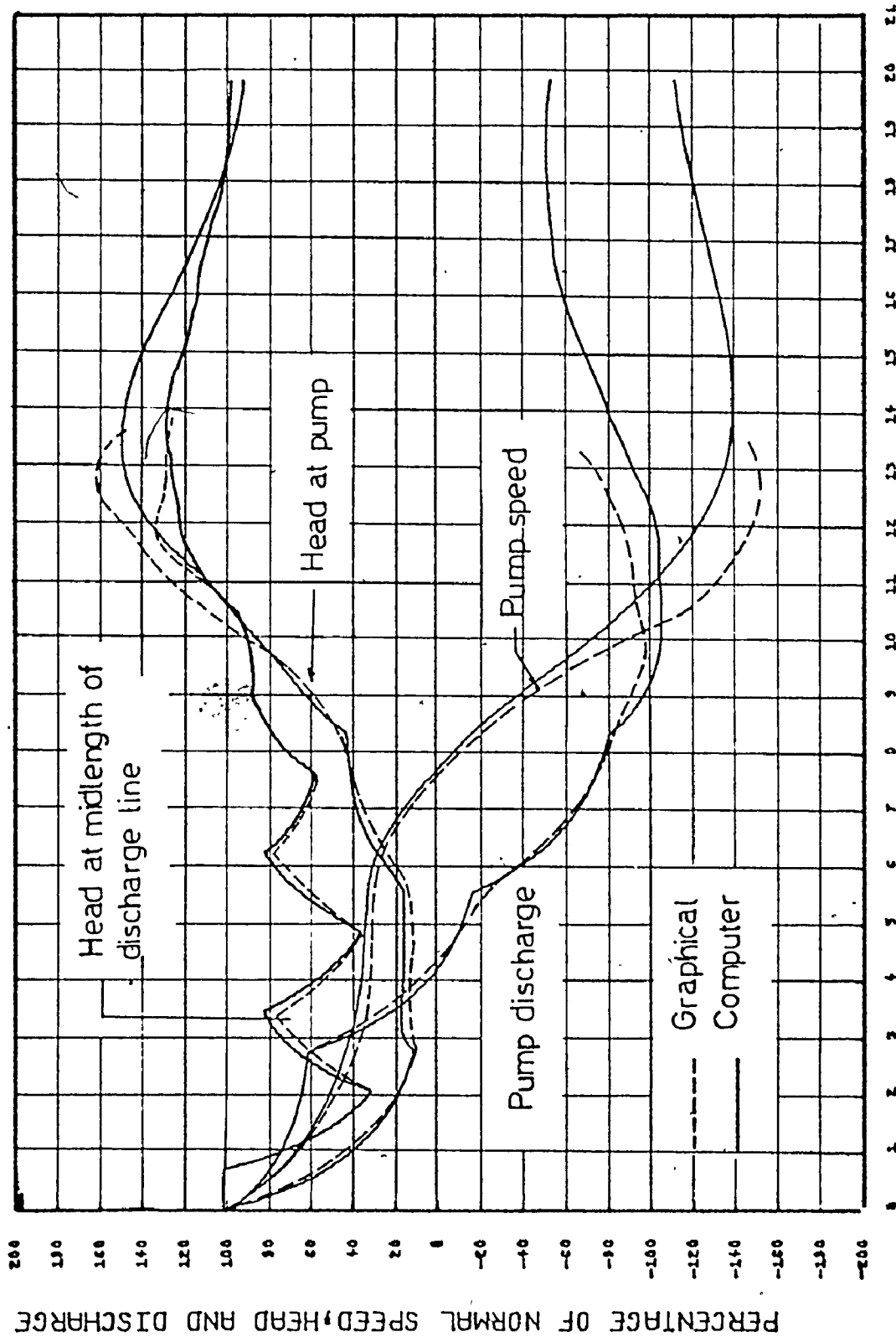


FIG. 5.11: TRANSIENT PRESSURE GRADIENTS DUE TO POWER FAILURE AT PUMP MOTORS

Pump discharge	$q_R = 33.7$ cu.ft/sec (for 3 pumps)
Pumping head	$h_R = 220$ ft
Motor speed	$N_R = 1760$ rpm
Inertia for each pump and motor	$WR^2 = 384.9$ lb.ft ²
Pump efficiency	$\eta_R = 84.7\%$
Pressure wave celerity	$a = 2820$ ft/sec
Pump specific speed	$N_s = 1998$ (gpm units)

In the graphical solution, friction was neglected and it was assumed that the pumping head is equal to the static head. In the computer program, the complete pump characteristics for the zones of normal, energy dissipation, and turbine operation as given in Figs. A.1 and A.2, and in Table A.1 are used. A time history of the flow, motor speed, and head at the pump and midlength of discharge line as obtained from the computer program is plotted in Fig. 5.12. Superimposed on it, are the results obtained from the graphical solution. The agreement is especially good in the zones of normal pump and energy dissipation.

Kinno and Kennedy⁽⁵⁶⁾ derived water hammer charts that can predict the maximum and minimum heads at the pump and at the midlength of discharge line. The charts can also predict the time of flow reversal at the pump. Table 5.1 gives a comparison of the results obtained from (a) the graphical solution, (b) water hammer charts, and (c) the computer program, for the same pump discharge line shown in Fig. 5.11 (in Table 5.1 the heads are related to the rated pumping head). Also, in Fig. 5.11 is presented a plot of the maximum and minimum pressures along the pipeline resulting from shut-down of the pumps.



TIME IN SECONDS AFTER POWER FAILURE

FIG. 5.12: TRANSIENT CONDITIONS DUE TO POWER FAILURE - COMPARISON BETWEEN GRAPHICAL ANALYSIS AND COMPUTER RESULTS

PERCENTAGE OF NORMAL SPEED, HEAD AND DISCHARGE

Method	Minimum head at pump	Minimum head at midlength	Maximum head at pump	Maximum head at midlength	Time of flow reversal at pump (seconds)
Graphical Analysis	0.08	0.31	1.61	1.35	4.22
Water hammer charts (56)	0.10	0.32	1.54	1.28	4.19
Computer Program	0.12	0.31	1.46	1.29	4.23

TABLE 5.1: COMPARISON WITH PARMAKIAN'S GRAPHICAL ANALYSIS AND KINNO'S CHARTS

5.2.2 Pumps with Butterfly Discharge Valves Connected Directly to the Suction Reservoir.

The Tracy Pumping Plant. The Tracy Pumping Plant is located in the Central Valley Project near Tracy, California. Briefly, the pumping plant consists of six large pumping units with each pair of pumps connected through a wye branch to a 15-foot diameter reinforced concrete pipe. The general arrangement and description of the plant is given by Parmakian (66).

Data used for water hammer calculations are:

Length of pump discharge line	$L = 5130 \text{ ft}$
Diameter of discharge line	$D = 15 \text{ ft}$
Pressure wave celerity	$a = 2930 \text{ ft/sec}$
Pump discharge	$q_R = 767 \text{ ft}^3/\text{sec}$
Rated pumping head	$h_R = 197 \text{ ft}$
Motor speed	$N_R = 180 \text{ rpm}$
Motor inertia	$WR^2 = 3500000 \text{ lb.ft}^2$
Pump and entrained water inertia	$WR^2 = 540000 \text{ lb.ft}^2$
Pump efficiency	$\eta_R = 0.73$
Specific speed	$N_s = 1834 \text{ (gpm units)}$

Each pump has a butterfly valve on the discharge side. Upon power failure at the pump motors, the butterfly valves close rapidly under the action of a servomotor. This mechanism rotates the flap through the first two thirds of the angular movement in 14 seconds and the remaining one third in an additional 46 seconds⁽⁶⁶⁾. The valve has an open area of about 47.9 square feet and a 82 degree angle of rotation of the valve leaf. The open area of the butterfly valve normal to the axis of the pipe is approximately

$$A_v = 47.9 \left(1 - \frac{\sin \theta}{\sin 82^\circ}\right)$$

The flow through the butterfly valve is

$$q = C_d A_v \sqrt{2gh_{Lv}}$$

Assuming a coefficient of discharge of 0.7⁽⁶⁶⁾, the initial head loss through the valve is 8 ft.

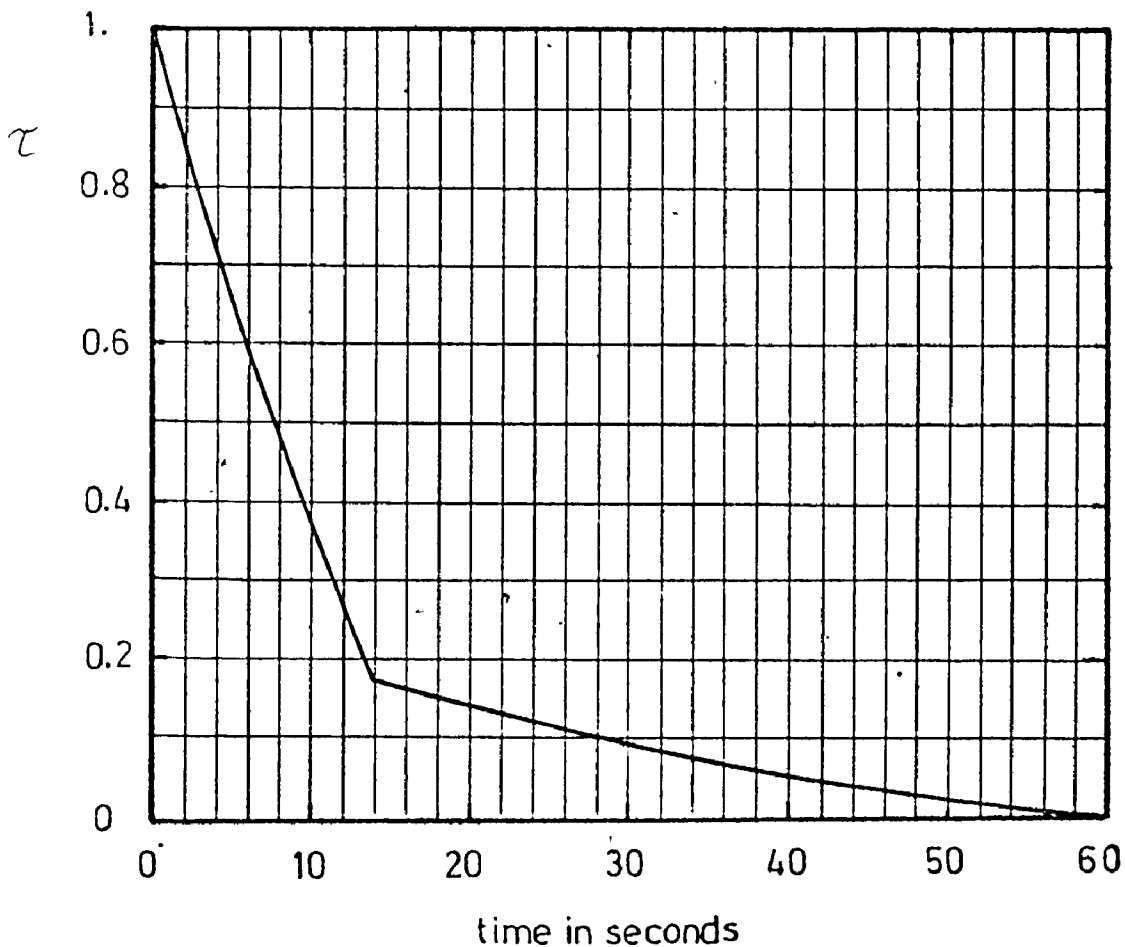
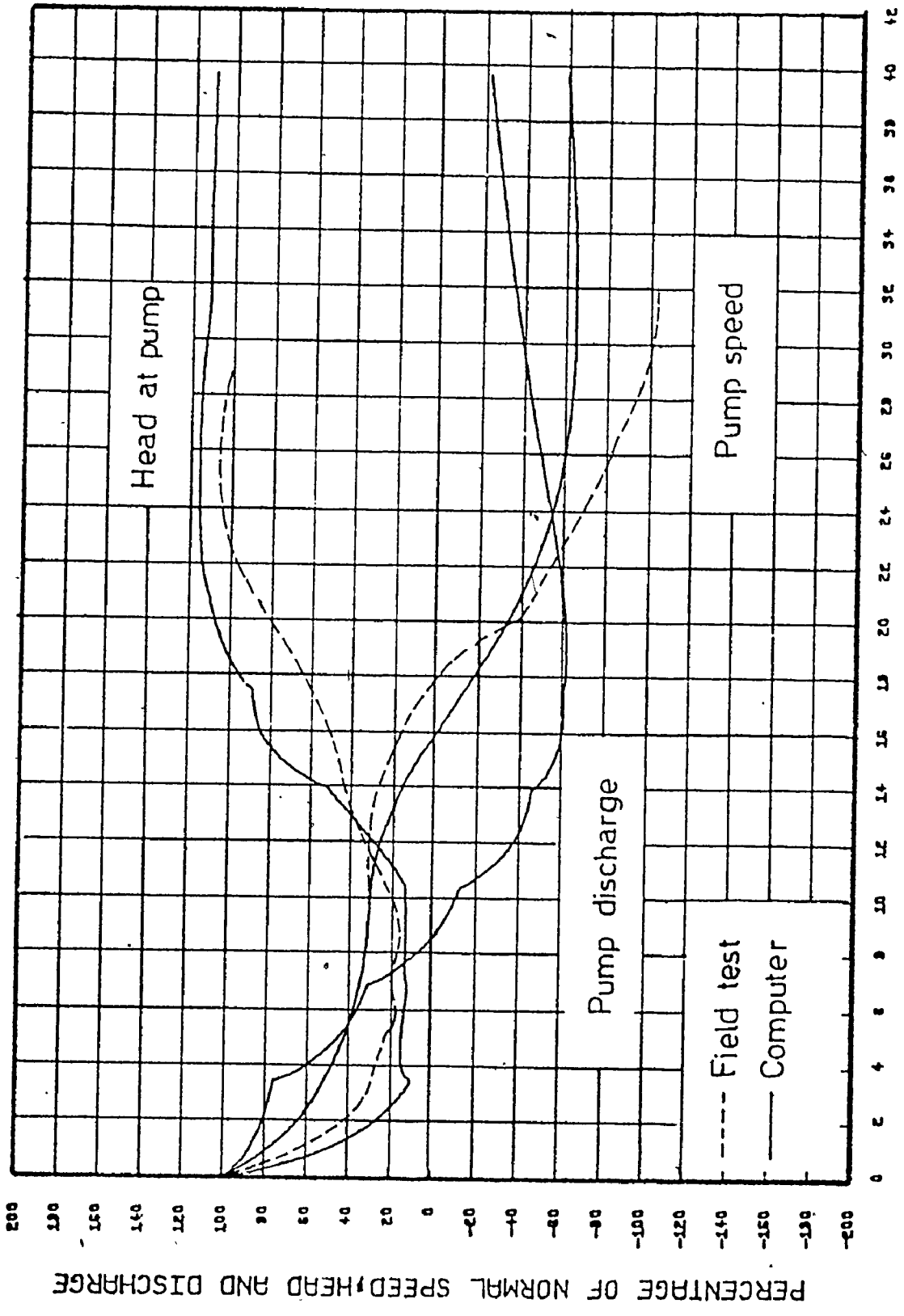


FIG. 5.13: THE TRACY PUMPING PLANT - BUTTERFLY VALVE CLOSURE RELATION

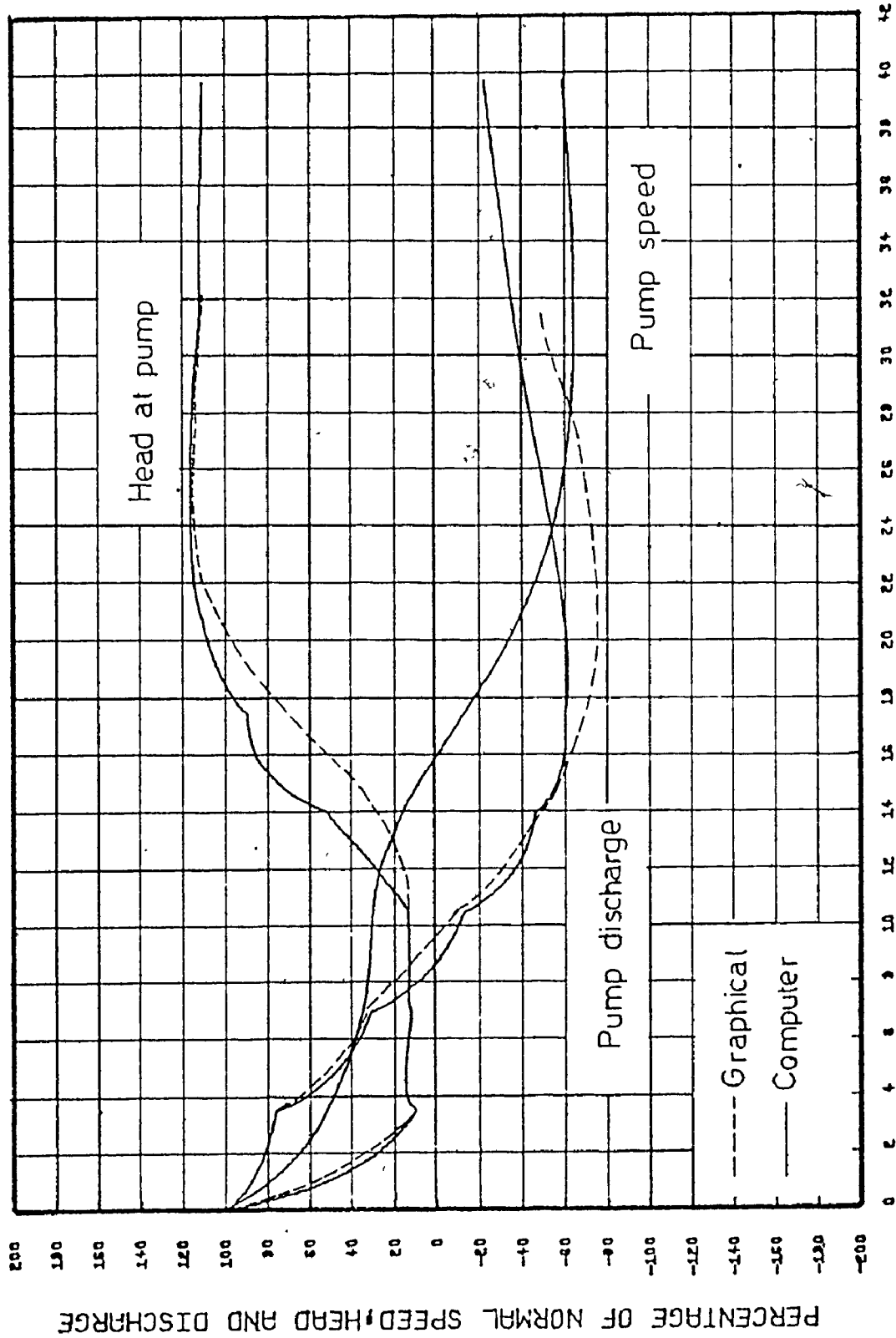
The valve closure relationship is plotted in Fig. 5.13. Figures 5.14 and 5.15 present a comparison between (a) computer results, (b) field tests, and (c) the graphical solution by Parmakian⁽⁶⁶⁾. The comparison is especially good in the zone of normal pump operation, but the computer



TIME IN SECONDS AFTER POWER FAILURE

FIG. 5.14: THE TRACY PUMPING PLANT - TRANSIENT CONDITIONS DUE TO POWER FAILURE - COMPARISON BETWEEN FIELD TESTS AND COMPUTER RESULTS

PERCENTAGE OF NORMAL SPEED, HEAD AND DISCHARGE



TIME IN SECONDS AFTER POWER FAILURE

FIG. 5.15: THE TRACY PUMPING PLANT - TRANSIENT CONDITIONS DUE TO POWER FAILURE - COMPARISON BETWEEN GRAPHICAL ANALYSIS AND COMPUTER RESULTS

7

gives somewhat lower values for the pump speed reversal when compared with that obtained from field tests. The maximum head at the pump as obtained from the computer program is about 10% higher than that observed from field tests, but it is nearly the same as that obtained from the graphical analysis. The discrepancy between the test results and those obtained from both the graphical analysis and the computer program may be due to the incorrect assumption of the coefficient of discharge which was assumed, as suggested by Parmakian⁽⁶⁶⁾, to be taken 0.7.

5.2.3 Pumps Connected to Both Suction and Delivery Pipes.

The Granby Pumping Plant. The Granby Pumping Plant is located on the Colorado-Big Thompson Project near Granby, Colorado. The general arrangement of the plant is given by Parmakian⁽⁴⁸⁾. Three pumps in parallel feed the pipeline. In the actual pipeline there are butterfly valves on both the inlet and discharge outlet of each pump. Upon power failure at the pump motors, the butterfly valves close rapidly under the action of a servomotor. Water hammer tests were run for one, two, and three pumps in operation. For lack of complete valve closure data, we can check the results obtained from the computer program against the tests in which the butterfly valves were held open after power failure. We can also check the downsurge, which is not affected by the valve closure.

Data relevant for water hammer calculations are:

Length of discharge pipe	$L_d = 3650.0 \text{ ft}$
Length of suction pipe	$L_s = 574.0 \text{ ft}$

Pressure wave celerity	$a = 3200 \text{ ft/sec}$
Pump discharge	$q_R = 200 \text{ cu.ft/sec}$
Pumping head	$h_R = 131 \text{ ft}$
Motor speed	$N_R = 327 \text{ rpm}$
Motor inertia	$WR^2 = 410000 \text{ lb.ft}^2$
Inertia of pump and entrained water	$WR^2 = 64500 \text{ lb.ft}^2$
Pump efficiency	$\eta_R = 0.72$
Specific speed	$N_s = 2310$

The water hammer tests were conducted with a pump intake submergence of 60.0 ft. Neglecting friction losses, the discharge head at the pump is 191.0 ft. A field test was run for one pump in operation, with the discharge valve held open after power failure. Figure 5.16 presents the pump speed, pump discharge, head at pump, and head at midlength of discharge pipe as well as a similar plot for 3 pump operation. A comparison between (a) test observations, (b) computer results, and (c) results from water hammer charts by Parmakian⁽⁴⁹⁾ is presented in Table 5.2. In order to use the water hammer charts by Parmakian, two independent parameters need to be estimated, viz ρ : the pipeline constant, and $K = K_1(2L/a)$: a constant which includes the effect of pump and motor inertia and the wave travel time. K and ρ are given by:

$$K = \frac{91600h_R q_R}{WR^2 \eta_R N_R^2}$$

$$2\rho = \frac{av_o}{gh_o}$$

Using the data given for the Granby Pumping Plant:

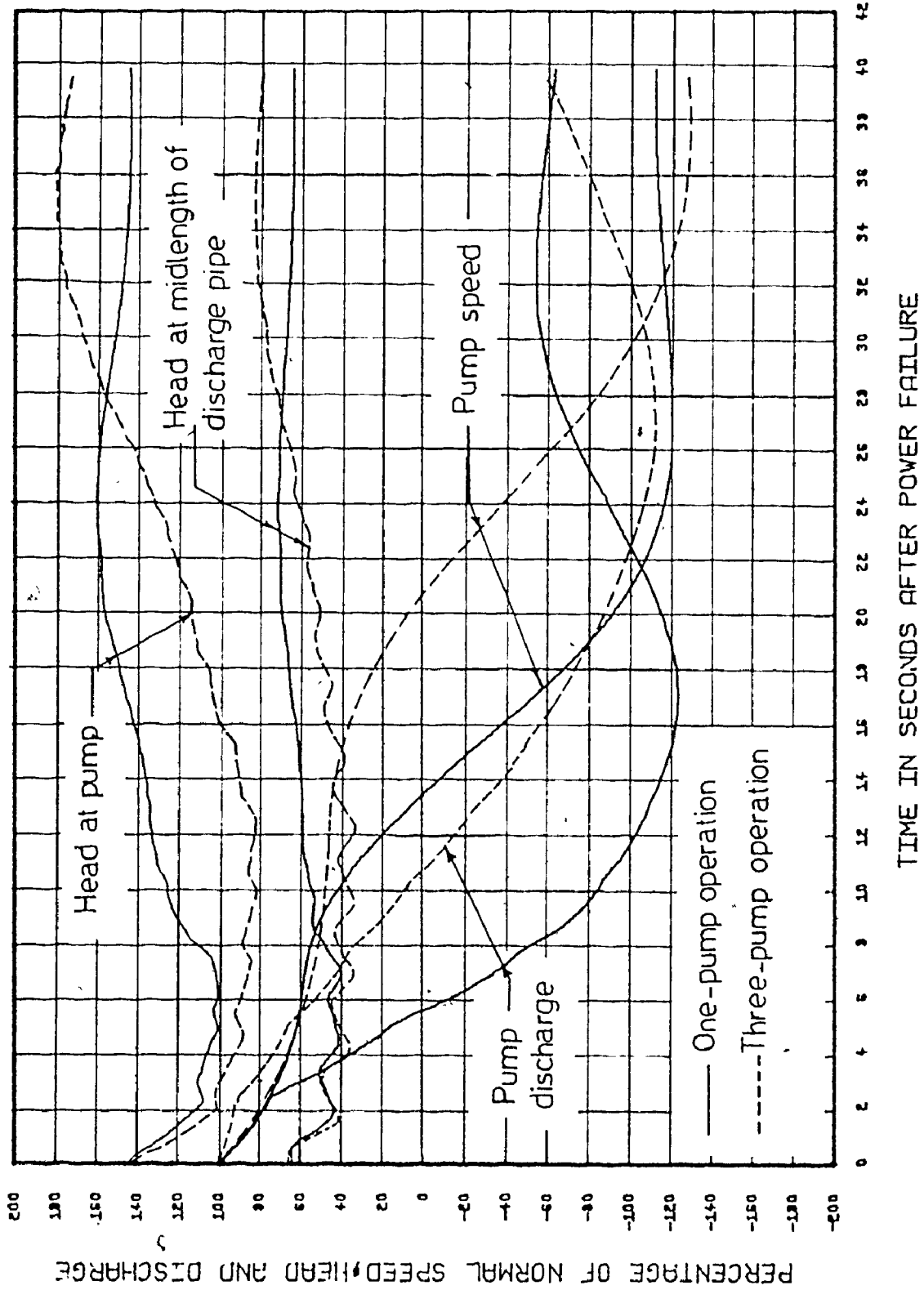


FIG. 5.16: THE GRANBY PUMPING PLANT - TRANSIENT CONDITIONS DUE TO POWER FAILURE

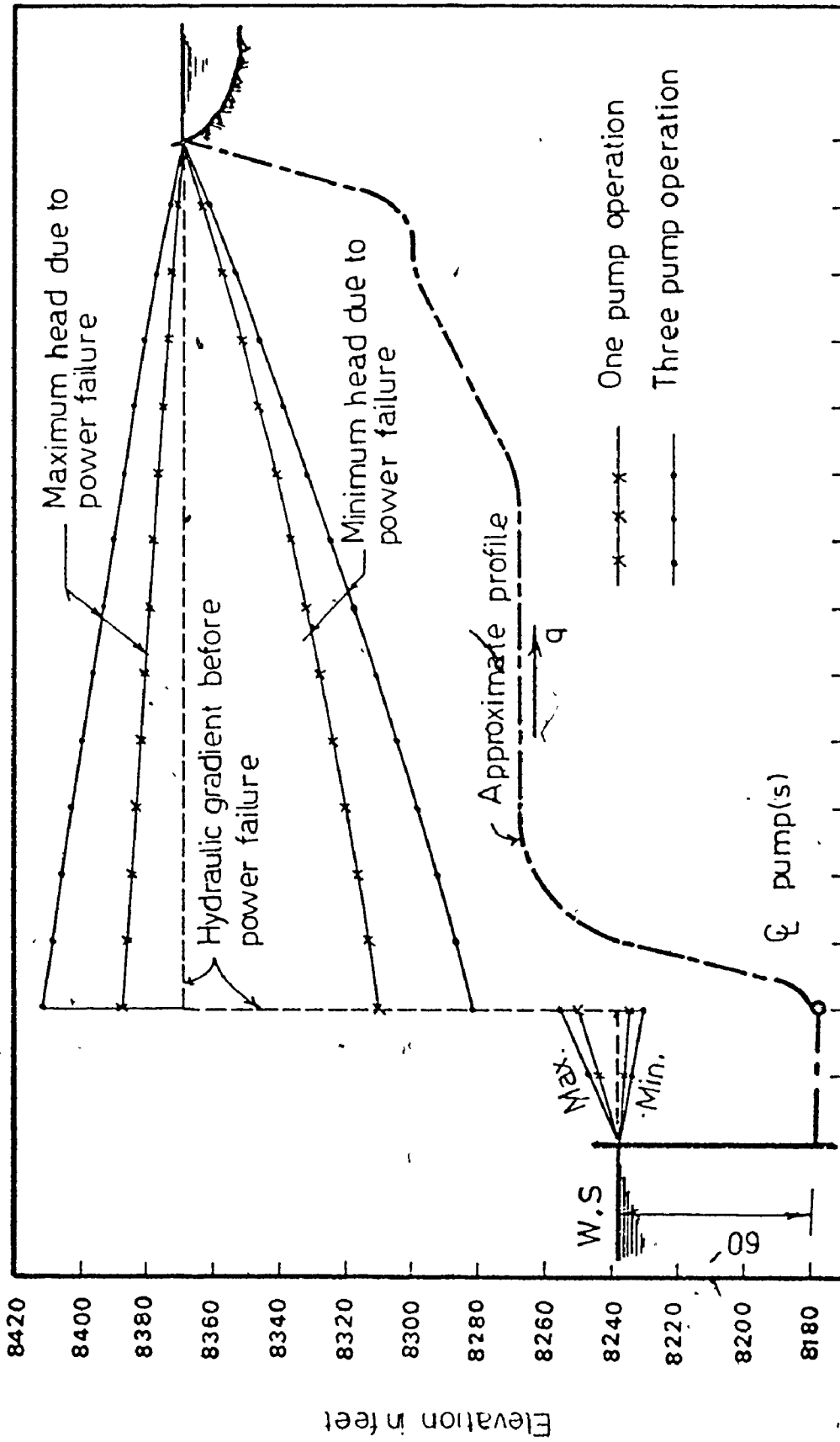


FIG. 5.17: THE GRANBY PUMPING PLANT - TRANSIENT PRESSURE GRADIENTS DUE TO POWER FAILURE

Method	Upsurge at Pump	Upsurge at Midlength	Downsurge at Pump	Downsurge at Midlength	Time of Flow Reversal (sec)	Maximum Reverse Speed	Time of Max. Reverse Pump Speed (sec)	Time of Zero Pump Speed (sec)
Field Test	0.175	-	0.526	-	-	1.27	-	-
Water Hammer Charts (49)	0.13	0.07	0.50	0.27	5.0	1.26	26.2	12.5
Computer Results	0.142	0.076	0.462	0.265	5.60	1.22	26.5	13.5

TABLE 5.2: THE GRANBY PUMPING PLANT - TRANSIENT CONDITIONS DUE TO POWER FAILURE - COMPARISON BETWEEN COMPUTER RESULTS AND (a) FIELD TESTS; (b) WATER HAMMER CHARTS

$$2\rho = 1.60$$

$$\frac{2L}{a} = 2.28$$

$$K \frac{2L}{a} = 0.15$$

In addition, Fig. 5.17 presents a plot of the maximum and minimum pressures along the pipeline for both one pump and three pump operation (the butterfly valve was held open after pump shut-down).

5.2.4 Effect of Valve Operation at the Pump. To illustrate the effect of valve operation at the pump discharge side on the transient conditions following pump shut-off, consider the Tracy Pumping Plant arrangement⁽⁶⁶⁾. Three different cases are simulated: (a) no discharge valves at pump, (b) non-return valve (check valve) which closes under the effect of the reverse flow, and (c) the two-stage gradual valve closure shown in Fig. 5.13. Results are plotted in Fig. 5.18. From these plots we conclude that the downsurge is not affected by the valve operation, while the upsurge reaches a maximum value of 168.0 ft, with the non-return valve at the pump. The minimum upsurge occurred with the two-stage butterfly valve (the first stage is rapid, while the second is slow). Generally, valves are primarily installed to prevent reverse flow, which could damage both pump and motor⁽⁶⁷⁾. Such valves also prevent the draining of the pipeline, and consequent loss of water or flooding of the wet well. The relation between flow and gate position⁽⁶⁸⁾ is important; this should be determined carefully to insure accurate evaluation

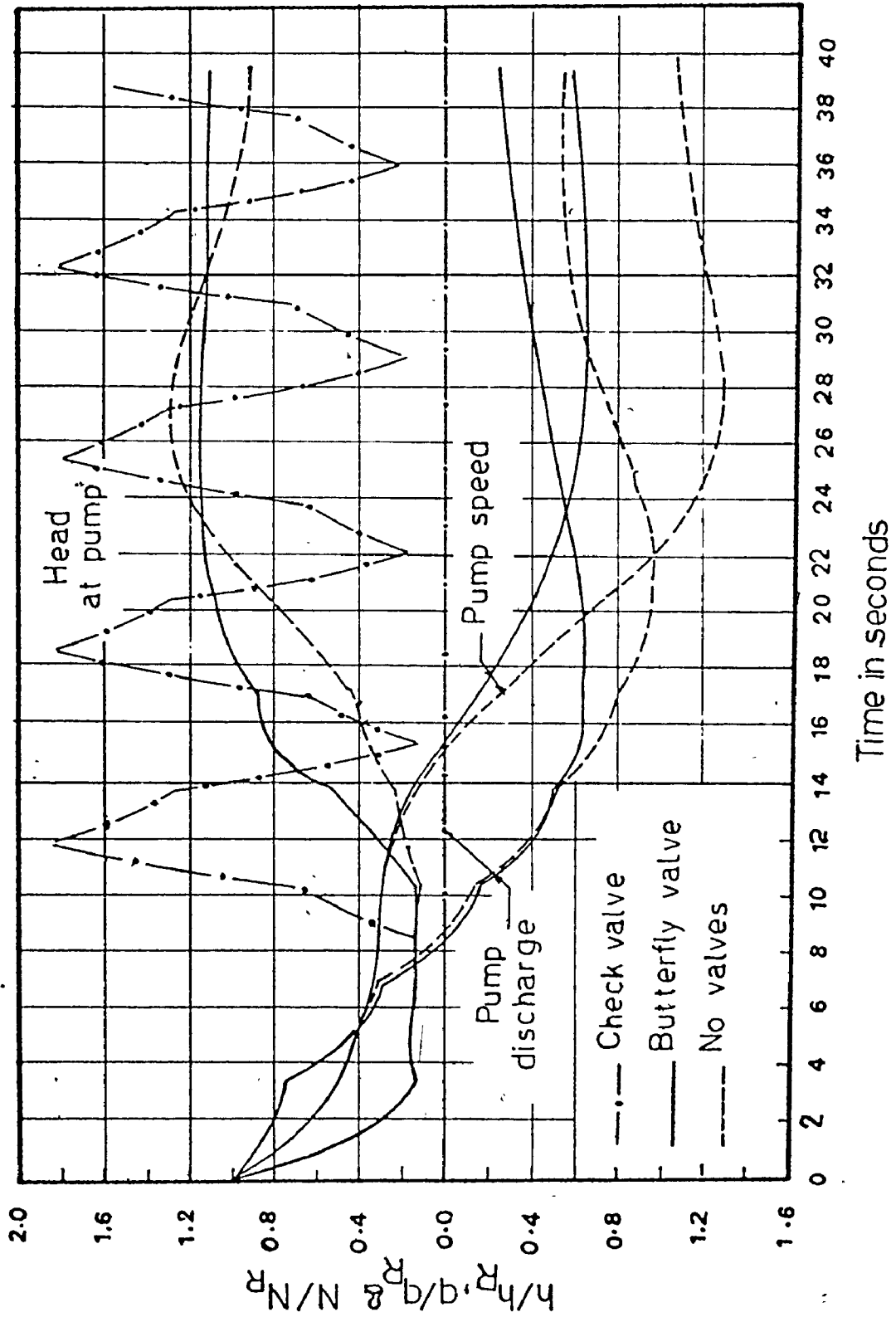


FIG. 5.18: EFFECT OF VALVE OPERATION AT THE PUMP ON THE PRESSURE TRANSIENTS

of water hammer transients.

5.2.5 Effect of the Inertia of Rotating Elements. To illustrate the effect of the inertia of the pump, motor and entrained water; data for the Tracy Pumping Plant⁽⁶⁶⁾ are used. Two cases have been considered: the first; without any discharge valves at the pump, and the second; with a check valve placed at the pump discharge side. In each case, three computer runs were made: the first, with the actual inertia; the second, with the inertia doubled; and the third, with the inertia tripled. Figure 5.19 presents the pressure variation at the pump and midlength of discharge pipe when no discharge valves are used at the pump, while Fig. 5.20 presents the same plot, but with a check valve at the pump. It was assumed that the check valve closes at the instant of flow reversal. In addition, in Figs. 5.21 and 5.22, the envelopes of maximum and minimum pressure for the above two cases and the three different inertias are plotted. These figures demonstrate that increasing the pump and motor inertia can reduce both the upsurges and downsurges.

5.2.6 Effect of Friction on Water Hammer Pressures. Generally we consider two types of pumping⁽⁶⁹⁾: (a) most of the pumping head is used to lift water while the friction losses are small, and (b) most of the pumping head is used to overcome friction resistance. Case (a) is associated with relatively short pipes and small friction losses. Case (b) is associated with relatively long pipes with high friction losses.

To illustrate the effect of the type of loading on the water

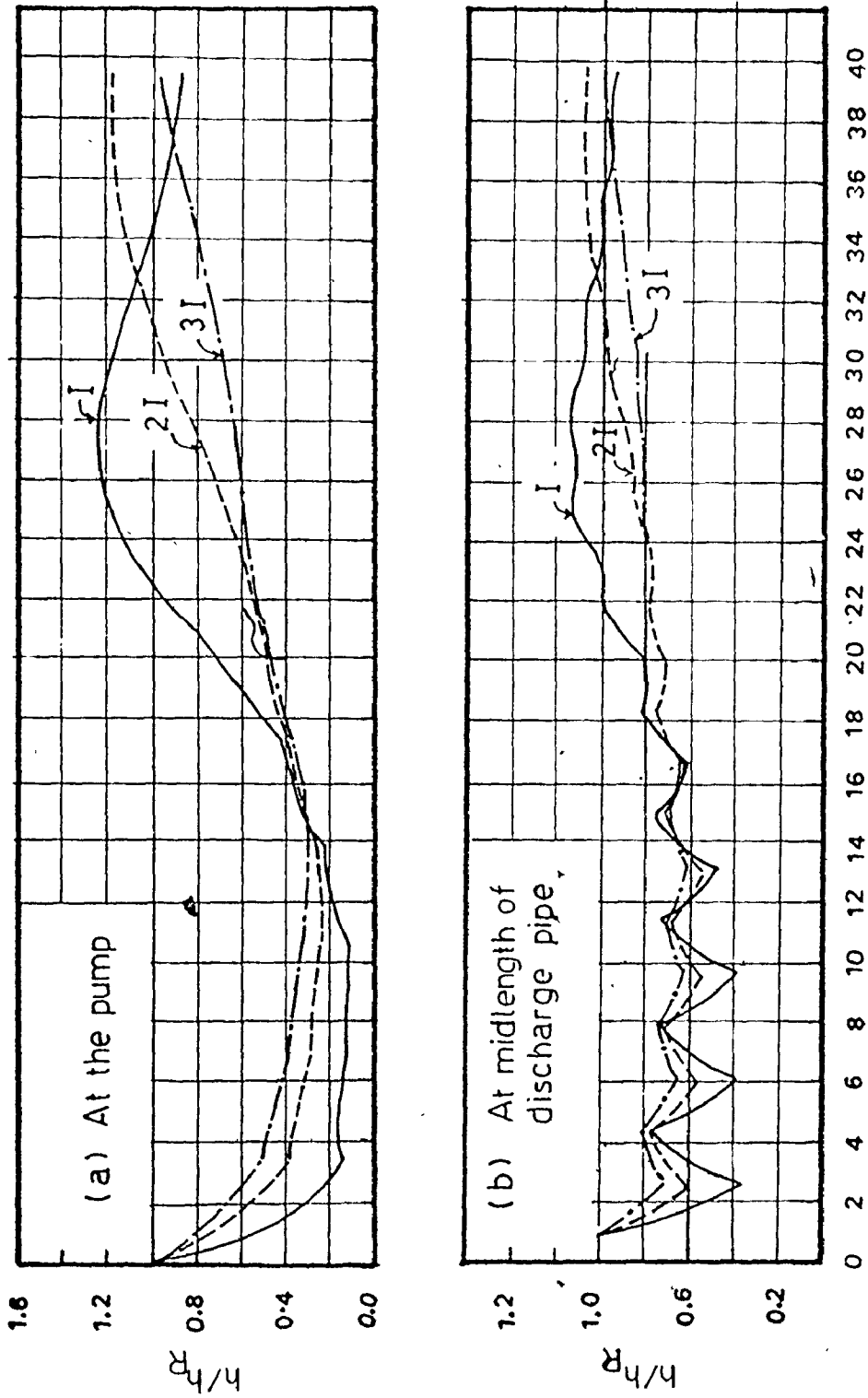
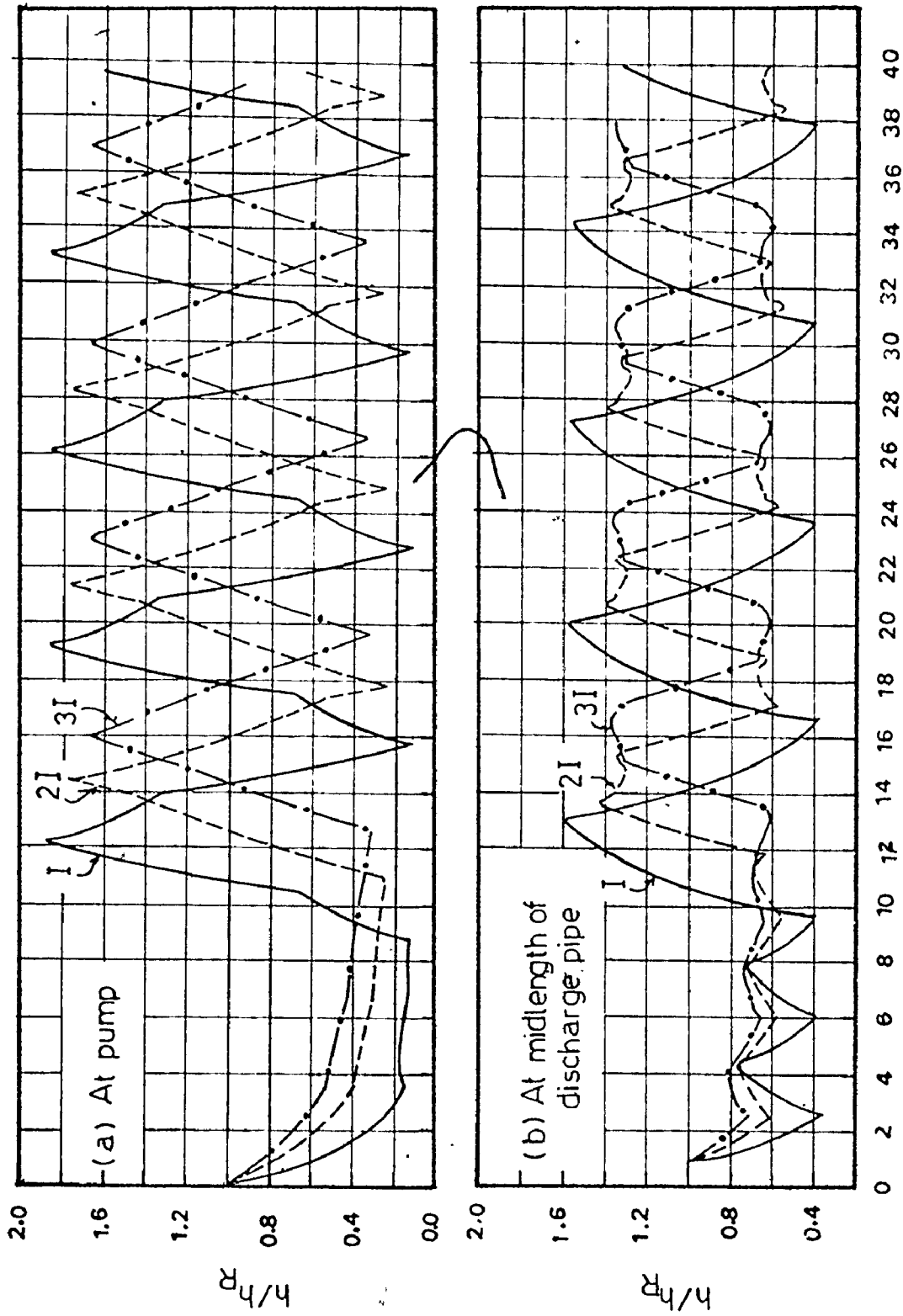


FIG. 5.19: EFFECT OF PUMP AND MOTOR INERTIA ON THE PRESSURE TRANSIENTS - NO VALVES AT THE PUMP



Time in seconds

FIG. 5.20: EFFECT OF PUMP AND MOTOR INERTIA ON THE PRESSURE TRANSIENTS - CHECK VALVE AT THE PUMP

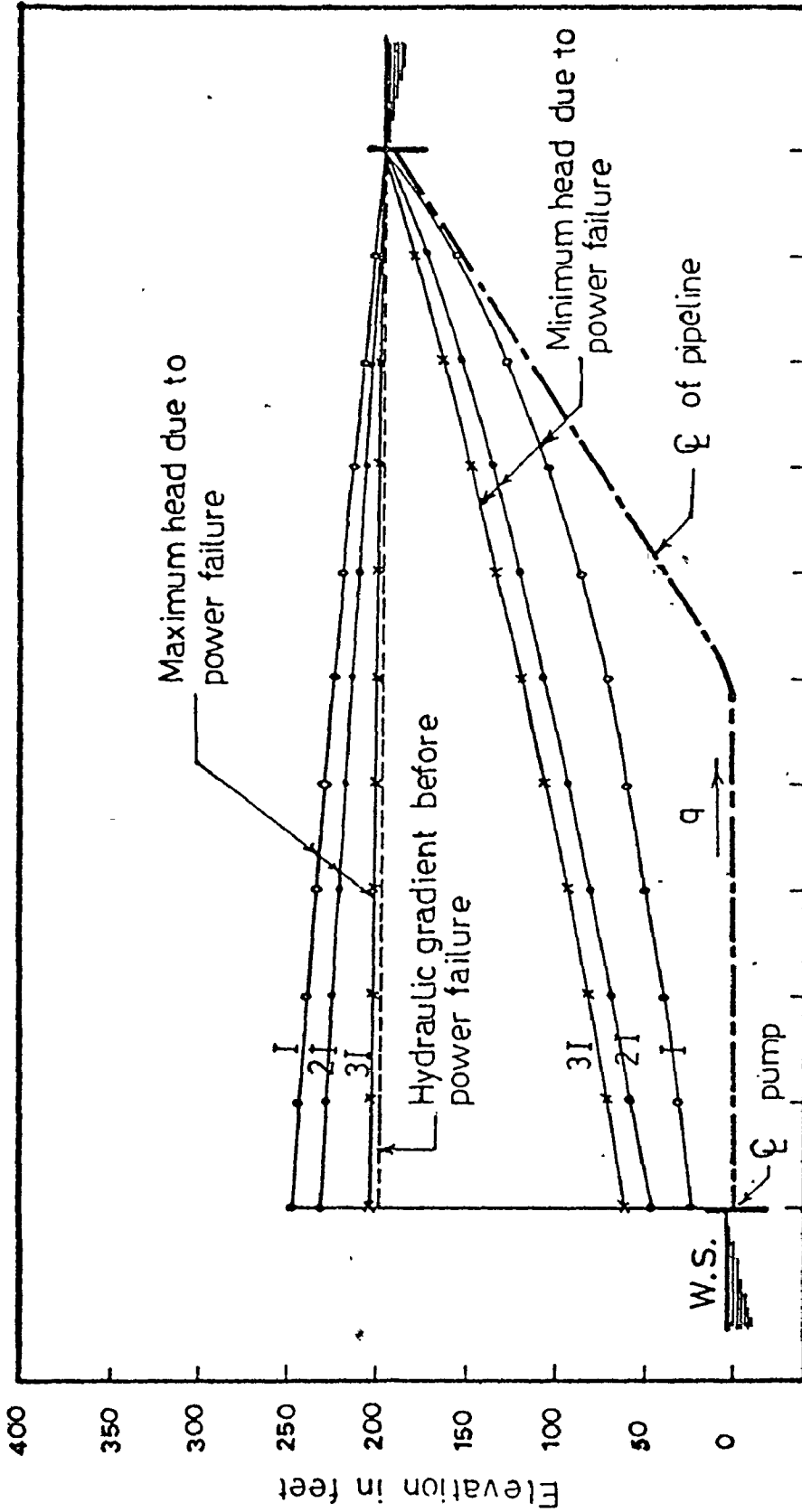


FIG. 5.21: EFFECT OF PUMP AND MOTOR INERTIA ON THE TRANSIENT PRESSURE GRADIENTS - NO VALVES AT THE PUMP

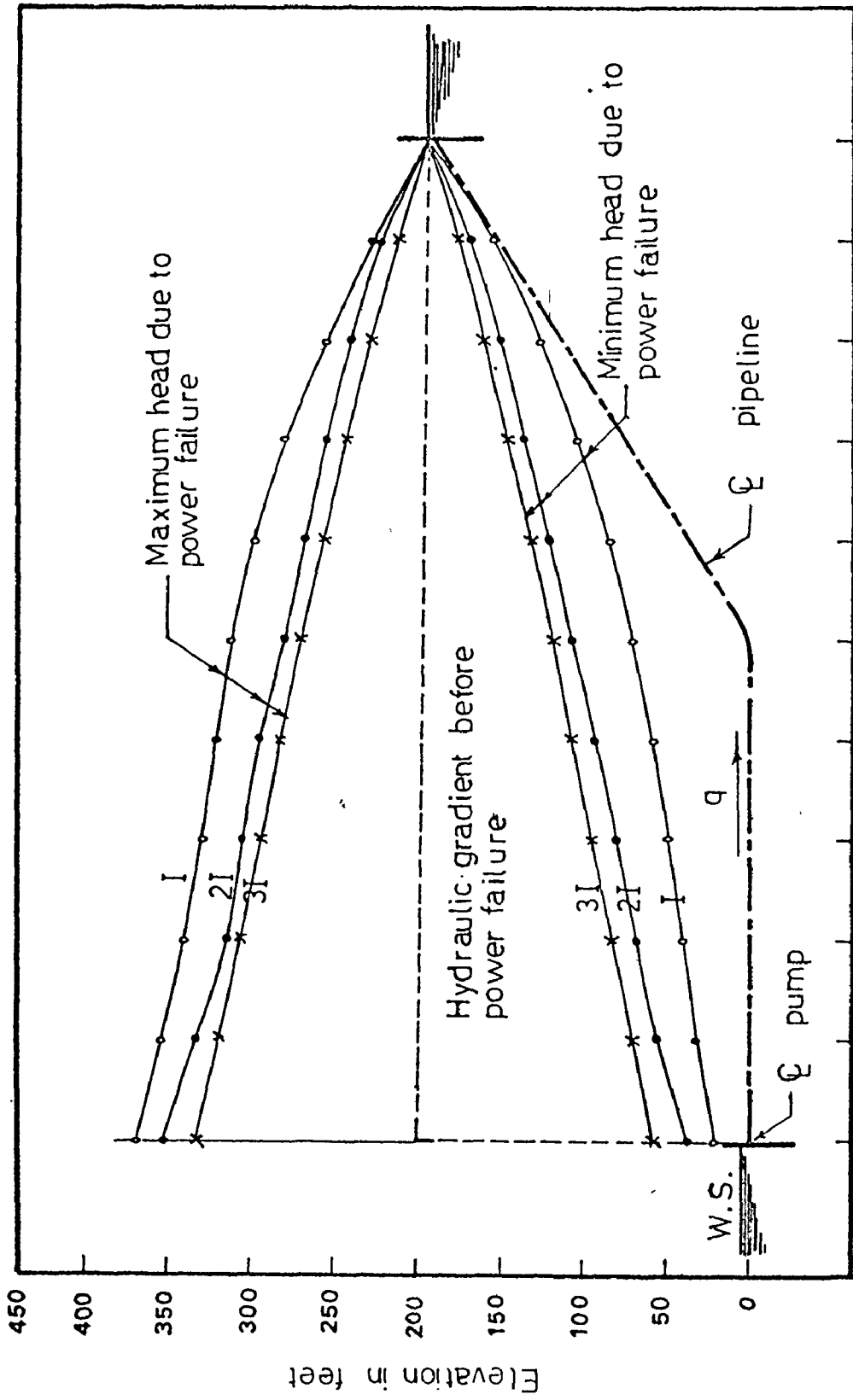


FIG. 5.22: EFFECT OF PUMP AND MOTOR INERTIA ON THE TRANSIENT PRESSURE GRADIENTS - CHECK VALVE AT THE PUMP

hammer transients following pump shut-off, data for the Tracy Pumping Plant⁽⁶⁶⁾ are used. The pumping head remains the same while the friction losses are increased to 40.0 ft. Figure 5.23 presents the pump discharge, pump speed, and the head at the pump due to pump shut-off. The envelopes of maximum and minimum pressure along the pipeline are plotted in Fig. 5.24. The maximum pressure will not exceed the steady state pressure at any point in the pipeline, which agrees with the results obtained by Kinno and Kennedy⁽⁵⁶⁾: they found that if the steady state friction loss is greater than approximately 0.18 to 0.20 of the initial pumping head, then the maximum head at the pump and midlength of the discharge line will not exceed the initial steady state head. In this case, underpressures rather than overpressures are dangerous. The zone of negative pressure, at high points on the pipeline, is indicated in Fig. 5.24. Doubling the pump-motor inertia will eliminate any negative pressure in the pipeline.

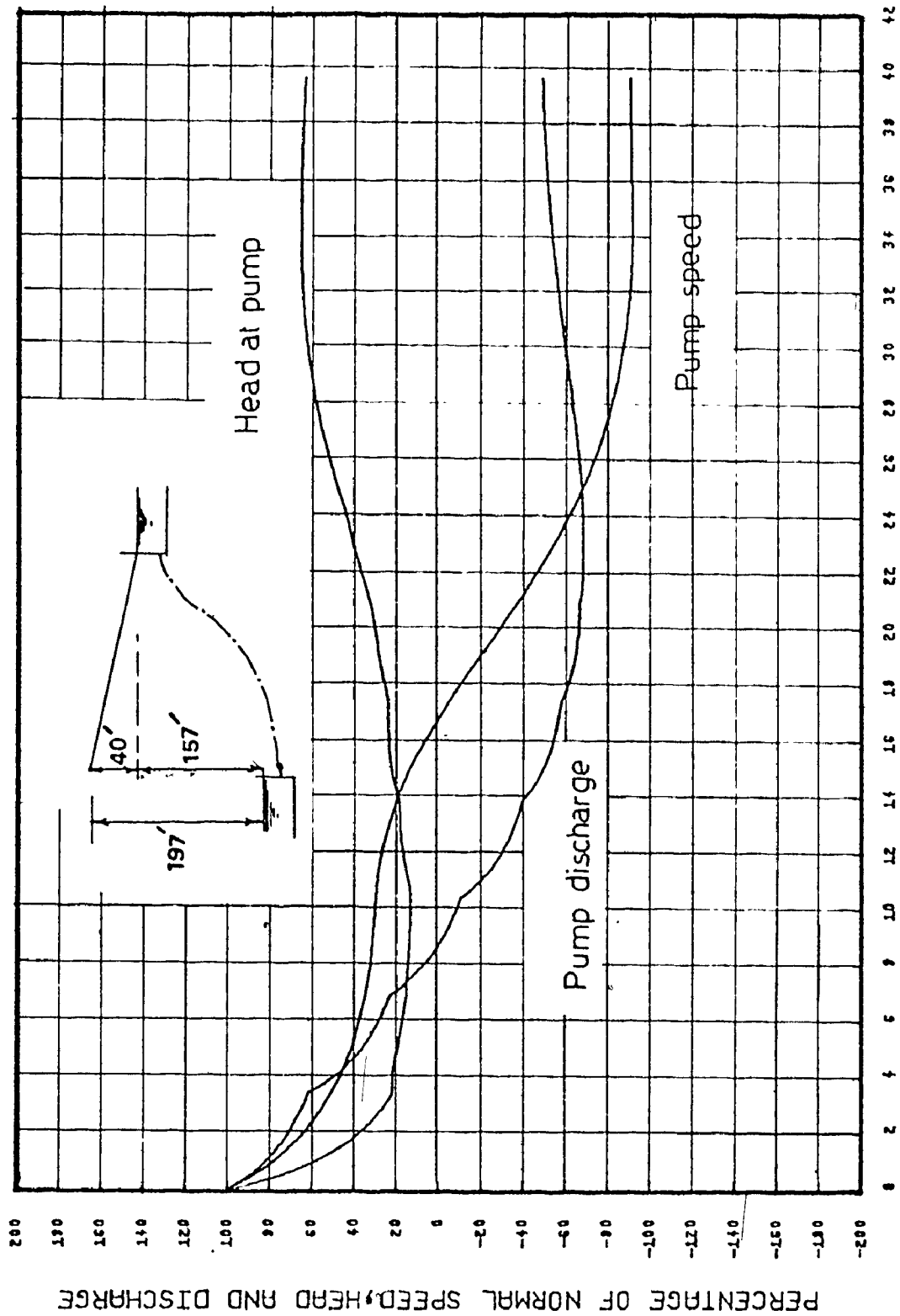


FIG. 5.23: TRANSIENT CONDITIONS DUE TO POWER FAILURE - CASE OF HIGH FRICTION LOSSES

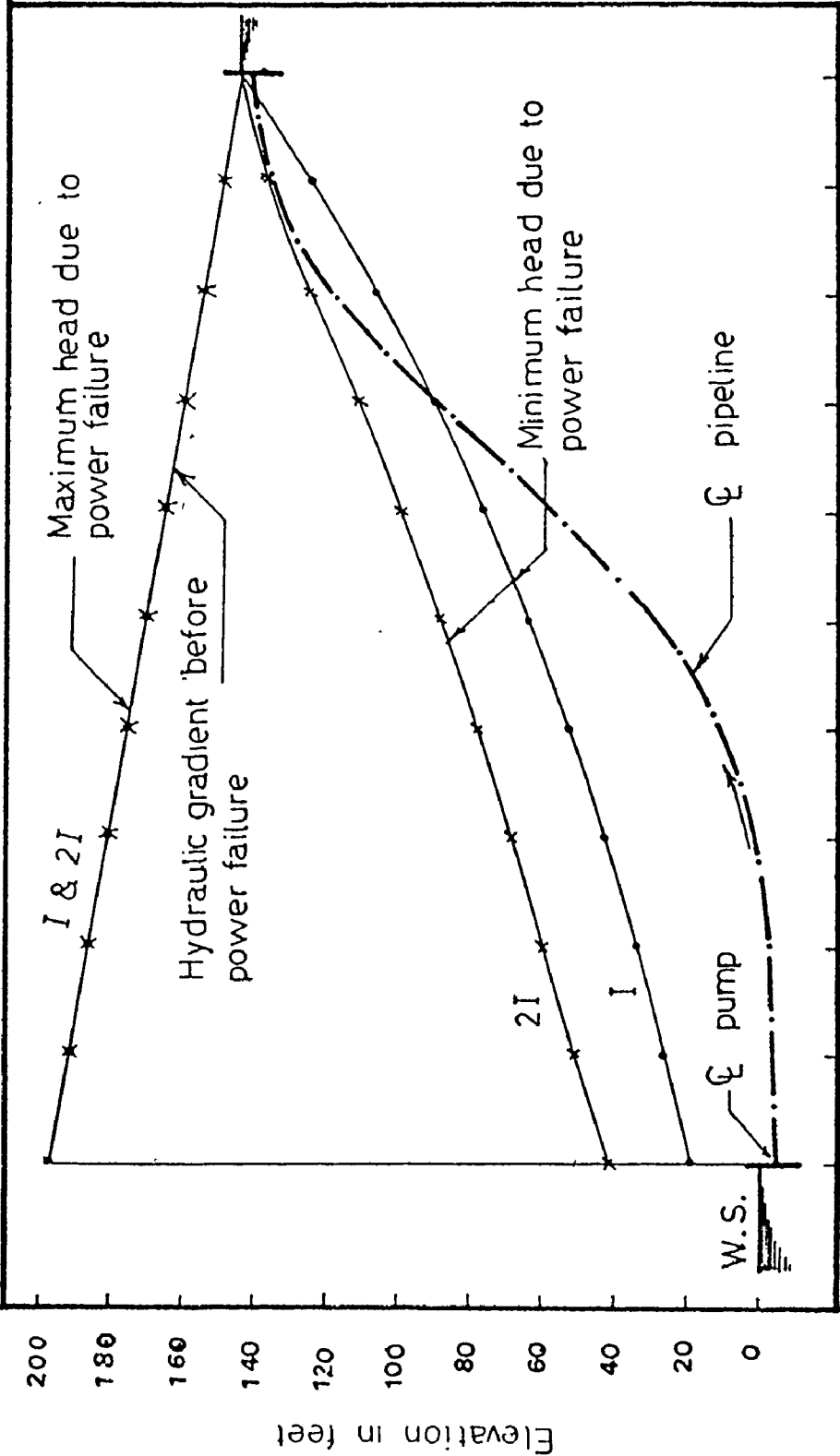


FIG. 5.24: TRANSIENT PRESSURE GRADIENTS DUE TO POWER FAILURE - CASE OF HIGH FRICTION LOSSES

6. THE ANCASTER PUMP STATION AND FORCEMAIN

6.1 Introduction

The pipeline profile is sketched in Fig. 6.1. The forcemain rises rapidly near the pump house. This convex profile, governed by the ground profile, creates a water hammer problem associated with pump shut-down. Negative pressures would occur in most of the pipeline (without protection). As the inertia of the rotating elements is small, the negative pressure reaches the vapour pressure of water and the water column may separate.

The project includes two pumps, only one in operation initially:

Length of forcemain	$L = 4405.0 \text{ ft}$
Diameter of forcemain	$D = 14.0 \text{ in}$
Pumping discharge	$q_R \approx 1000.0 \text{ gpm}$
Pump head	$h_R \approx 157.5 \text{ ft}$
Motor speed	$N_R = 1750 \text{ ft}$
Rotational inertia of pump and motor	$WR^2 = 25.0 \text{ lb.ft}^2$
Pressure wave celerity	$a = 3500.0 \text{ ft/sec}$
Specific speed	$N_s = 1254.0 \text{ (gpm units)}$
Pump efficiency	$\eta_R = 0.73$

A discharge check valve is mounted at the pump in order to prevent flow reversal and drainage of the pipe which may result in flooding of the wet well.

After 20 years, a bigger pump impellor will be incorporated:

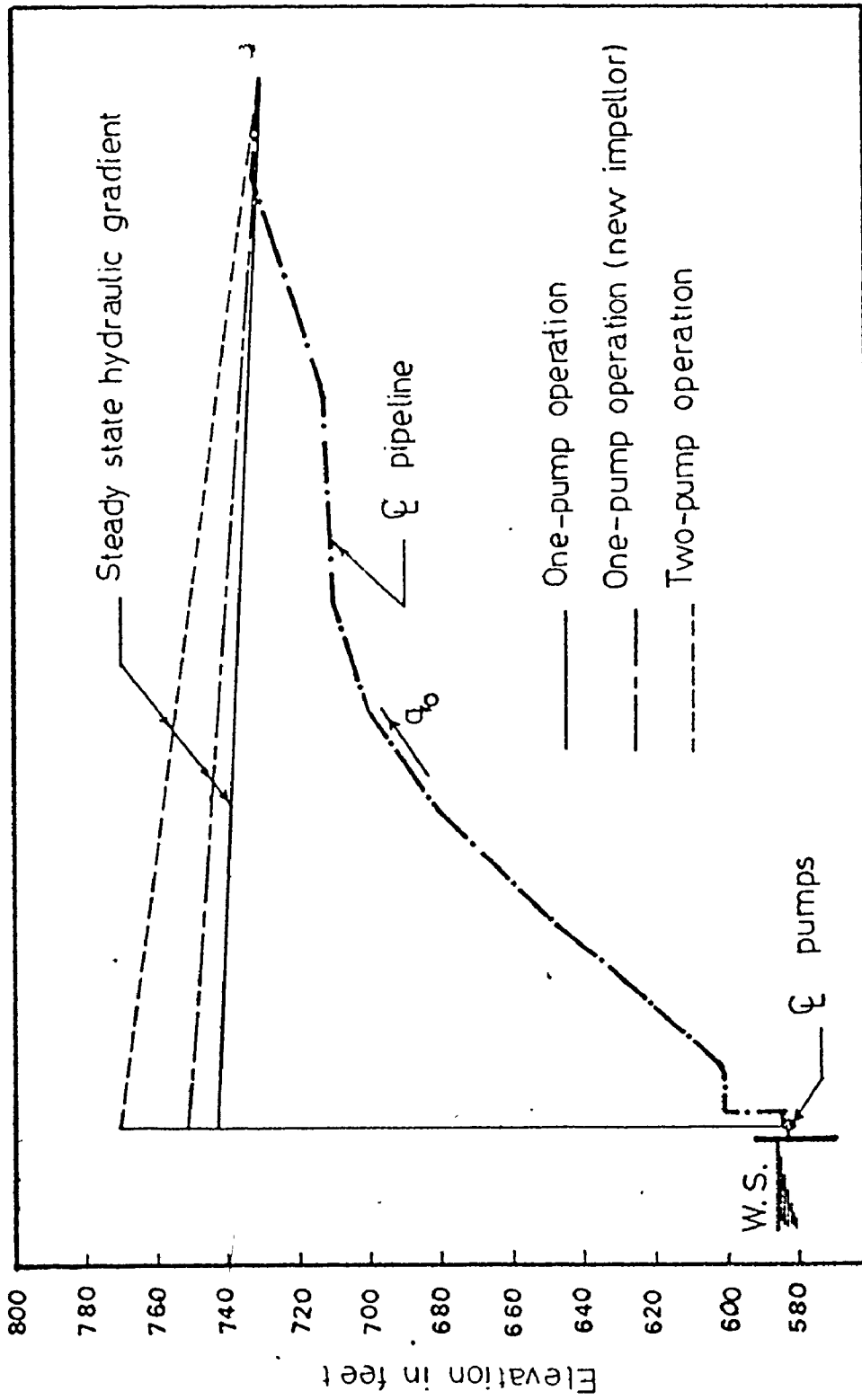


FIG. 6.1: THE ANCASTER FORCEMAIN - OPERATING HEADS

Pumping discharge	$q_R = 1375.0$ gpm
Pump head	$h_R = 165.0$ ft
Pump efficiency	$\eta_R = 0.75$

The ultimate design is for three pumps; two in operation at a time:

Pumping discharge	$q_R = 2080.0$ gpm
Pump head	$h_R = 185.0$ ft
Pump efficiency	$\eta_R = 0.72$

The steady state hydraulic gradients for the above three operating conditions are shown in Fig. 6.1. The three conditions were simulated, without protection devices, using the computer program. Figures 6.2, 6.3, and 6.4 present a print-out of the transient pressures after pump shut-off. Printing stops when the pressure reaches water vapour pressure. From these results we conclude as follows, for an unprotected pipeline:

1. One-pump operation (Fig. 6.2): Maximum down-surge will develop negative pressures less than water vapour pressure (-33.0 ft of head). This indicates that vapour pockets will form.
2. Two-pump operation (Fig. 6.3): At power failure, the down-surge would cause vapour pockets earlier and further upstream, most likely about 1200 ft. from the pump house.
3. One-pump operation; new impellor (Fig. 6.4): The results are essentially the same as (2) above.

It seems clear that a water hammer protective device is desirable.

0.00	"	182.59	182.67	183.15	183.63	184.11	184.59	185.07	185.55	186.03	186.51	26.75
	"	2.58	2.58	2.58	2.58	2.58	2.58	2.58	2.58	2.58	2.58	2.58
0.01	"	186.29	186.27	186.75	187.23	187.71	188.19	188.67	189.15	189.63	190.11	26.75
	"	2.58	2.58	2.58	2.58	2.58	2.58	2.58	2.58	2.58	2.58	2.58
0.13	"	186.31	186.29	186.77	187.25	187.73	188.21	188.69	189.17	189.65	190.13	26.75
	"	2.58	2.58	2.58	2.58	2.58	2.58	2.58	2.58	2.58	2.58	2.58
0.19	"	186.59	186.57	187.05	187.53	188.01	188.49	188.97	189.45	189.93	190.41	26.75
	"	2.58	2.58	2.58	2.58	2.58	2.58	2.58	2.58	2.58	2.58	2.58
0.25	"	187.05	187.03	187.51	187.99	188.47	188.95	189.43	189.91	190.39	190.87	26.75
	"	2.58	2.58	2.58	2.58	2.58	2.58	2.58	2.58	2.58	2.58	2.58
0.31	"	187.05	187.03	187.51	187.99	188.47	188.95	189.43	189.91	190.39	190.87	26.75
	"	2.58	2.58	2.58	2.58	2.58	2.58	2.58	2.58	2.58	2.58	2.58
0.39	"	188.57	188.55	189.03	189.51	189.99	190.47	190.95	191.43	191.91	192.39	26.75
	"	2.58	2.58	2.58	2.58	2.58	2.58	2.58	2.58	2.58	2.58	2.58
0.44	"	188.19	188.17	188.65	189.13	189.61	190.09	190.57	191.05	191.53	192.01	26.75
	"	2.58	2.58	2.58	2.58	2.58	2.58	2.58	2.58	2.58	2.58	2.58
0.50	"	188.67	188.65	189.13	189.61	190.09	190.57	191.05	191.53	192.01	192.49	26.75
	"	2.58	2.58	2.58	2.58	2.58	2.58	2.58	2.58	2.58	2.58	2.58
0.57	"	188.65	188.63	189.11	189.59	190.07	190.55	191.03	191.51	191.99	192.47	26.75
	"	2.58	2.58	2.58	2.58	2.58	2.58	2.58	2.58	2.58	2.58	2.58
0.62	"	188.63	188.61	189.09	189.57	190.05	190.53	191.01	191.49	191.97	192.45	26.75
	"	2.58	2.58	2.58	2.58	2.58	2.58	2.58	2.58	2.58	2.58	2.58
0.69	"	187.95	187.93	188.41	188.89	189.37	189.85	190.33	190.81	191.29	191.77	26.75
	"	2.58	2.58	2.58	2.58	2.58	2.58	2.58	2.58	2.58	2.58	2.58
0.75	"	18.00	18.03	18.06	18.09	18.12	18.15	18.18	18.21	18.24	18.27	26.75
	"	2.58	2.58	2.58	2.58	2.58	2.58	2.58	2.58	2.58	2.58	2.58

FIG. 6.2: THE ANCASTER FORCEMAIN - TRANSIENT HEADS AND VELOCITIES ALONG THE PIPELINE FOR ONE-PUMP OPERATION

9.90	H ^o	126:23	127:25	128:27	129:29	130:31	131:33	132:35	133:37	134:39	135:41	136:43	137:45	138:47	139:49	140:51
	V ^o	3:21	3:21	3:21	3:21	3:21	3:21	3:21	3:21	3:21	3:21	3:21	3:21	3:21	3:21	3:21
9.91	H ^o	126:25	127:27	128:29	129:31	130:33	131:35	132:37	133:39	134:41	135:43	136:45	137:47	138:49	139:51	140:53
	V ^o	3:21	3:21	3:21	3:21	3:21	3:21	3:21	3:21	3:21	3:21	3:21	3:21	3:21	3:21	3:21
9.92	H ^o	126:27	127:29	128:31	129:33	130:35	131:37	132:39	133:41	134:43	135:45	136:47	137:49	138:51	139:53	140:55
	V ^o	3:22	3:22	3:22	3:22	3:22	3:22	3:22	3:22	3:22	3:22	3:22	3:22	3:22	3:22	3:22
9.93	H ^o	126:29	127:31	128:33	129:35	130:37	131:39	132:41	133:43	134:45	135:47	136:49	137:51	138:53	139:55	140:57
	V ^o	3:22	3:22	3:22	3:22	3:22	3:22	3:22	3:22	3:22	3:22	3:22	3:22	3:22	3:22	3:22
9.94	H ^o	126:31	127:33	128:35	129:37	130:39	131:41	132:43	133:45	134:47	135:49	136:51	137:53	138:55	139:57	140:59
	V ^o	3:22	3:22	3:22	3:22	3:22	3:22	3:22	3:22	3:22	3:22	3:22	3:22	3:22	3:22	3:22
9.95	H ^o	126:33	127:35	128:37	129:39	130:41	131:43	132:45	133:47	134:49	135:51	136:53	137:55	138:57	139:59	140:61
	V ^o	3:22	3:22	3:22	3:22	3:22	3:22	3:22	3:22	3:22	3:22	3:22	3:22	3:22	3:22	3:22
9.96	H ^o	126:35	127:37	128:39	129:41	130:43	131:45	132:47	133:49	134:51	135:53	136:55	137:57	138:59	139:61	140:63
	V ^o	3:22	3:22	3:22	3:22	3:22	3:22	3:22	3:22	3:22	3:22	3:22	3:22	3:22	3:22	3:22
9.97	H ^o	126:37	127:39	128:41	129:43	130:45	131:47	132:49	133:51	134:53	135:55	136:57	137:59	138:61	139:63	140:65
	V ^o	3:22	3:22	3:22	3:22	3:22	3:22	3:22	3:22	3:22	3:22	3:22	3:22	3:22	3:22	3:22
9.98	H ^o	126:39	127:41	128:43	129:45	130:47	131:49	132:51	133:53	134:55	135:57	136:59	137:61	138:63	139:65	140:67
	V ^o	3:22	3:22	3:22	3:22	3:22	3:22	3:22	3:22	3:22	3:22	3:22	3:22	3:22	3:22	3:22

FIG. 6.3: THE ANCASTER FORCEMAIN - TRANSIENT HEADS AND VELOCITIES ALONG THE PIPELINE FOR ONE-PUMP OPERATION (NEW IMPELLOR)

.67	H*	132.25	132.25	132.25	132.25	132.25	132.25	132.25	132.25	132.25	132.25	132.25	132.25	132.25	132.25	132.25
	V*	4.16	4.16	4.16	4.16	4.16	4.16	4.16	4.16	4.16	4.16	4.16	4.16	4.16	4.16	4.16
.68	H*	132.25	132.25	132.25	132.25	132.25	132.25	132.25	132.25	132.25	132.25	132.25	132.25	132.25	132.25	132.25
	V*	4.16	4.16	4.16	4.16	4.16	4.16	4.16	4.16	4.16	4.16	4.16	4.16	4.16	4.16	4.16
.69	H*	132.25	132.25	132.25	132.25	132.25	132.25	132.25	132.25	132.25	132.25	132.25	132.25	132.25	132.25	132.25
	V*	4.16	4.16	4.16	4.16	4.16	4.16	4.16	4.16	4.16	4.16	4.16	4.16	4.16	4.16	4.16
.70	H*	132.25	132.25	132.25	132.25	132.25	132.25	132.25	132.25	132.25	132.25	132.25	132.25	132.25	132.25	132.25
	V*	4.16	4.16	4.16	4.16	4.16	4.16	4.16	4.16	4.16	4.16	4.16	4.16	4.16	4.16	4.16
.71	H*	132.25	132.25	132.25	132.25	132.25	132.25	132.25	132.25	132.25	132.25	132.25	132.25	132.25	132.25	132.25
	V*	4.16	4.16	4.16	4.16	4.16	4.16	4.16	4.16	4.16	4.16	4.16	4.16	4.16	4.16	4.16
.72	H*	132.25	132.25	132.25	132.25	132.25	132.25	132.25	132.25	132.25	132.25	132.25	132.25	132.25	132.25	132.25
	V*	4.16	4.16	4.16	4.16	4.16	4.16	4.16	4.16	4.16	4.16	4.16	4.16	4.16	4.16	4.16
.73	H*	132.25	132.25	132.25	132.25	132.25	132.25	132.25	132.25	132.25	132.25	132.25	132.25	132.25	132.25	132.25
	V*	4.16	4.16	4.16	4.16	4.16	4.16	4.16	4.16	4.16	4.16	4.16	4.16	4.16	4.16	4.16
.74	H*	132.25	132.25	132.25	132.25	132.25	132.25	132.25	132.25	132.25	132.25	132.25	132.25	132.25	132.25	132.25
	V*	4.16	4.16	4.16	4.16	4.16	4.16	4.16	4.16	4.16	4.16	4.16	4.16	4.16	4.16	4.16
.75	H*	132.25	132.25	132.25	132.25	132.25	132.25	132.25	132.25	132.25	132.25	132.25	132.25	132.25	132.25	132.25
	V*	4.16	4.16	4.16	4.16	4.16	4.16	4.16	4.16	4.16	4.16	4.16	4.16	4.16	4.16	4.16
.76	H*	22.61	7.51	-1.99	-11.53	-24.16	-33.00	-33.00	-33.00	-33.00	-33.00	-33.00	-33.00	-33.00	-33.00	-16.72
	V*	4.29	35.40	33.35	30.33	26.25	18.23	14.15	11.13	-0.95	3.00					
.77	H*	27.28	12.69	4.08	4.54	-19.99	-11.96	-12.18	-20.14	-25.32	-14.67					
	V*	4.17	4.17	4.17	4.17	4.17	4.17	4.17	4.17	4.17	4.17	4.17	4.17	4.17	4.17	4.17
.78	H*	22.61	7.51	-1.99	-11.53	-24.16	-33.00	-33.00	-33.00	-33.00	-33.00	-33.00	-33.00	-33.00	-33.00	-16.72
	V*	4.29	35.40	33.35	30.33	26.25	18.23	14.15	11.13	-0.95	3.00					

FIG. 6.4: THE ANCASTER FORCEMAIN - TRANSIENT HEADS AND VELOCITIES ALONG THE PIPELINE FOR TWO-PUMP OPERATION

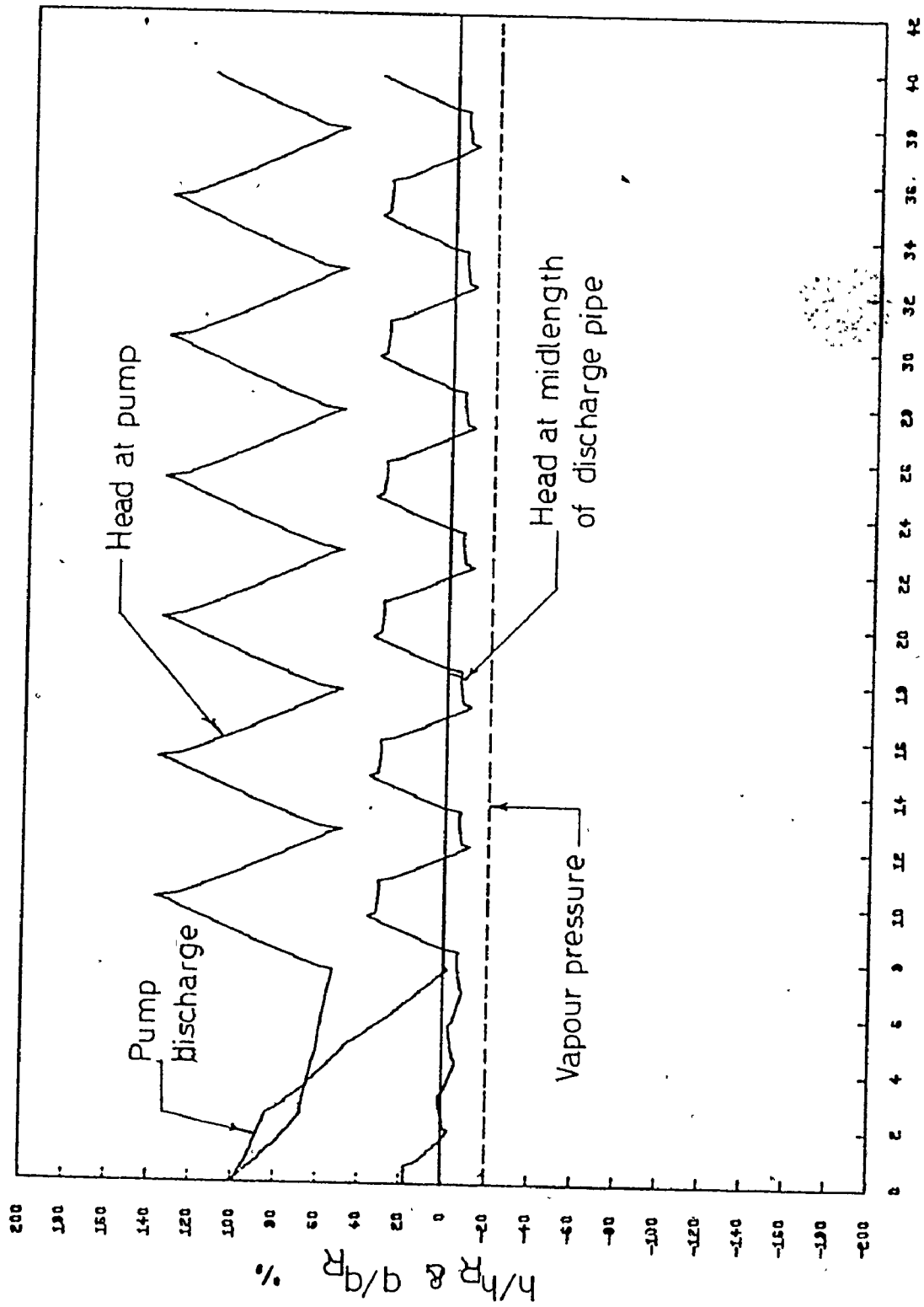
6.2 Protection of the Pipeline

In this section the advantages and disadvantages of different protection devices are discussed.

6.2.1 Increasing Inertia. Figures 6.5 and 6.6 present the pressure variations at the pump and midlength of discharge pipe for $WR^2 = 400.0 \text{ lb.ft.}^2$ for (a) one-pump operation and (b) two-pump operation. Figure 6.7 presents the maximum and minimum pressures along the pipeline for the above two conditions (the pipeline is divided into ten sections). The down-surge in both cases will produce acceptable negative pressures at high points in the pipeline. If these negative pressures are to be avoided, a further increase in inertia will be necessary.

The inertia can be increased by attaching a flywheel to the pump. Flywheels have the disadvantages⁽⁶²⁾ that: (a) more start-up power is required, (b) losses in the bearings reduce the overall efficiency, and (c) it would be difficult to mount the flywheel on the pumps already installed.

6.2.2 Surge Tanks. A surge tank may be used to protect the upper part of the pipe, although there are good reasons for avoiding such a solution. For interest, the computer program was used to locate the best position for such a tank. The peaks in the pipeline are preferred in order to reduce the tank height. The best position for the tank is shown in Fig. 6.8 where the envelopes of maximum and minimum pressure



TIME IN SECONDS AFTER POWER FAILURE

FIG. 6.5: THE ANCASTER FORCEMAIN - TRANSIENT CONDITIONS DUE TO POWER FAILURE FOR $WR2 = 400.0 \text{ lb.ft}^2$; FOR ONE-PUMP OPERATION

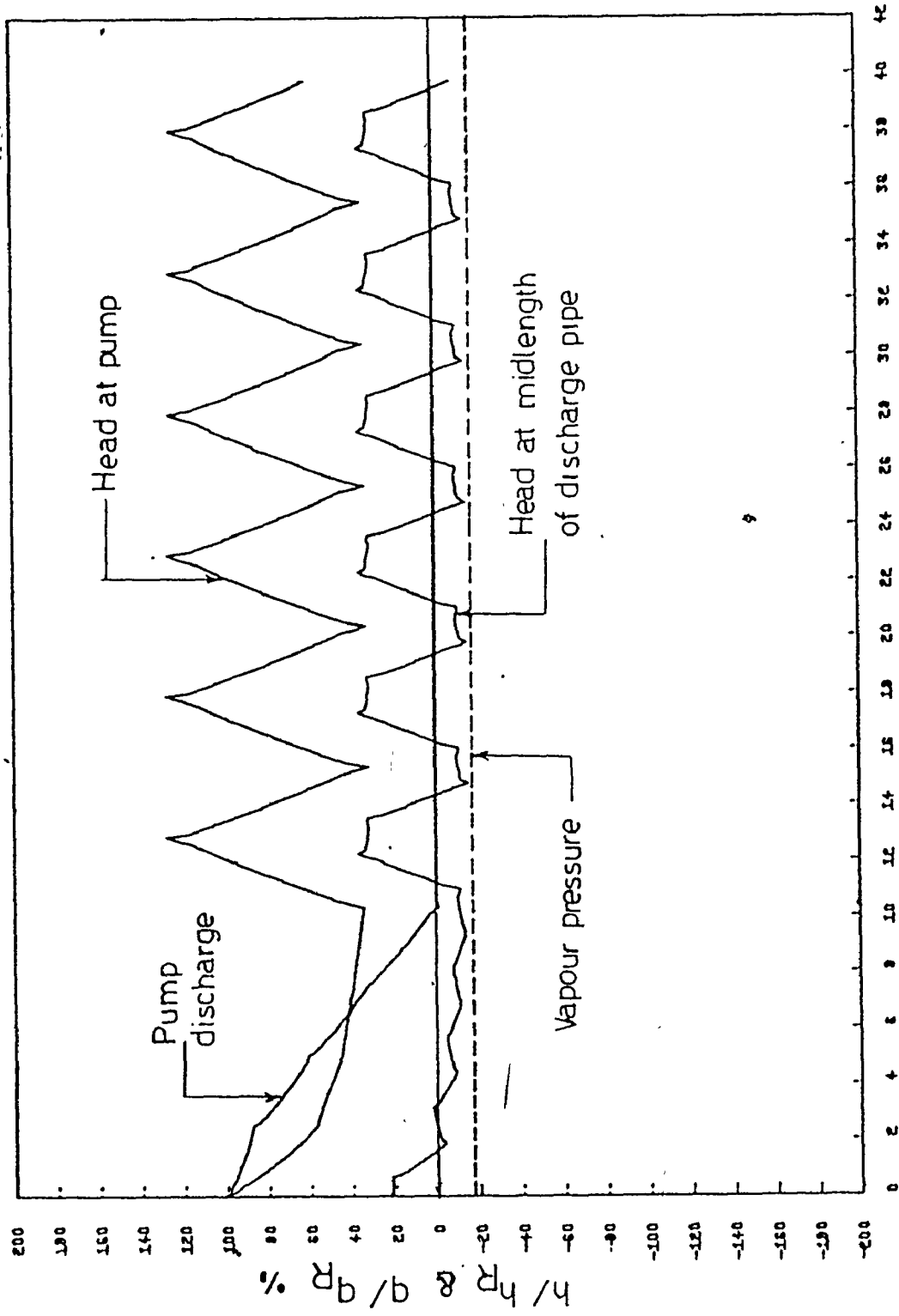


FIG. 6.6: THE ANCASTER FORCEMAIN - TRANSIENT CONDITIONS DUE TO POWER FAILURE FOR $WR^2 = 400.0 \text{ lb}\cdot\text{ft}^2$; FOR TWO-PUMP OPERATION

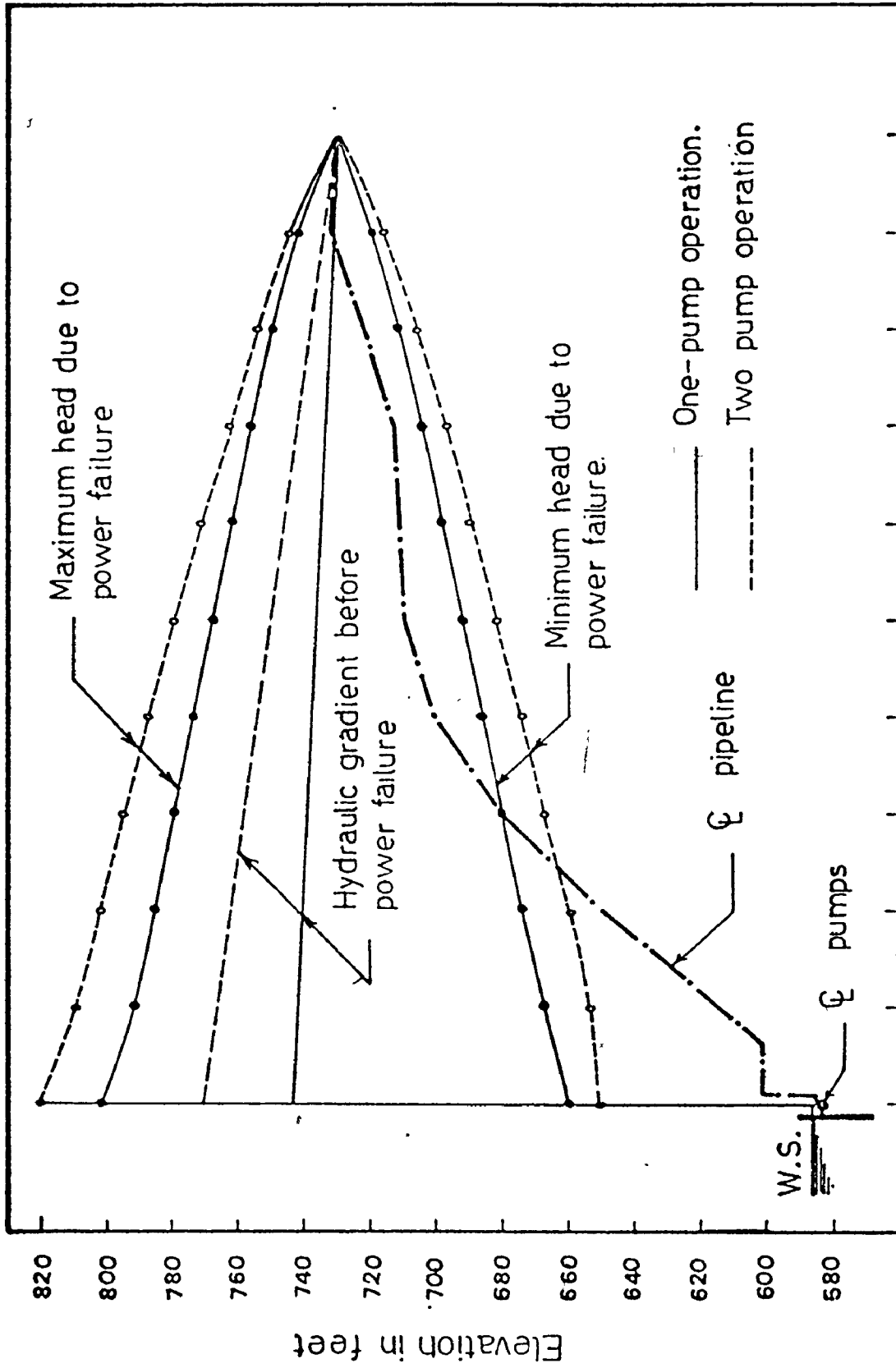


FIG. 6.7: THE ANCASTER FORCEMAIN - TRANSIENT PRESSURE GRADIENTS FOR WR2 = 400.0 lb.ft²

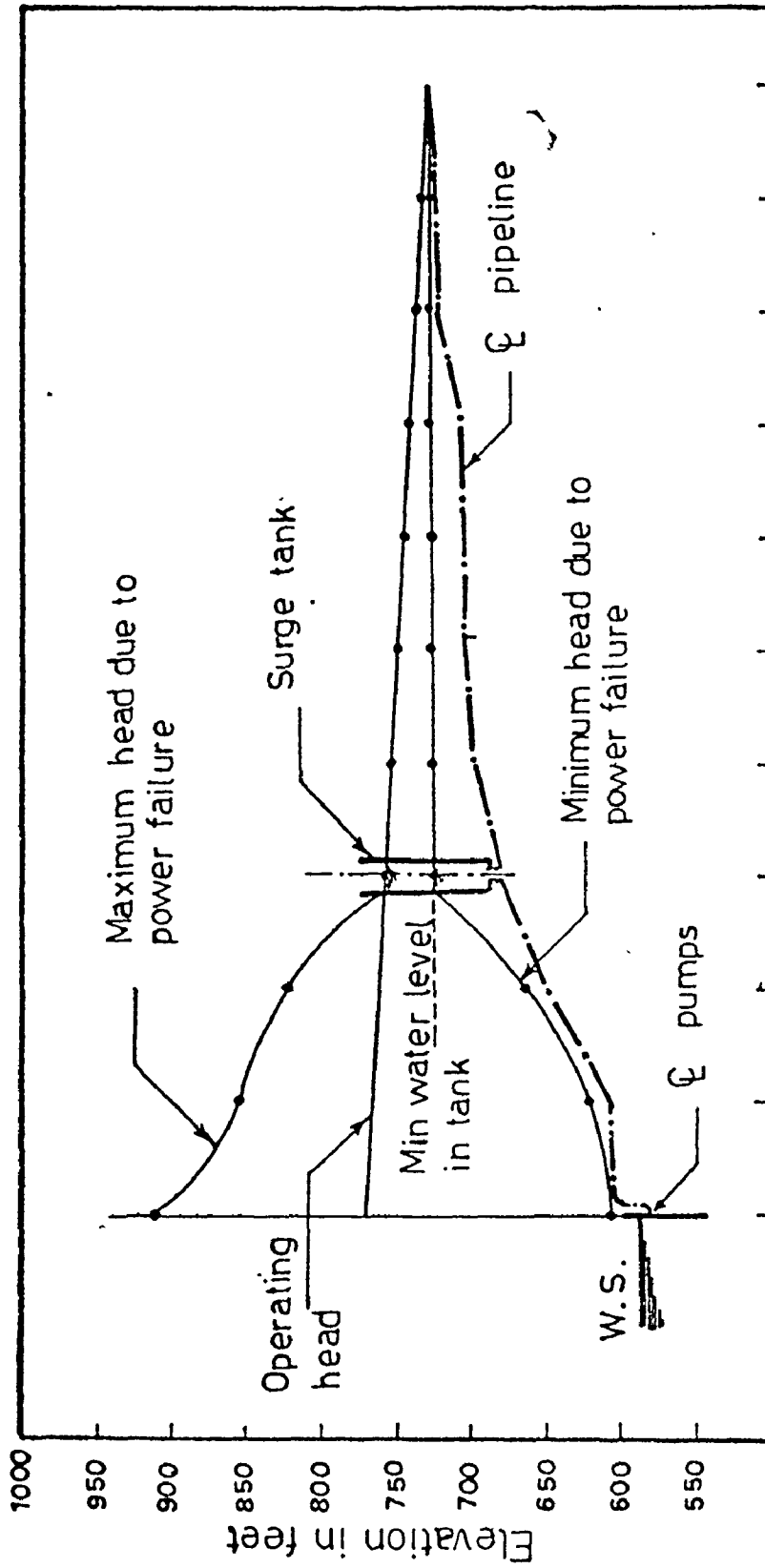


FIG. 6.8: THE ANCASTER FORCEMAIN - EFFECT OF SURGE TANK ON THE TRANSIENT PRESSURE GRADIENTS: ULTIMATE DESIGN CONDITIONS

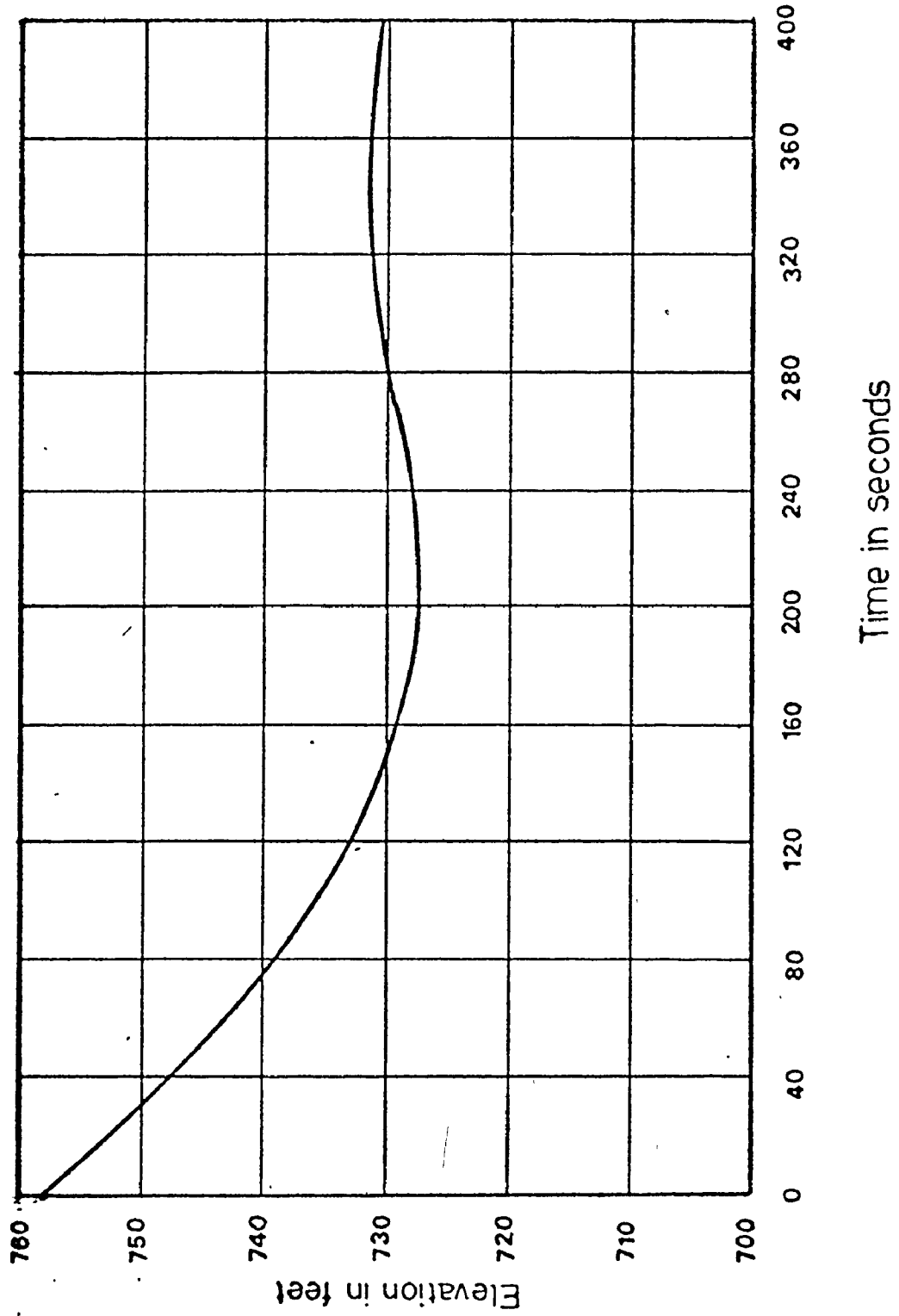


FIG. 6.9: THE ANCASTER FORCEMAIN - SURGE LEVELS IN SURGE TANK

along the pipeline are plotted. Figure 6.9 presents the surge tank oscillations as obtained from the program (based on the ultimate design conditions). High pressures will occur in the pipeline between the pumps and the tank. The minimum required height of the tank is 79.0 ft for two pump operation.

Such a surge tank is clearly not to be recommended, for reasons including height, limited protection, and freezing.

6.2.3 One-Way Surge Tanks. Although one-way surge tanks (or discharge tanks) can be used to protect the pipeline, this solution was not recommended because (a) excavation, (b) sewage should not be allowed to become stagnant in the tank, and (c) the check valves could become clogged. The difficulties associated with discharge tank operation are discussed elsewhere⁽⁷⁰⁾. However, for interest, the computer program was run to locate the most effective position for such a tank. Figure 6.10 shows the recommended position for the tank, and the resulting maximum and minimum pressures along the pipeline (for one-pump operation). Figure 6.11 presents pump discharge, head at the tank, and head at the pump following pump shut-down, as obtained from the computer program. Negative, but acceptable, pressures appear in the pipeline. In the pipeline between the pump and the tank, high pressures will obtain. For pump operation with the future impellor (after 20 years), and the ultimate design condition (two-pump operation), this discharge tank cannot protect the pipeline; vapour pockets will again develop in the pipeline. Two discharge tanks with in-line valves could protect the pipeline in this case.

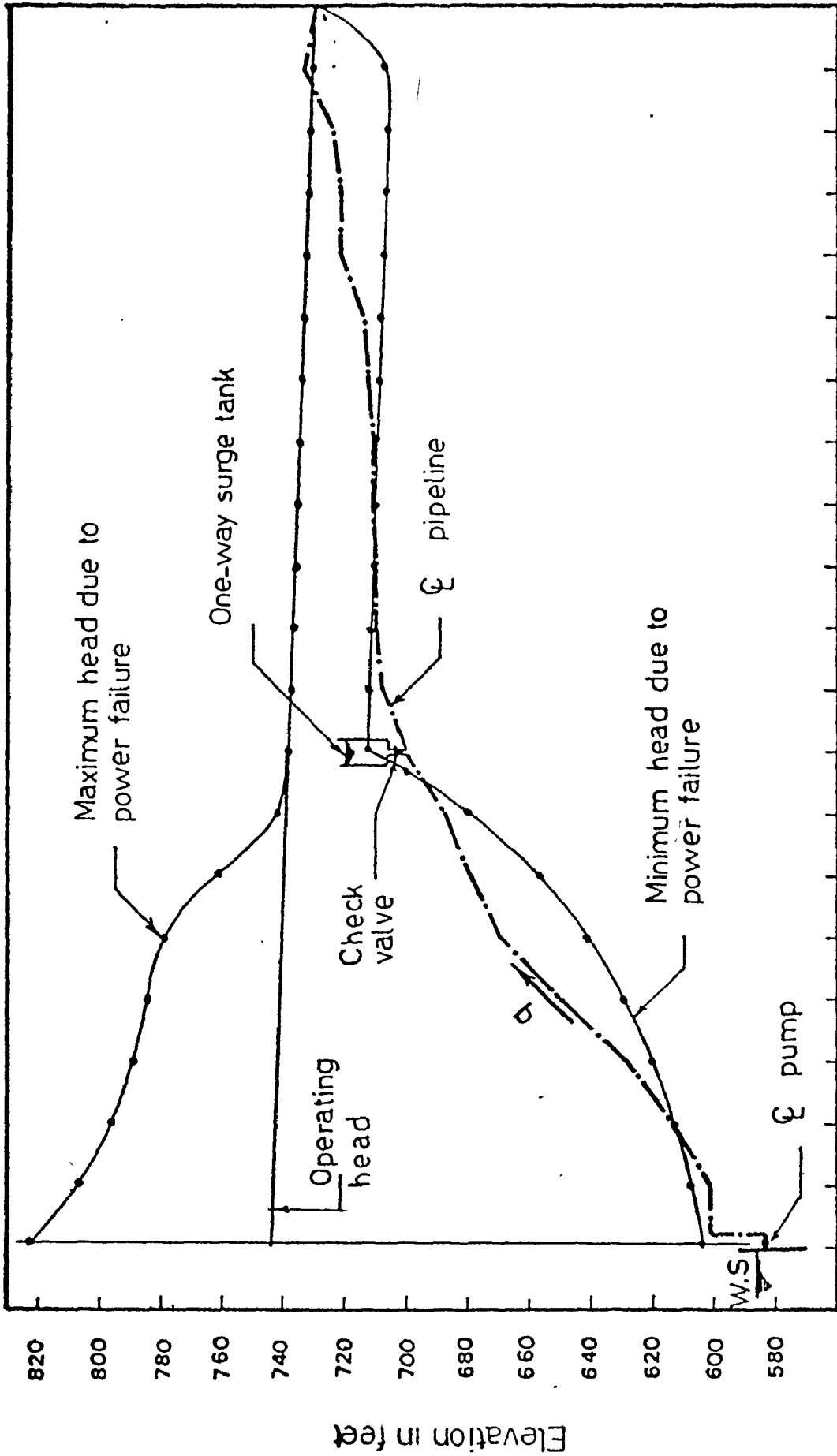


FIG. 6.10: THE ANCASTER FORCEMAIN - EFFECT OF ONE-WAY SURGE TANK ON THE TRANSIENT PRESSURE GRADIENTS: ONE-PUMP OPERATION

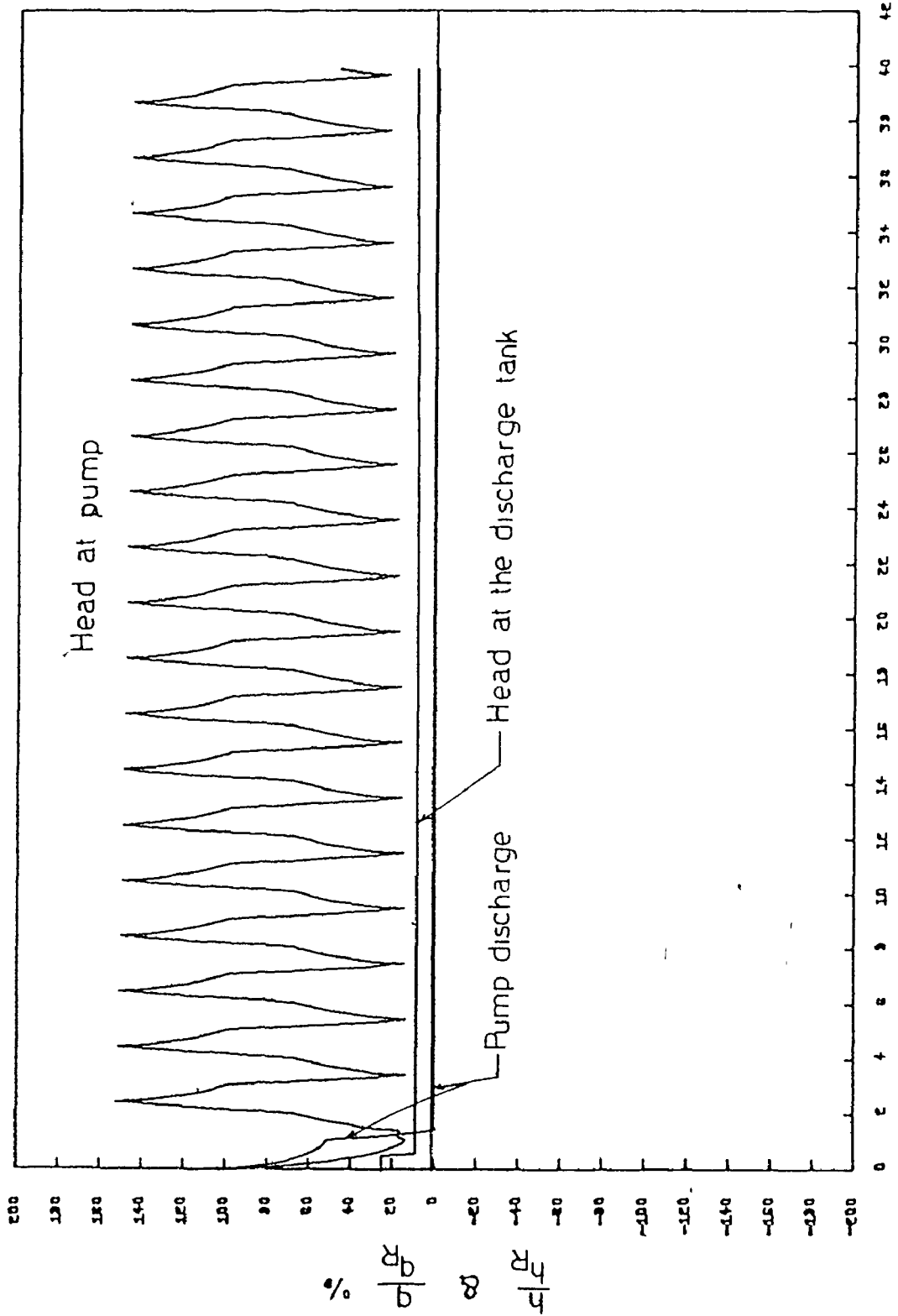


FIG. 6.11: THE ANCASTER FORCEMAIN - TRANSIENT CONDITIONS DUE TO POWER FAILURE; WITH A ONE-WAY SURGE TANK

6.2.4 Air Vessel. An air vessel at the pumps can protect the whole pipeline. For preliminary design for the air vessel, charts by Evans⁽⁵²⁾ can be used. The design of the air vessel is based on ultimate two-pump operation; since it can serve the same purpose, and more efficiently, for the initial running conditions. The program was run for different air chamber capacities. The minimum capacity that could eliminate harmful water hammer effects was determined as follows:

Diameter of air chamber	= 4.0 ft
Height of air chamber	= 15.0 ft
Initial volume of air	= 125.0 ft ³
Initial volume of water (sewage)	= 60.0 ft ³

The resulting water hammer maximum and minimum pressures along the pipeline (with the air vessel installed) are plotted in Fig. 6.12. Three cases were simulated: (a) initial one-pump operation, (b) one-pump operation (new impellor), and (c) ultimate two-pump operation. The results indicate that negative pressures will be completely eliminated from the pipeline for the initial one-pump operation. For the future operating conditions, negative pressures in the pipeline will be considerably lower than the water vapour pressure. If these negative pressures are not to be permitted, then a bigger air chamber will be necessary. In Figs. 6.13 and 6.14, the transient pressures at the air chamber and midlength of discharge pipe are plotted, based on the initial operating conditions. A smaller air chamber can be used for one-pump operation. The tank capacity can be reduced by throttling the inlet to the air chamber to restrict the flow into the chamber, while keeping the outflow as free as possible. An orifice for that purpose

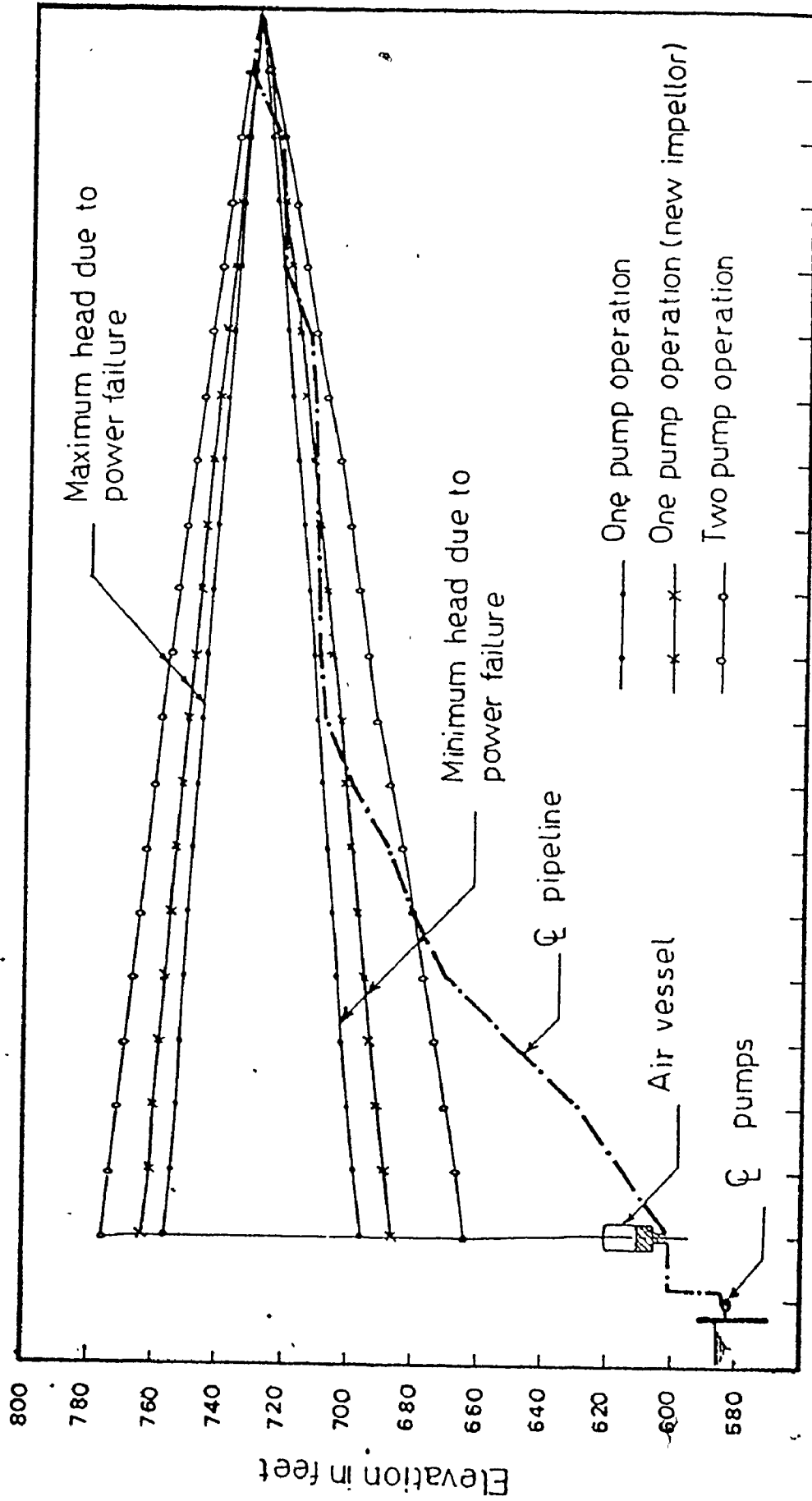


FIG. 6.12: THE ANCASTER FORCEMAIN - EFFECT OF PRESSURE VESSEL ON THE TRANSIENT PRESSURE GRADIENTS

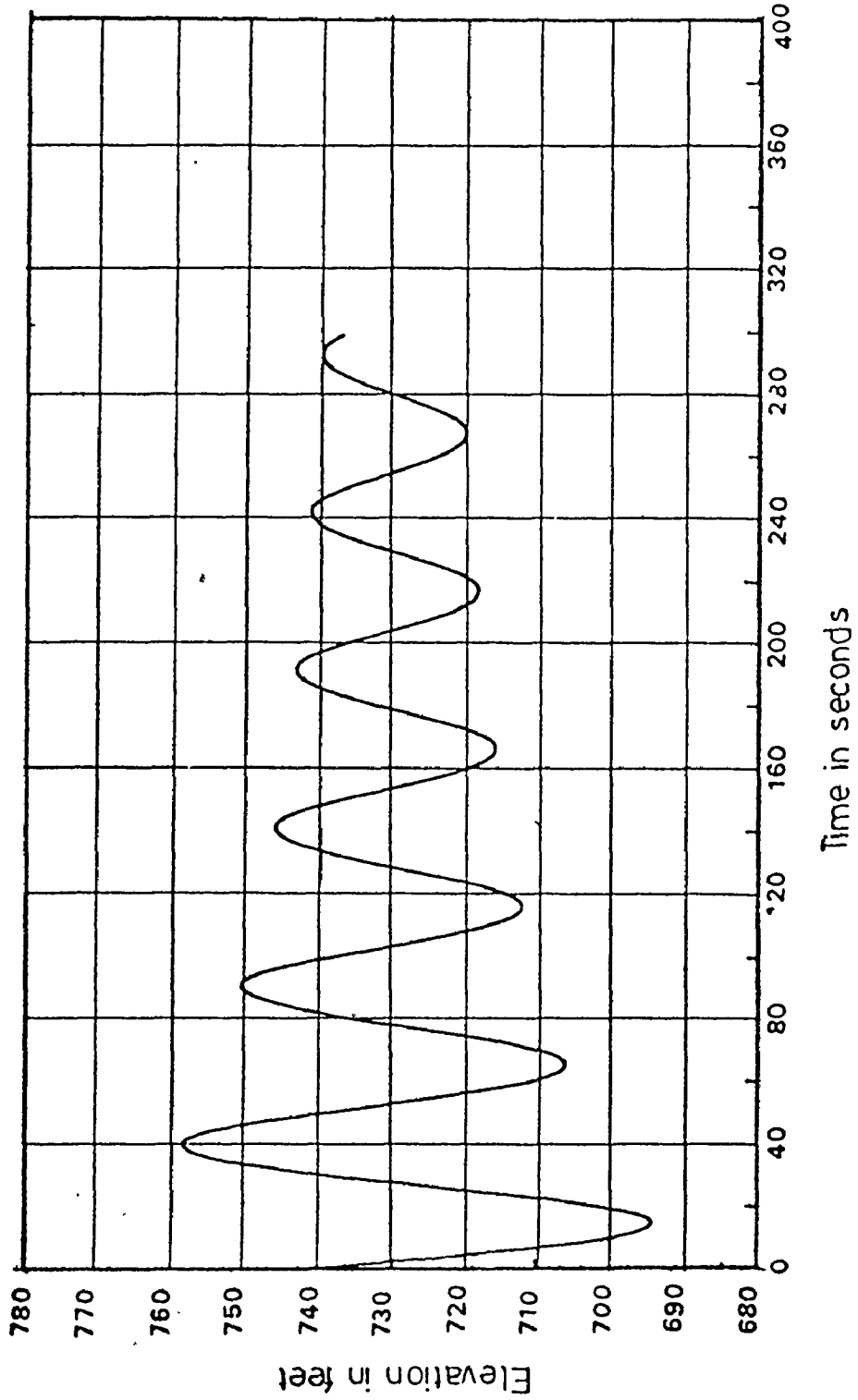


FIG. 6.13: THE ANCASTER FORCEMAIN - PRESSURE VARIATIONS AT THE AIR VESSEL

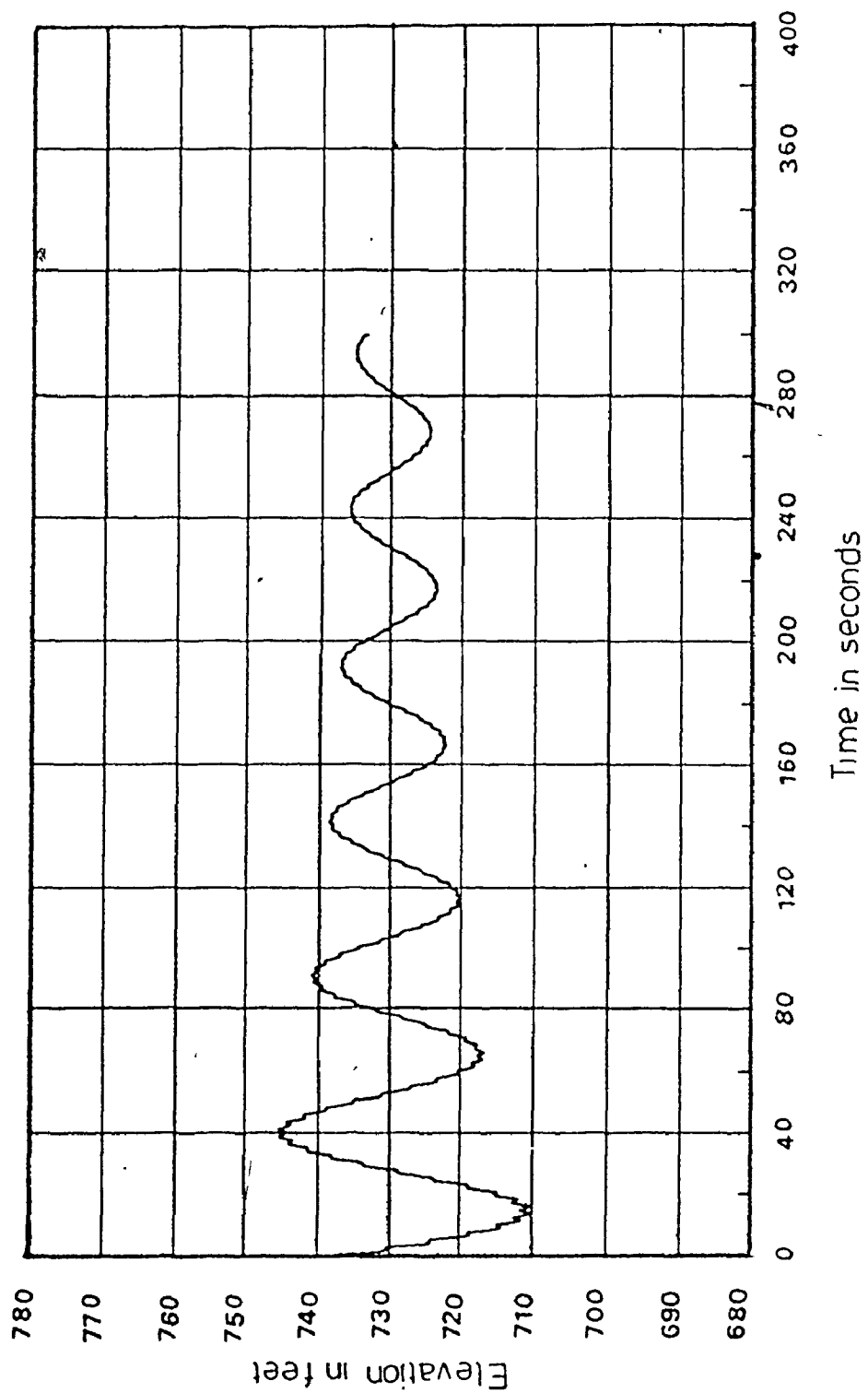


FIG. 6.14: THE ANCASTER FORCEMAIN - PRESSURE VARIATIONS AT THE MIDLENGTH OF DISCHARGE LINE; WITH THE AIR VESSEL INSTALLED

is described by Evans⁽⁵²⁾.

6.2.5 Air Vents. Air vents may be used to protect the pipeline by injecting air into the low pressure sections. However, this solution is not recommended as (a) air injected into the pipeline would eventually discharge at the top manhole within which a messy situation would soon develop, and (b) air would also noisily discharge through the cover or cause a nuisance in the houses connected to that manhole.

6.3 Conclusion

The best protection for this pipeline is an air chamber near the pump (inside the pump house). The positions of the automatic switches should be determined carefully with regard to the water level fluctuations during the transients. It is possible to use a smaller air chamber for the initial conditions, and to add further air chamber(s) for the future conditions.

7. CONCLUSIONS

1. A general computer program is developed which can solve many transient flow problems. The program can be used by non-programmers with limited understanding of transient problems. The program is written in dimensionless form and can be used for any system of units, so long as the units are consistent throughout.
2. The explicit method of characteristics proved to be accurate and stable, although it may require excessive calculations if time increment Δt is made relatively small. To satisfy the condition of stability ($\Delta t = \frac{\Delta x}{a}$), and to decrease the computation time and cost, Δx should be set as large as possible. Δx is limited by the fact that all critical points on the pipeline should be represented.
3. The logical arrangement of the program allows the flexibility to handle a large number of surge-control devices placed anywhere in the pipeline. This is of value in choosing the most effective protective device as demonstrated for the Ancaster forcemain (Chapter 6).
4. A comparison between the computer results and test observations, graphical analysis, or the water hammer charts available in the literature showed that the program is dependable and accurate to an acceptable degree. However it has not been possible to examine the computer results for any complex system, because of the lack of published data.
5. Plotted results are easily interpreted and provide the designer with a useful picture of the physical behaviour of the system. This insight would not be so readily gained from an examination of tabular output.

6. A numerical study of valve operation at the pump demonstrated that a two-stage valve closure (at first is rapid and then slow), similar to that used at the Tracy Pumping Plant, is most effective in reducing upsurges. The use of a check valve with slam closure feature creates the highest upsurges. Transient pressures in the zone of normal pump operation are not affected by valve operation. Increasing the inertia of rotating elements (pump, motor, and entrained water) can reduce the upsurges and downsurges, whether a valve is used at the pump discharge side or not.
7. In some pump-discharge lines, increasing the inertia of rotating elements can be a satisfactory means of eliminating (or at least reducing) harmful water hammer effects. However, pump manufacturers do not produce pumps having more rotational inertia than is necessary to deliver the rated discharge. Large inertia pumps may be cheaper than the cost of constructing a surge-control device, or may reduce the cost of the device necessary. Tests should be conducted by manufacturers to evaluate the exact rotational inertia of pumps; including entrained water, as this estimate is important in evaluating the least cost method of reducing pressure transients.
8. Recommendations: The method developed in this study should be applied to pipelines of variable diameters and friction, as well as branched pipes and pipe net-works. The pump data published by Donsky⁽⁵¹⁾ for three specific speeds are the only published data available in the literature. It is recommended that tests be conducted for pumps having other specific speeds, especially in the zones of energy dissipation and turbine operation. Consulting engineers and professional companies should be encouraged to publish their water hammer test results.

BIBLIOGRAPHY

References 2-47 were cited by F.M. Wood (see page 1)

1. Wood, F. M., History of Water-Hammer, C. E. Report No. 65. Civil Eng. Dept., Queen's University, Kingston, April 1970.
2. Euler, L., "Principia pro motu sanguinis per arterias determinando" Opera Postuma Tomus Alter XXXIII 1775.
3. Newton, I., The Principia (Cajori translation).
4. Euler, L., "De la Propagation du Son" Memoires de l'Acad. d. Wiss. Berlin 1759.
5. Lagrange, J. L., Mecanique Analytique 1788.
6. Monge, G., "Graphical integration, etc." Ann. des Ing. sortis des Ecoles de Gand 1789.
7. Laplace, P. S., Celestial Mechanics (4 Volumes) Bowditch translation.
8. Wertheim, Pogg (Ann. d. Phys. und Chemie) Vol. 77, 1848.
9. Riemann, B., Partielle Differentialgleichungen, Braunschweig 1869.
10. Weber, W., "Propagation of waves through water or other incompressible fluids in elastic pipes" Akad. d. Wiss. Leipzig Berichte 1865.
11. Weber, W., (as above) 1850. Weber, E. and Wellenlehre, . (text book) Leipzig 1825.
12. Kundt. Pogg Vol. 153.
13. Dvorak. Pogg Vol. 154, 1875.

14. Marey, Dr., "Mouvement des Ondes Liquides pour servir a la Theorie du Pouls" Travaux du Laboratoire de M. Marey, 1875.
15. Resal, H., "Movement of an incompressible fluid in an elastic pipe" Journal de Math. pures et Appliquees, 1876.
16. Korteweg, D. J., "Uber die Fortpflanzungsgeschwindigkeit der Schalles in Elastischen Rohren" Ann. d. Physik u. Chemie 1878.
17. Michaud, J., "Coups de Belier dans les conduites" Bulletin de la Soc. Vaudoise des Ing. et des Architectes, Lausanne 1878.
18. Gromeka, V. I., "Concerning the propagation velocity of water-hammer waves in elastic pipes" Scientific Soc. of Univ. of Kazan, May 1883.
19. Weston, E. B. Trans. ASCE 1885.
20. Church, I. P. Journal of the Franklin Inst. 1890.
21. Church, I. P. Cornell Civil Engineer. 1898.
22. Carpenter, R. C., "Experiments on Water-hammer" Trans. ASME 1893-4.
23. Frizell, J. P., "Pressures from velocity changes in pipes" Trans. ASCE 1898.
24. Joukowski, N., Paper to Polytechnic Soc. Moscow, Spring of 1898.
(English translation by Miss O. Simin. Proc. AWWA, 1904).
25. Allievi, L., (a) "General theory of pressure variation in Pipes" Ann. d. Ing. et Archit. Ital. Dec. 1902.
(b) "Mouvement de l'eau dans les Tuyaux de Conduite" Revue de Mecanique, Jan. March 1904.
(c) "Theorie Generale du Mouvement varie, etc." Dunod. Paris 1904.
(d) "Notes" Atti d. Cole d. Ing. e. Arch. Milan 1913.
(e) English translation by E. E. Halmos ASME 1925.

26. Warren, M. M., "Penstock and Surge Tank Problems" Trans. ASCE 1915.
27. Constantinescu, G., Ann. des Mines de Roumaine, Dec. 1919 - Jan. 1920.
(abstract in Le Genie Civil Vol. 76, No. 15).
28. Gibson, N. R. "Pressures in Penstocks caused by gradual closing of turbine gates" Trans. ASCE 1920.
29. Strowger and Kerr. "Speed Changes of Hydraulic Turbines for sudden changes of load" ASME June 1926.
30. Löwy, R., "Druckschwankungen in Druckrohrleitungen" Springer 1928.
31. Schnyder, O., "Druckstösse in Pumpensteigleitungen" Schweizerische Bauzeitung. Nov., Dec. 1929.
32. Bergeron, Louis, "Variations de regime dans les conduites d'eau" Comptes Rendus des Travaux de la Soc. Hydrotech. de France 1931.
33. Schnyder, O., "Über druckstösse in Rohrleitungen" Wasserkraft u. Wasserwirtschaft. Heft 5, 1932.
34. "Symposium on Water-Hammer" ASME and ASCE. Chicago, June 1933 (also a Supplement to the Symposium).
35. Angus, R. W., "Simple Graphical Solutions for Pressure Rise in Pipe and Pump Discharge Lines" Journal EIC Feb. 1935.
36. Allievi, L., Air Chambers for Discharge Pipes.
37. Angus, R. W., Air Chambers and Valves in relation to water-hammer.
38. De Juhasz. Hydraulic Phenomena in Fuel-injection Systems for Diesel Engines.
39. Knapp, F. Operation of emergency shut-off valves in pipe lines.
40. Knapp, R. T. Complete Characteristics of Centrifugal Pumps and their use in the prediction of transient behavior.

41. Schnyder, O., Comparison between calculated and test results on water-hammer in Pumping Plants.
42. Strowger, Relation of Relief valves and Turbine characteristics in the determination of water-hammer.
43. Wood, F. M., "The application of Heaviside's operational calculus to the solution of problems in Water-Hammer".
44. Angus, R. W., "Water-Hammer Pressures in Compound and Branches Pipes" Proc. ASCE 1938.
45. Lupton, H. R., "Graphical Analysis of Pressure Surges in Pumping Systems" Journal Inst. of Water Engrs. 1953.
46. Richards, R. T., "Water Column Separation in Pump Discharge Lines" Trans. ASME 1956.
47. Kittredge, C. P., "Hydraulic Transients in Centrifugal Pump Systems" Trans. ASME 1956.
48. Parmakian, John, "Pressure Surges at Large Pump Installations" Trans. ASME, Vol. 75, August 1953, pp. 995-1006.
49. Parmakian, John. Waterhammer Analysis. Prentice-Hall, Inc., New York, 1955.
50. Parmakian, John, "One-Way Surge Tanks for Pumping Plants", Transactions of the ASME, October 1958, pp. 1563-1572.
51. Donsky, Benjamin, "Complete Pump Characteristics and the Effect of Specific Speeds on Hydraulic Transients", Journal of Basic Engineering, Transactions of the ASME, December 1961, pp. 685-699.
52. Evans, W. E., and Crawford, C. C., "Design Charts For Air Chambers on Pump Lines", Proc. Separate No. 273, ASCE, Paper No. 2710, Sept. 1953.

53. Streeter, V. L., and Chintu Lai, "Waterhammer Analysis Including Fluid Friction", Journal of the Hydraulics Division, Proc., ASCE, Vol. 88, HY3, May 1962, pp. 79-112.
54. Streeter, V. L., "Valve Stroking to Control Water Hammer", Journal of the Hydraulic Division, ASCE, Vol. 89, HY2, pp. 39-66, March 1963.
55. Streeter, V. L., "Waterhammer Analysis of Pipelines", Journal of the Hydraulics Division, Proc., ASCE, Vol. 90, No. HY4, July 1964, pp. 151-172.
56. Kinno, H., and Kennedy, J. F., "Waterhammer Charts for Centrifugal Pump Systems", Journal of the Hydraulic Division, Proc., ASCE, Vol. 91, HY3, May 1965, pp. 247-270.
57. Stephenson, D., "Discharge Tanks for Suppressing Water Hammer in Pumping Lines", Proceedings of the 1st International Conference on Pressure Surges, Canterbury, England, Paper F3, BHRA Fluid Engineering, 1972.
58. Martin, C. S., "Method of Characteristics Applied to Calculations of Surge Tank Oscillations", Proceedings of the 1st International Conference on Pressure Surges, Canterbury, England, Paper E1, BHRA Fluid Engineering, 1972.
59. Streeter, V. L., "Unsteady Flow Calculations by Numerical Methods", Journal of Basic Engineering, Trans., ASME, June 1972, pp. 457-466.
60. Sheer, T. J., "Water Hammer Studies for a Pumping Line Protected by One-Way Surge Tank",

61. Streeter, V. L. Fluid Mechanics, McGraw-Hill Book Company, New York, 1971.
62. Pickford, John. Analysis of Surge, Macmillan and Co. Ltd., 1969.
63. Thomas, G. O., "Determination of Pump Characteristics for a Computerized Transient Analysis", Proceedings of the 1st International Conference on Pressure Surges, Canterbury, England, Paper A3, BHRA Fluid Engineering, 1972.
64. Donsky, B., Discussion of Reference No. 63.
65. Stephenson, D., "Water Hammer Protection of Pumping Lines", Trans. S.A.I.C.E., December 1972.
66. Parmakian, John, "Pressure Surge Control at Tracy Pumping Plant", Proc. Sep. No. 361, ASCE, Vol. 79, December 1953.
67. Livingston, A. C., and Wilson, J. N., "Effects of Valve Operation", Symposium on "Surges in Pipelines", Proc., The Institution of Mechanical Engineers, Vol. 180, Part 3E, Paper 3, 1965-66, Westminster, London.
68. Angus, R. W., Discussion of Reference No. 48.
69. Streeter, V. L., and Wylie, E. B., Hydraulic Transients, McGraw-Hill, 1967.
70. Donsky, B., Discussion of Reference No. 50.

NOTATION

The following symbols are used in this thesis:

- A = cross sectional area of pipe;
 A_R = cross sectional area of surge tank riser;
 A_T = cross sectional area of surge tank;
 A_{ves} = cross sectional area of air vessel;
 a = celerity of pressure wave;
 b = pipe wall thickness;
 C = a subscript which denotes values calculated after time increment Δt ;
 c_1 = pipe rigidity, or a factor of pipe restriction;
 D = diameter of pipe;
 D_T = diameter of surge tank;
 D_R = diameter of surge tank riser;
 D_{ves} = diameter of air vessel;
 E = modulus of elasticity of pipe wall material;
 f = darcy-weisbach friction factor;
 g = acceleration due to gravity;
 H = dimensionless piezometric head;
 H_{CL} = calculated dimensionless head at the left hand side of an in-line device, after time increment Δt ;
 H_{CR} = calculated dimensionless head at the right hand side of an in-line device, after time increment Δt ;
 H_j = the Joukowski head (av_o/g);
 H_{Ld} = steady state dimensionless head loss across the downstream valve;

H_{Ls} = steady state dimensionless head loss across the upstream valve;

H_{Lv} = dimensionless head loss across the pump discharge valve;

H_{rd} = dimensionless water surface elevation in the downstream reservoir, measured from an arbitrary datum;

H_{ru} = dimensionless water surface elevation in the upstream reservoir, measured from datum;

H' = total dynamic head of the pump divided by the rated head;

ΔH_o = dimensionless steady state head loss across an in-line valve;

ΔH_v = dimensionless steady state head loss across the pump discharge valve;

h = piezometric head;

h_d = water surface elevation in the downstream reservoir measured from the pipe centerline;

h_{bar} = parometric head;

h_{CL} = calculated head at the left hand side of an in-line device, at the end of time increment Δt ;

h_{CR} = calculated head at the right hand side of an in-line device, at the end of time increment Δt ;

h_f = friction head;

h_{Ld} = steady state head loss across the downstream valve;

h_{Ls} = steady state head loss across the upstream valve;

h_{Lv} = head loss across the pump discharge valve;

h_R = rated pump head;

h_{rd} = water surface elevation in the downstream reservoir, measured from datum;

h_{ru} = water surface elevation in the upstream reservoir, measured from datum;

h_s = water surface elevation in the upstream reservoir, measured from the pipe centerline;

h_{ss} = system static head;

- h_g^* = absolute head in the air chamber;
 Δh_o = steady state head loss across in-line valve;
 Δh_v = steady state head loss across the pump discharge valve;
 I = polar moment of inertia;
 K = bulk modulus of elasticity of liquid;
 L = length of pipe;
 N = pump speed, number of reaches;
 N_R = rated pump speed;
 N_S = pump specific speed;
 n = number of pumps;
 n' = polytropic exponent;
 Q = dimensionless discharge ($= q/q_o$);
 Q_T = dimensionless discharge into discharge tank ($= q_T/q_o$);
 Q' = pump discharge divided by rated discharge;
 q = discharge;
 q_o = steady state discharge;
 q_R = rated discharge;
 q_{rr} = steady state discharge divided by the rated pump discharge;
 q_T = discharge into surge tank;
 S = maximum surge at surge tank, measured from the operating level;
 T = pump torque, dimensionless time;
 T_R = rated torque;
 ΔT = dimensionless time increment;
 t = time;
 tdh = total dynamic head;
 Δt = time increment;

- V = volume of air in the air chamber;
 v = velocity;
 v_o = steady state velocity;
 WR^2 = rotational inertia;
 X = dimensionless length along the pipe;
 ΔX = dimensionless length increment;
 x = length along the pipe;
 Δx = length increment;
 Z_{pn} = dimensionless pump elevation;
 z_b = elevation of the pipe at its connection to the surge tank, measured from datum;
 z_d = elevation of the pipe at the downstream end;
 z_p = pump elevation measured from datum;
 z_u = elevation of the pipe at the upstream end;
 z_{ves} = height of air vessel;
 z_w = initial height of water in air vessel;
 α = pump speed divided by the rated speed;
 β = pump torque divided by the rated torque;
 η_R = pump efficiency at rated conditions;
 γ = specific weight of fluid;
 μ = poisson's ratio for the pipe wall material;
 ρ = pipeline constant;
 τ = a known function of time; and
 ω = angular velocity of pump.

PUMP CHARACTERISTICS

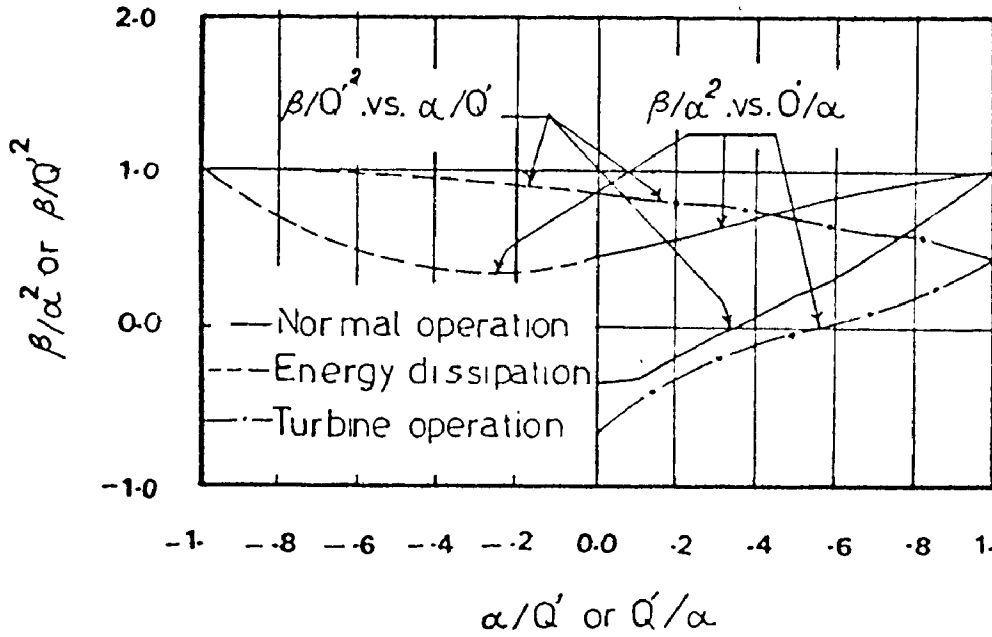


FIG. A.1: DIMENSIONLESS-HOMOLOGOUS TORQUE DATA FOR CENTRIFUGAL PUMPS - $N_s = 1800$ (gpm units)

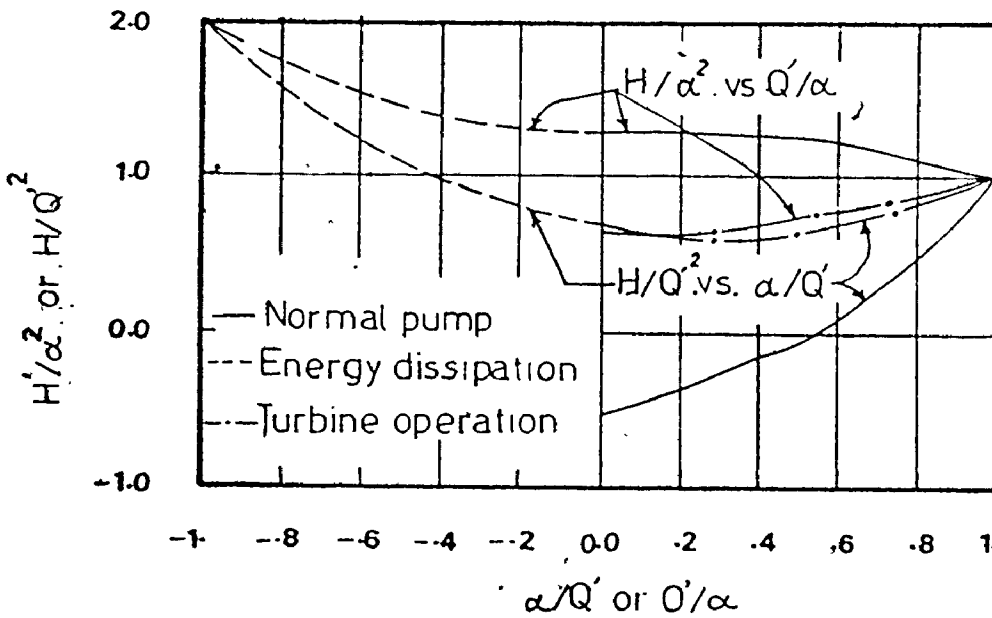


FIG. A.2: DIMENSIONLESS-HOMOLOGOUS HEAD DATA FOR CENTRIFUGAL PUMPS - $N_s = 1800$ (gpm units)

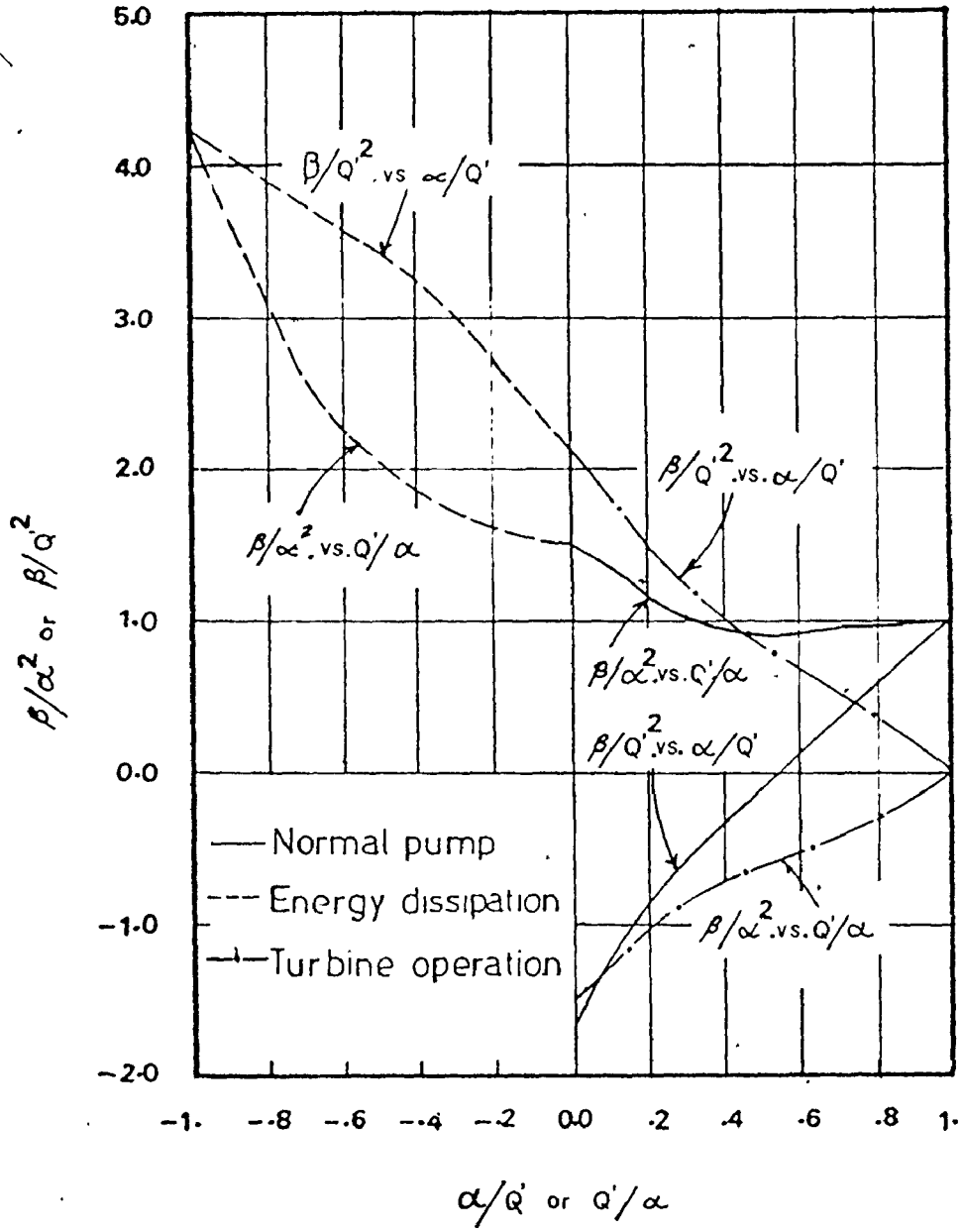


FIG. A.3: DIMENSIONLESS-HOMOLOGOUS TORQUE DATA FOR MIXED FLOW PUMPS - $N_s = 7600$ (gpm units)

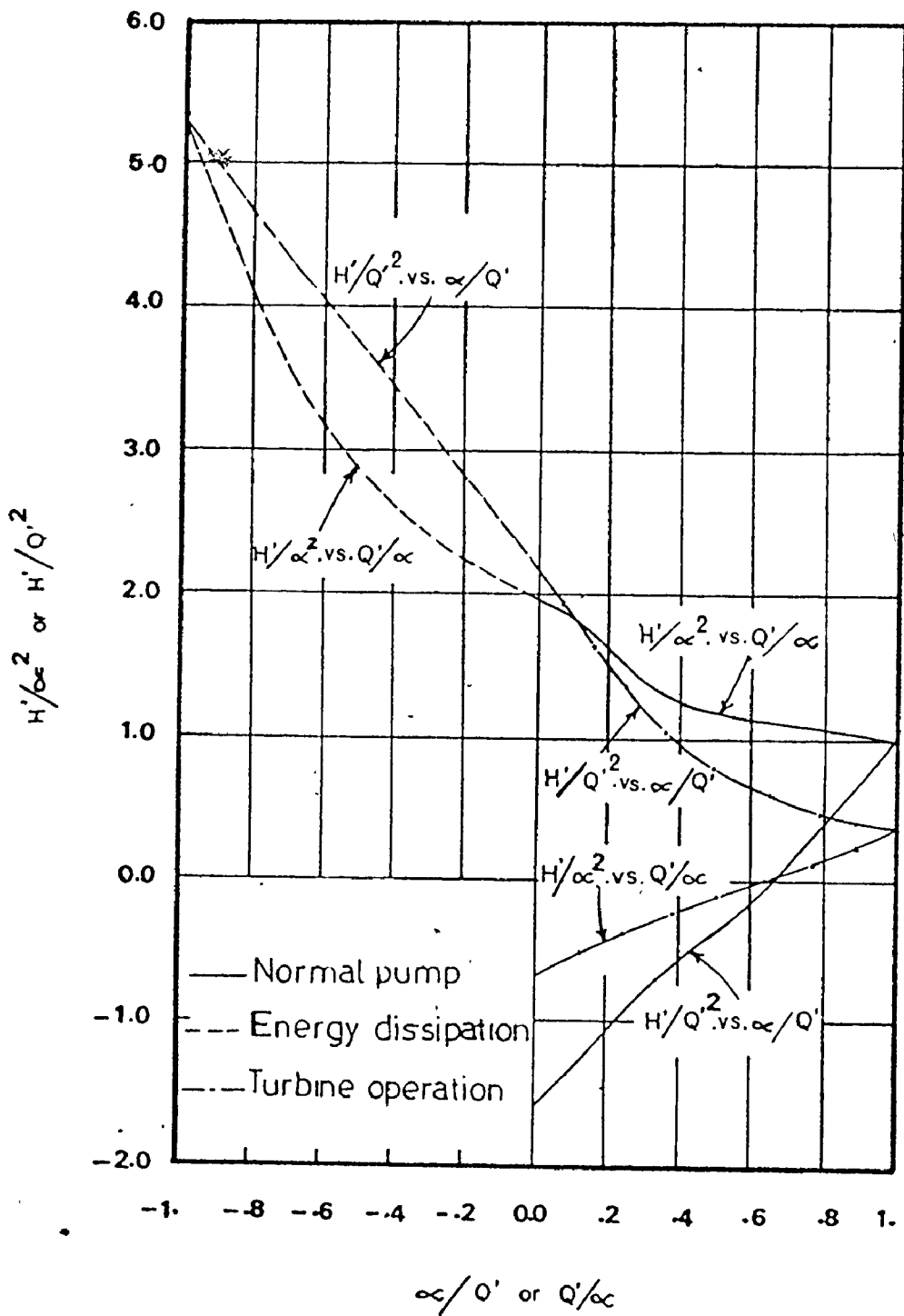


FIG. A.4: DIMENSIONLESS-HOMOLOGOUS HEAD DATA FOR MIXED FLOW PUMPS - $N_s = 7600$ (gpm units)

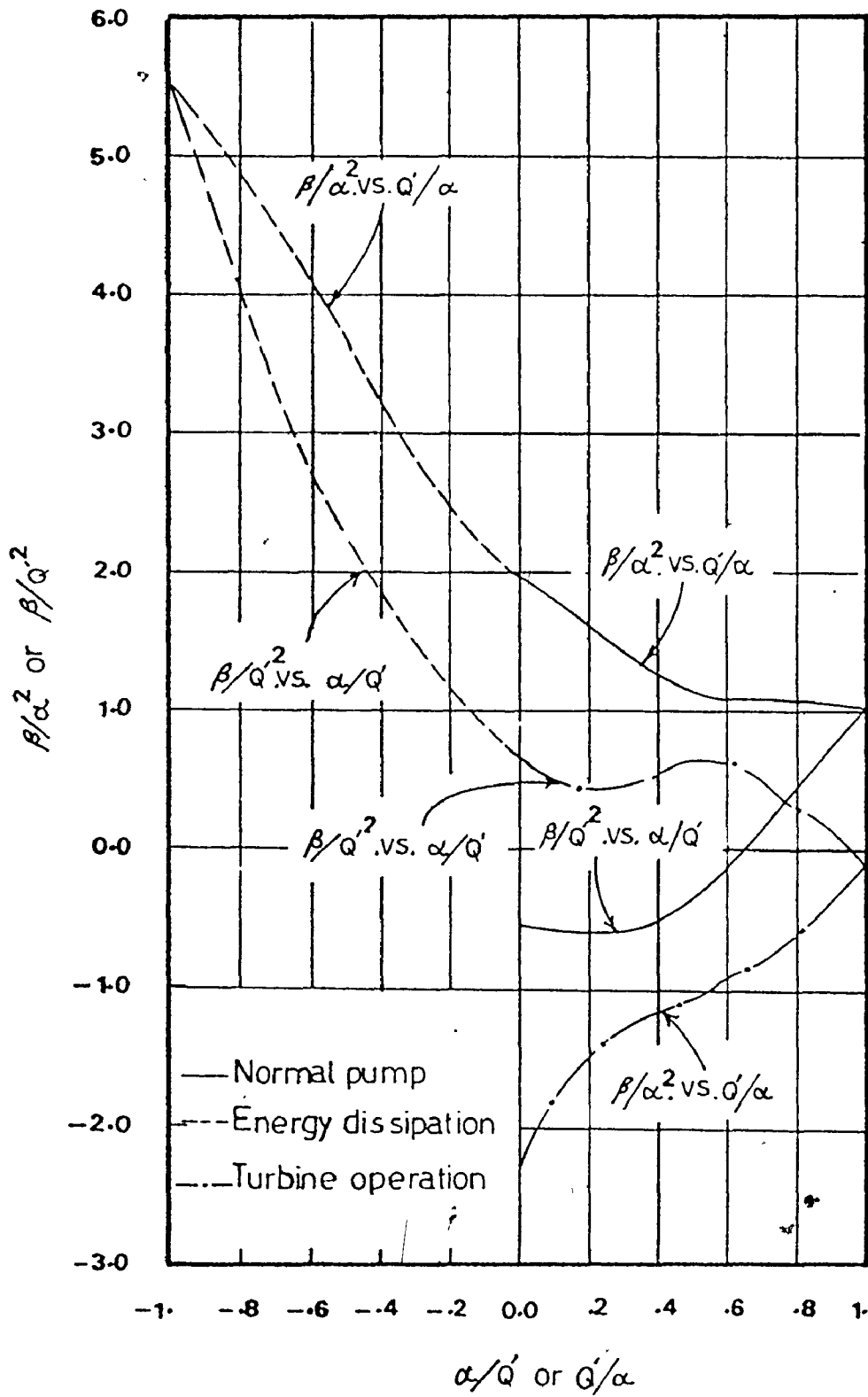


FIG. A.5: DIMENSIONLESS-HOMOLOGOUS TORQUE DATA FOR AXIAL FLOW PUMPS - $N_s = 13500$ (gpm units)

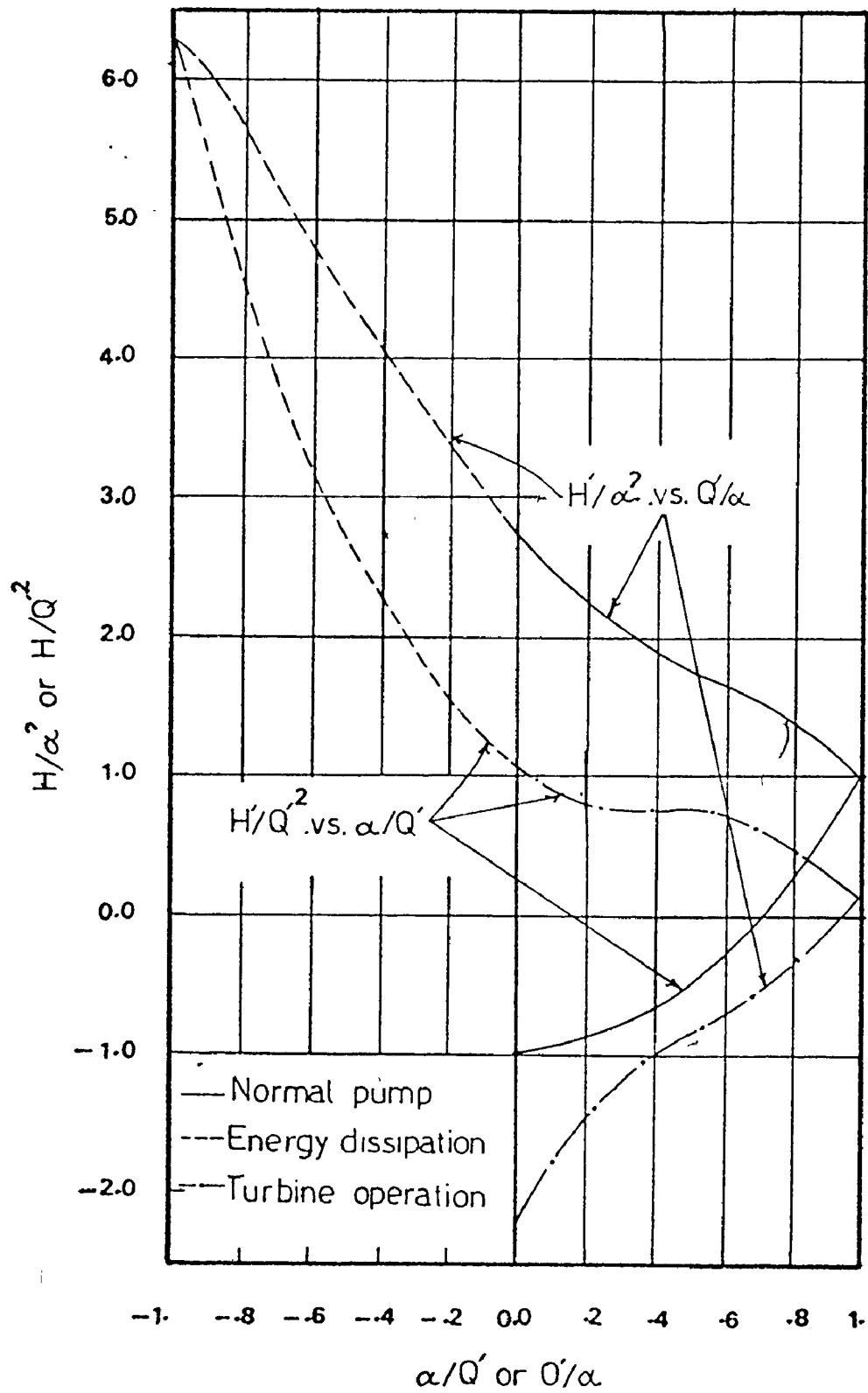


FIG. A.6: DIMENSIONLESS-HOMOLOGOUS HEAD DATA FOR AXIAL FLOW PUMPS - $N_s = 13500$ (gpm units)

$$\frac{\alpha}{Q'} \text{ or } \frac{Q'}{\alpha}$$

	0.0	0.1	0.2	0.3	0.4	0.5	0.6	0.7	0.8	0.9	1.0	
Zone of Normal Pump Operation	β/Q'^2	-0.37	-0.29	-0.19	-0.05	0.07	0.21	0.31	0.48	0.65	0.82	1.00
	β/α^2	0.45	0.50	0.57	0.63	0.71	0.77	0.83	0.89	0.93	0.97	1.00
	H'/Q'^2	-0.56	-0.47	-0.38	-0.27	-0.17	-0.08	0.11	0.29	0.49	0.73	1.00
	H'/α^2	1.29	1.29	1.28	1.27	1.26	1.24	1.21	1.17	1.12	1.06	1.00
Zone of Energy Dissipation	β/Q'^2	0.86	0.89	0.91	0.93	0.96	0.98	0.99	1.00	1.01	1.02	1.04
	β/α^2	0.45	0.39	0.37	0.37	0.38	0.42	0.48	0.58	0.70	0.85	1.04
	H'/Q'^2	0.69	0.74	0.80	0.88	0.97	1.09	1.21	1.37	1.54	1.75	1.99
	H'/α^2	1.29	1.29	1.31	1.35	1.38	1.43	1.50	1.60	1.71	1.84	1.99
Zone of Turbine Operation	β/Q'^2	0.86	0.83	0.80	0.80	0.75	0.70	0.65	0.60	0.56	0.51	0.45
	β/α^2	-0.68	-0.50	-0.33	-0.20	-0.10	-0.04	0.02	0.11	0.20	0.32	0.45
	H'/Q'^2	0.69	0.66	0.63	0.63	0.64	0.66	0.70	0.76	0.83	0.91	1.01
	H'/α^2	0.63	0.65	0.67	0.68	0.70	0.73	0.76	0.81	0.86	0.93	1.01

TABLE A.1: DIMENSIONLESS-HOMOLOGOUS TORQUE AND HEAD DATA FOR CENTRIFUGAL PUMPS -
 $N_s = 1800$ (gpm units)

$$\frac{\alpha}{Q'} \text{ or } \frac{Q'}{\alpha}$$

	0.0	0.1	0.2	0.3	0.4	0.5	0.6	0.7	0.8	0.9	1.0	
Zone of Normal Pump Operation	β/Q'^2	-1.65	-1.17	-0.83	-0.55	-0.30	-0.11	0.12	0.36	0.60	0.82	1.00
	β/α^2	1.48	1.29	1.14	1.01	0.93	0.91	0.92	0.95	0.97	0.99	1.00
	H'/Q'^2	-1.56	-1.31	-1.04	-0.76	-0.53	-0.35	-0.13	0.13	0.42	0.72	1.00
	H'/α^2	1.96	1.83	1.62	1.38	1.25	1.21	1.15	1.11	1.07	1.03	1.00
Zone of Energy Dissipation	β/Q'^2	2.10	2.37	2.67	2.97	3.21	3.40	3.56	3.73	3.96	4.06	4.22
	β/α^2	1.48	1.53	1.60	1.68	1.83	2.03	2.24	2.59	3.06	3.61	4.22
	H'/Q'^2	2.17	2.48	2.79	3.11	3.42	3.72	4.03	4.29	4.62	4.95	5.26
	H'/α^2	1.96	2.07	2.20	2.37	2.58	2.83	3.14	3.54	4.03	4.60	5.26
Zone of Turbine Operation	β/Q'^2	2.10	1.78	1.48	1.22	1.00	0.83	0.67	0.51	0.36	0.19	0.00
	β/α^2	-1.50	-1.25	-1.02	-0.83	-0.70	-0.63	-0.53	-0.43	-0.32	-0.18	0.00
	H'/Q'^2	2.17	1.83	1.49	1.18	0.94	0.77	0.67	0.57	0.49	0.43	0.38
	H'/α^2	-0.67	-0.54	-0.42	-0.31	-0.21	-0.12	-0.01	0.09	0.17	0.26	0.38

TABLE A.2: DIMENSIONLESS-HOMOLOGOUS TORQUE AND HEAD DATA FOR MIXED FLOW PUMPS -
 $N_s = 7600$ (gpm units)

$$\frac{\alpha}{Q'} \text{ or } \frac{Q'}{\alpha}$$

		0.0	0.1	0.2	0.3	0.4	0.5	0.6	0.7	0.8	0.9	1.0
Zone of Normal Pump	β/Q'^2	-0.56	-0.60	-0.62	-0.60	-0.54	-0.39	-0.15	0.11	0.41	0.71	1.00
	β/α^2	1.96	1.80	1.61	1.41	1.24	1.13	1.09	1.06	1.05	1.03	1.00
	H'/Q'^2	-1.00	-0.95	-0.88	-0.79	-0.67	-0.50	-0.28	-0.03	0.27	0.61	1.00
	H'/α^2	2.73	2.49	2.27	2.07	1.90	1.76	1.65	1.53	1.40	1.23	1.00
Zone or Energy Dissipation	β/Q'^2	0.67	0.88	1.16	1.49	1.86	2.25	2.75	3.35	4.07	4.80	5.52
	β/α^2	1.95	2.17	2.46	2.82	3.23	3.67	4.10	4.50	4.88	5.22	5.52
	H'/Q'^2	1.08	1.29	1.57	1.91	2.29	2.70	3.18	3.80	4.56	5.40	5.29
	H'/α^2	2.73	3.04	3.37	3.74	4.11	4.47	4.80	5.20	5.66	6.05	6.29
Zone or Turbine Operation	β/Q'^2	0.67	0.49	0.42	0.44	0.51	0.63	0.61	0.49	0.27	0.15	-0.15
	β/α^2	-2.33	-1.83	-1.50	-1.32	-1.20	-1.10	-0.95	-0.79	-0.61	-0.40	-0.15
	H'/Q'^2	1.08	0.89	0.79	0.77	0.77	0.77	0.73	0.64	0.49	0.32	0.13
	H'/α^2	-2.20	-1.79	-1.46	-1.20	-1.00	-0.86	-0.72	-0.55	-0.35	-0.12	0.13

TABLE A.3: DIMENSIONLESS-HOMOLOGOUS TORQUE AND HEAD DATA FOR AXIAL FLOW PUMPS -
 $N_s = 13500$ (gpm units)


```

COMMON /198/ Q01(3),M1(1),S1(1),X1(1),Y1(1),Z1(1),V1(1),C1(1)
COMMON /248/ ...
COMMON /398/ ...
COMMON /498/ ...
COMMON /598/ ...
COMMON /698/ ...
COMMON /798/ ...
COMMON /898/ ...
COMMON /998/ ...

CALL TAUDV
IF ICHC.EQ.21 GO TO 201
...
CALL SPEED
...

```

```

REAL INERT
...
20 GO TO 14
...
30 CALL ...
...
40 ...
...
50 ...
...
60 ...
...
70 ...
...
80 ...
...
90 ...
...
100 ...
...
110 ...
...
120 ...
...
130 ...
...
140 ...
...
150 ...
...
160 ...
...
170 ...
...
180 ...
...
190 ...
...
200 ...
...
210 ...
...
220 ...
...
230 ...
...
240 ...
...
250 ...
...
260 ...
...
270 ...
...
280 ...
...
290 ...
...
300 ...
...
310 ...
...
320 ...
...
330 ...
...
340 ...
...
350 ...
...
360 ...
...
370 ...
...
380 ...
...
390 ...
...
400 ...
...
410 ...
...
420 ...
...
430 ...
...
440 ...
...
450 ...
...
460 ...
...
470 ...
...
480 ...
...
490 ...
...
500 ...
...
510 ...
...
520 ...
...
530 ...
...
540 ...
...
550 ...
...
560 ...
...
570 ...
...
580 ...
...
590 ...
...
600 ...
...
610 ...
...
620 ...
...
630 ...
...
640 ...
...
650 ...
...
660 ...
...
670 ...
...
680 ...
...
690 ...
...
700 ...
...
710 ...
...
720 ...
...
730 ...
...
740 ...
...
750 ...
...
760 ...
...
770 ...
...
780 ...
...
790 ...
...
800 ...
...
810 ...
...
820 ...
...
830 ...
...
840 ...
...
850 ...
...
860 ...
...
870 ...
...
880 ...
...
890 ...
...
900 ...
...
910 ...
...
920 ...
...
930 ...
...
940 ...
...
950 ...
...
960 ...
...
970 ...
...
980 ...
...
990 ...
...
END

```

SUBROUTINE TAUDV

TO COMPUTE PUMP SPEEDS AT EACH TIME INTERVAL

